

# A Reactive Multicomponent Transport Model for Saturated Porous Media

© Henning Prommer & Vincent Post

User's Manual v2.10  
<http://www.pht3d.org>  
August, 2010

## Disclaimer

The PHT3D v2.10 software described in this manual has been tested for a range of benchmark problems and other applications, as demonstrated in this document and by peer-reviewed publications. However, the program and the manual are provided “as is” and no warranty is made as to the fitness for a particular purpose, functioning and accuracy of the program. For any errors found, please notify the program authors

Henning Prommer ([Henning.Prommer@csiro.au](mailto:Henning.Prommer@csiro.au))

or

Vincent Post ([vincent.post@flinders.edu.au](mailto:vincent.post@flinders.edu.au))

## Preface

PHT3D is a three-dimensional reactive multicomponent transport code for saturated porous media. The here described version of PHT3D (v2.10) incorporates MT3DMS (Release 5.3), a program for the simulation of three-dimensional advective-dispersive multi-species transport, and PHREEQC-2 (Release 2.17), the U.S. Geological Survey geochemical code for the quantification of reactive processes.

The current version of MT3DMS is based on MT3D, originally developed by Chunmiao Zheng at S.S. Papadopulos & Associates, Inc. and documented for the United States Environmental Protection Agency. MT3DMS was written by Chunmiao Zheng and P. Patrick Wang with the iterative solver routine by Tsun-Zee Mai. Funding for MT3DMS development was provided, in part, by U.S. Army Corps of Engineers Waterways Experiment Station.

PHREEQC-2 was developed by D.L. Parkhurst at U.S. Geological Survey and C.A.J. Appelo. PHREEQC, in its original version, is a computer program written in the C programming language that is designed to perform a wide variety of low-temperature aqueous geochemical calculations. PHREEQC is based on an ion-association aqueous model and has capabilities for (1) speciation and saturation-index calculations; (2) batch-reaction and one-dimensional (1D) transport calculations involving reversible reactions, which include aqueous, mineral, gas, solid-solution, surface-complexation, and ion-exchange equilibria, and irreversible reactions, which include specified mole transfers of reactants, kinetically controlled reactions, mixing of solutions, and temperature changes; and (3) inverse modeling, which finds sets of mineral and gas mole transfers that account for differences in composition between waters, within specified compositional uncertainty limits

As the two public-domain codes PHREEQC-2 and MT3DMS form the core of the PHT3D code, the underlying work of David Parkhurst, Tony Appelo, Chunmiao Zheng, Patrick Wang and all of their co-workers is greatly acknowledged.



# Contents

<b>List of Figures</b>	<b>xi</b>
<b>List of Tables</b>	<b>xiii</b>
<b>1 Introduction</b>	<b>1</b>
1.1 Background . . . . .	1
1.2 Model features . . . . .	3
1.3 What is new in PHT3D v2.10 . . . . .	5
1.4 Limitations . . . . .	6
1.5 Acknowledgments . . . . .	7
1.5.1 Funding support . . . . .	7
1.5.2 Technical support . . . . .	7
<b>2 Model Concept</b>	<b>9</b>
2.1 Hydrological Transport . . . . .	9
2.2 Geochemical Reactions . . . . .	10
2.3 Coupling Procedure . . . . .	10
<b>3 Model structure</b>	<b>15</b>
3.1 Program design . . . . .	15
3.2 Units . . . . .	18
3.3 Model output . . . . .	18
3.4 Temporal discretisation . . . . .	19
<b>4 Model input</b>	<b>21</b>
4.1 PHT3D Input Files . . . . .	21
4.2 Input instructions for the PHREEQC-2 database file . . . . .	22
4.3 Input instructions for the PHREEQC-2 interface package file . . . . .	27
<b>5 Benchmark problems and application Examples</b>	<b>39</b>
5.1 Example 1: Single Species Transport with Monod Kinetics . . . . .	40
5.1.1 Introduction . . . . .	40
5.1.2 Spatial discretisation and flow problem . . . . .	41
5.1.3 Data input for the database file . . . . .	42
5.1.4 Data input for the PHREEQC interface package file . . . . .	44
5.1.5 Data input for the basic transport package file . . . . .	45
5.1.6 Data input for the advection package file . . . . .	46

5.1.7	Data input for the source/sink mixing package file . . . . .	46
5.1.8	Simulation results . . . . .	47
5.2	Example 2: Transport and mineral precipitation/dissolution . . .	48
5.2.1	Introduction . . . . .	48
5.2.2	Spatial discretisation and flow problem . . . . .	48
5.2.3	Data input for the database file . . . . .	48
5.2.4	Data input for the PHREEQC interface package file . . . . .	51
5.2.5	Data input for the basic transport package file . . . . .	52
5.2.6	Data input for the advection package file . . . . .	53
5.2.7	Data input for the dispersion package file . . . . .	54
5.2.8	Data input for the source/sink mixing package file . . . . .	54
5.2.9	Simulation results . . . . .	54
5.3	Example 3: Migration of precipitation/dissolution fronts . . . . .	56
5.3.1	Introduction . . . . .	56
5.3.2	Spatial discretisation and flow problem . . . . .	56
5.3.3	Data input for the database file . . . . .	56
5.3.4	Data input for the PHREEQC interface package file . . . . .	57
5.3.5	Data input for the basic transport package file . . . . .	58
5.3.6	Data input for the advection package file . . . . .	60
5.3.7	Data input for the dispersion package file . . . . .	61
5.3.8	Data input for the source/sink mixing package file . . . . .	61
5.3.9	Simulation results . . . . .	61
5.4	Example 4: Cation exchange - flushing of a sodium-potassium ni- trate solution with calcium chloride . . . . .	64
5.4.1	Introduction . . . . .	64
5.4.2	Spatial discretisation and flow problem . . . . .	64
5.4.3	Data input for the database file . . . . .	65
5.4.4	Data input for the PHREEQC interface package file . . . . .	67
5.4.5	Data input for the basic transport package file . . . . .	68
5.4.6	Data input for the advection package file . . . . .	70
5.4.7	Data input for the dispersion package file . . . . .	70
5.4.8	Data input for the source/sink mixing package file . . . . .	70
5.4.9	Simulation results . . . . .	71
5.5	Example 5: Cation exchange during artificial recharge . . . . .	72
5.5.1	Introduction . . . . .	72
5.5.2	Spatial discretisation and flow problem . . . . .	72
5.5.3	Data input for the database file . . . . .	72

5.5.4	Data input for the PHREEQC interface package file . . . . .	73
5.5.5	Data input for the basic transport package file . . . . .	74
5.5.6	Data input for the advection package file . . . . .	75
5.5.7	Data input for the dispersion package file . . . . .	76
5.5.8	Data input for the source/sink mixing package file . . . . .	76
5.5.9	Simulation results . . . . .	76
5.6	Example 6: Cation exchange and precipitation/dissolution during tenside injection . . . . .	78
5.6.1	Introduction . . . . .	78
5.6.2	Spatial discretisation and flow problem . . . . .	78
5.6.3	Data input for the database file . . . . .	79
5.6.4	Data input for the PHREEQC interface package file . . . . .	81
5.6.5	Data input for the basic transport package file . . . . .	82
5.6.6	Data input for the advection package file . . . . .	84
5.6.7	Data input for the dispersion package file . . . . .	85
5.6.8	Data input for the source/sink mixing package file . . . . .	85
5.6.9	Simulation results . . . . .	85
5.7	Example 7: Kinetic, sequential/parallel degradation of multiple species . . . . .	87
5.7.1	Introduction . . . . .	87
5.7.2	Spatial discretisation and flow problem . . . . .	88
5.7.3	Data input for the database file . . . . .	88
5.7.4	Data input for the PHREEQC interface package file . . . . .	91
5.7.5	Data input for the basic transport package file . . . . .	92
5.7.6	Data input for the advection package file . . . . .	94
5.7.7	Data input for the dispersion package file . . . . .	95
5.7.8	Data input for the source/sink mixing package file . . . . .	95
5.7.9	Simulation results . . . . .	95
5.8	Example 8: Kinetic, sequential degradation of chlorinated hydro- carbons . . . . .	97
5.8.1	Introduction . . . . .	97
5.8.2	Spatial discretisation and flow problem . . . . .	98
5.8.3	Data input for the database file . . . . .	98
5.8.4	Data input for the PHREEQC interface package file . . . . .	103
5.8.5	Data input for the basic transport package file . . . . .	104
5.8.6	Data input for the advection package file . . . . .	105
5.8.7	Data input for the dispersion package file . . . . .	105

5.8.8	Data input for the source/sink mixing package file . . . . .	106
5.8.9	Simulation results . . . . .	106
5.9	Example 9: Kinetic degradation of BTEX using multiple electron acceptors . . . . .	108
5.9.1	Background . . . . .	108
5.9.2	Spatial discretisation and flow problem . . . . .	109
5.9.3	Data input for the database file . . . . .	110
5.9.4	Data input for the PHREEQC interface package file . . . . .	115
5.9.5	Data input for the basic transport package file . . . . .	117
5.9.6	Data input for the advection package file . . . . .	119
5.9.7	Data input for the dispersion package file . . . . .	119
5.9.8	Data input for the source sink/mixing package file . . . . .	119
5.9.9	Simulation results . . . . .	119
5.10	Example 10: Dissolution, degradation and geochemical response . . . . .	121
5.10.1	Introduction . . . . .	121
5.10.2	Spatial discretisation and flow problem . . . . .	121
5.10.3	Data input for the database file . . . . .	122
5.10.4	Data input for the PHREEQC interface package file . . . . .	126
5.10.5	Data input for the basic transport package file . . . . .	128
5.10.6	Data input for the advection package file . . . . .	128
5.10.7	Data input for the dispersion package file . . . . .	129
5.10.8	Simulation results . . . . .	129
5.11	Example 11: Biogeochemical and isotopic changes during BTEX/PAH degradation . . . . .	131
5.11.1	Introduction . . . . .	131
5.11.2	Field Site . . . . .	131
5.11.3	Model Setup . . . . .	132
5.11.4	Reaction Network . . . . .	132
5.11.5	Carbon Isotope Fractionation . . . . .	137
5.11.6	Sulfate Reduction and Sulfur Isotope Fractionation . . . . .	139
5.11.7	Contaminant Source Geometry, Source Composition and Dissolution Kinetics . . . . .	140
5.11.8	Data input for the PHREEQC interface package file . . . . .	140
5.11.9	Simulated Fate of BTEX and PAH . . . . .	145
5.11.10	Simulated Carbon Isotope Signatures . . . . .	146
5.11.11	Simulated Sulfate Reduction and Sulfate Isotope Signatures . . . . .	148
5.12	Example 12: Transport and surface complexation of uranium . . . . .	151

5.12.1	Introduction . . . . .	151
5.12.2	Spatial discretisation and flow problem . . . . .	151
5.12.3	Data input for the database file . . . . .	151
5.12.4	Data input for the PHREEQC interface package file . . . . .	153
5.12.5	Data input for the basic transport package . . . . .	155
5.12.6	Data input for the advection package . . . . .	156
5.12.7	Data input for the dispersion package . . . . .	156
5.12.8	Data input for the source/sink package . . . . .	156
5.12.9	Simulation results . . . . .	156
5.13	Example 13: Modelling of an oxidation experiment . . . . .	160
5.13.1	Introduction . . . . .	160
5.13.2	Spatial discretisation and flow problem . . . . .	160
5.13.3	Data input for the database file . . . . .	162
5.13.4	Data input for the PHREEQC interface package file . . . . .	164
5.13.5	Data input for the basic transport package . . . . .	167
5.13.6	Data input for the advection package . . . . .	169
5.13.7	Data input for the dispersion package . . . . .	171
5.13.8	Data input for the source/sink package . . . . .	171
5.13.9	Simulation results . . . . .	171
<b>6</b>	<b>File formats</b>	<b>173</b>
6.1	ASCII Output file format . . . . .	173
<b>7</b>	<b>Further information</b>	<b>175</b>
7.1	Web resources . . . . .	175



## List of Figures

3.1	Flowchart for the main program of the PHT3D code . . . . .	16
3.2	Flowchart for the main program of the PHT3D code . . . . .	17
3.3	Temporal discretisation scheme in PHT3D . . . . .	20
5.1	Example 1 - PHT3D simulation of single-species transport with Monod-type biodegradation in comparison with the analytical solution of Parlange et al. (1984). . . . .	47
5.2	Example 2 - Simulation results for PHT3D and MST1D: Aqueous and mineral concentrations after 21000 s . . . . .	55
5.3	Example 3 - Comparison of selected aqueous component and mineral concentrations. . . . .	62
5.4	Example 4 - Comparison of simulated cation concentrations. . . . .	71
5.5	Example 5 - Comparison of simulated chloride and cation concentrations 16 <i>m</i> from the injection point . . . . .	77
5.6	Example 6 - Comparison of simulated tenside and cation concentrations . . . . .	86
5.7	Example 7 - Reaction network . . . . .	87
5.8	Example 7 - Comparison of simulated concentrations after 40 days simulation time . . . . .	96
5.9	Example 8 - Model grid and location of the contaminant source . . . . .	99
5.10	Example 8 - Simulated PCE and VC concentrations after 3 years (PHT3D = dashed lines, RT3D = solid lines) . . . . .	107
5.11	Example 9 - Comparison of concentration contours between PHT3D (dashed lines) and RT3D (solid lines) simulations for hydrocarbon, oxygen, nitrate and iron(II) concentrations. . . . .	120
5.12	Example 10 - Model grid, boundary conditions, hydraulic conductivity zonation and location of contaminant source used in Example 10 . . . . .	122
5.13	Example 10 - Head contours and streamlines of the hereogeneous flow field. . . . .	124
5.14	Example 10 - Simulated aqueous and mineral concentration after 500 days simulation time. . . . .	130
5.15	Study site. . . . .	133
5.16	Example 11 - Simulated concentration contours of toluene. . . . .	145
5.17	Example 11 - Modelled electron flux. . . . .	147

5.18	Example 11 - Simulated concentration contours and associated isotope signatures. . . . .	148
5.19	Example 11 - Selected simulated concentration profiles. . . . .	150
5.20	Example 12 - Simulated and experimental normalized tracer breakthrough. . . . .	157
5.21	Example 12 - Simulated and measured normalized uranyl breakthrough curves (Experiment 7). . . . .	158
5.22	Example 12 - Top: Simulated concentrations profiles of uranyl; Bottom: Simulated pH profiles (Experiment 7). Note that there is a typing error in Kohler et al. 1996 for the label of the profiles at 3h (pers. comm. Gary Gurtis) . . . . .	159
5.23	Example 13 - Simulated and measured breakthrough curves. . . . .	172

## List of Tables

3.1	Units to be used for the data input of a PHT3D simulation . . . . .	18
5.1	Parameters and chemical concentrations used in Example 1. . . . .	40
5.2	Flow and transport parameters used in Example 2. . . . .	48
5.3	Aqueous concentrations used in Example 2. . . . .	53
5.4	Mineral concentrations used in Example 2. . . . .	54
5.5	Flow and transport parameters used in Example 3. . . . .	56
5.6	Aqueous concentrations used in Example 3. . . . .	59
5.7	Mineral concentrations used in Example 3. . . . .	59
5.8	Flow and transport parameters used in Example 4. . . . .	64
5.9	Aqueous concentrations used in Example 4. . . . .	68
5.10	Initial exchanger concentrations used in Example 4. . . . .	69
5.11	Flow and transport parameters used in Example 5. . . . .	73
5.12	Aqueous concentrations used in Example 5. . . . .	74
5.13	Initial exchanger concentrations used in Example 5. . . . .	74
5.14	Flow and transport parameters used in Example 6. . . . .	78
5.15	Aqueous concentrations used in Example 6. . . . .	82
5.16	Initial mineral and exchanger concentrations used in Example 6. . . . .	83
5.17	Flow and transport parameters used in Example 7. . . . .	88
5.18	Reaction rate constants and stoichiometric yields used in Example 7. . . . .	93
5.19	Aqueous concentrations used in Example 7. . . . .	93
5.20	Flow and transport parameters used in Examples 8 and 9. . . . .	98
5.21	Aqueous concentrations used in Example 9. . . . .	117
5.22	Flow and transport parameters used in Example 10. . . . .	122
5.23	Concentrations of mobile aqueous components used in Example 10. . . . .	123
5.24	Mineral concentrations used in Example 10. . . . .	123
5.25	Flow/transport model parameters used in Example 11 . . . . .	134
5.26	Initial (ambient) and upgradient boundary water composition used in Example 11, corresponding to measured values from an upgradi- ent infiltration well. . . . .	136
5.27	Example 11 - Stoichiometry of degradation reactions that include microbial growth, assuming that 10% of the organic carbon is in- corporated into biomass. . . . .	138
5.28	Flow and transport model setup and discretisation used in Example 12. . . . .	152
5.29	Reaction network definition for Example 12. . . . .	153

5.30	Compositions of initial and inflow solutions in Example 12. . . . .	154
5.31	Flow/transport model setup and spatial/temporal discretisation used in Example 13. . . . .	161
5.32	Ion exchange and surface complexation reactions defined for Exam- ple 13. . . . .	165
5.33	Cation exchange capacities of exchangers defined for Example 13.	170
5.34	Compositions of initial and inflow solutions in Example 13. . . . .	170

## Introduction

### 1.1 Background

The extension of the original single-species transport code MT3D (Zheng, 1990) to the multi-species transport simulator MT3DMS (Zheng and Wang, 1999) provided the starting point for the development of a number of models that simulate coupled hydrological transport of multiple chemical species and the chemical reactions among these species. For example, RT3D (Clement, 1997) couples the implicit ordinary differential equation (ODE) solver LSODA (Hindmarsh, 1983) to MT3DMS to solve arbitrary kinetic reaction problems. RT3D provides a number of predefined reaction packages, e.g., for biodegradation of oxidisable contaminants consuming one or more electron acceptors and for sequential decay chain-type reactions of chlorinated hydrocarbons (CHCs). The BIOREDOX model (Carey et al., 1999), SEAM3D (Waddill and Widdowson, 1998) and MT3D99 (Zheng, 1999) also simulate the fate of specific pollutants, i.e., BTEX and CHCs by solving purely kinetic biodegradation reactions. On the other hand, Guerin and Zheng (1998) presented GMT3D, a multi-component transport code that addresses a different range of reactive processes such as aqueous complexation and mineral dissolution/precipitation reactions by coupling the geochemical package MODPHRQ (Brown et al., 1991) to MT3DMS. While the afore-mentioned so-called 'multi-species' codes solve the transport equation separately for each aqueous complex, GMT3D and other 'multi-component' codes solve for total aqueous component concentrations (Yeh and Tripathi, 1989; Steefel and MacQuarrie, 1996). However, in GMT3D and comparable codes such as MINTRAN (Walter et al., 1994), all of the reactions included are treated as equilibrium reactions. This limits the applicability of the model to groundwater systems where all reactions of those chemicals included in a particular simulation proceed relatively fast compared to the groundwater flow, i.e., the local equilibrium assumption (LEA) is valid. Cases where the LEA often does not hold include, for example, the biodegradation reactions of many common organic substances and mineral weathering reactions. In order to partially overcome these limitations, Prommer et al. (1999b) incorporated reaction modules for specific kinetically controlled processes (biodegradation, NAPL dissolution) into a model coupling MT3DMS and the earlier, equilibrium-based PHREEQC code (Parkhurst, 1995). That code formed the first version of the here described reactive multi-component transport code PHT3D. After the release of PHREEQC-2 (Parkhurst and Appelo, 1999) and its incorporation into PHT3D the earlier kinetic subroutines became redundant. That version and a range of

benchmark examples were documented as PHT3D v1.0 (Prommer, 2002) and its major features were also summarised in Prommer et al. (2003).

The present document describes the latest version (v2.10) of PHT3D, which handles now a wide range of mixed equilibrium/kinetic geochemical reactions. While other codes with comparable features exist, PHT3D combines the advantages of the well-established, modular and robust MODFLOW/MT3DMS flow and transport simulator family with the extremely versatile capabilities and the reliability of the PHREEQC-2 code (Parkhurst and Appelo, 1999). Thus, a great variety of reactive transport problems can be addressed for complex hydraulic systems and boundary conditions. Primarily, PHT3D model applications will target rather complex geochemical problems, i.e., multi-component problems where transport and reactions of all major ions are included and pH, pe and, typically, water-rock (or water-sediment) interactions are simulated. However, simpler reaction networks can of course also be simulated, although computationally less effective if compared to some purpose-build simpler models. As the reaction simulations of the coupled model is based on PHREEQC-2, reaction kinetics can easily be formulated through user-defined rate expressions within the database. Reactive processes such as NAPL dissolution, microbial growth/decay or isotopic fractionation can thus conveniently be included through modifications of the original, extensible PHREEQC-2 database. Both models, MT3DMS and PHREEQC-2 are widely used in the groundwater/geochemistry communities and are individually well tested and documented. Previous modeling studies using PHT3D were, for example, carried out to study

- the biogeochemistry of landfill leachate plumes (Prommer et al., 2006)
- aromatic and chlorinated hydrocarbon spills (Prommer et al., 2002b; Vencelides et al., 2007; Colombani et al., 2009)
- the fate of pesticides (Prommer et al., 2006)
- reactive transport of arsenic and uranium (Jung et al., 2009; Ma et al., 2009; Wallis et al., 2010)
- trace metal remediation by in-situ reactive zones (Prommer et al., 2007)
- the fate of an ammoniacal liquor contamination
- an emplaced creosote source experiment

- the isotopic fractionation during natural attenuation of organic pollutants (van Breukelen and Prommer, 2008; Pooley et al., 2009; Prommer et al., 2009)
- the geochemical evolution under islands in the Okavango Delta, Botswana (Bauer-Gottwein et al., 2007)
- biogeochemical changes during ASR (aquifer storage and recovery) of reclaimed water (Greskowiak et al., 2005)
- temperature-dependent pyrite oxidation during a deep-well injection experiment (Prommer and Stuyfzand, 2005)
- the fate of a pharmaceutical residue during artificial recharge of groundwater (Greskowiak et al., 2006)
- remediation of acid mine drainage by permeable reactive barriers
- the reactive transport of chlorinated or brominated solvents in a permeable Fe(0)-filled reactive barriers (Prommer et al., 2008; Cohen et al., 2008)
- the role of transverse dispersion on reactive contaminant transport (Ham et al., 2004, 2007)
- the geochemical evolution of the capture zone of drinking water supply wells

An up-to-date list of PHT3D-related publications is maintained on the PHT3D web-site under <http://www.pht3d.org/public.html>

## 1.2 Model features

The current version of PHT3D implements most, but not all features provided by the unmodified MT3DMS simulator (Version 5.30, released February 2010). This includes in particular a choice between different solution schemes for advective transport:

- Upstream Finite Difference (FD) method
- Method of Characteristics (MOC) scheme
- Modified Method of Characteristics (MMOC) scheme
- Hybrid Method of Characteristics (HMOC) scheme

- Third-order TVD (total-variation-diminishing) scheme (ULTIMATE)

Note that these different schemes may show quite different performances and in some cases can fail to produce a correct solution, depending on the nature of the investigated simulation problem as well as the selected discretisation. Typically the use of the TVD or the MMOC scheme appear to perform most reliable while the HMOC and MOC scheme often do not work well in cases where redox reactions occur. PHT3D users are encouraged to study the theoretical background provided by Zheng and Wang (1999). Chemical fluxes and reactions associated with external sinks/sources such as

- wells
- rivers
- recharge
- evapotranspiration

can be included in PHT3D simulations. For the reaction step, MT3DMS and PHREEQC-2 have been interfaced such that PHT3D simulations might include

- equilibrium complexation reaction/speciation within the aqueous phase
- kinetically controlled reactions within the aqueous phase such as biodegradation
- equilibrium dissolution and precipitation of minerals
- kinetic dissolution and precipitation of minerals
- single or multi-site cation exchange (equilibrium)
- single or multi-site surface complexation reactions

The structure of PHT3D permits to define kinetically reacting immobile components. Typical environmental processes such as microbial activity and NAPL (non aqueous phase liquids) dissolution can be defined, incorporated and simulated. Those and other processes might be, without modification of the PHT3D source code, and in a convenient way, included through a PHREEQC-2 database file.

The model allows the simulation of complex geochemical transport problems whereby users may find it helpful that the PHT3D model is built from two well-known, existing tools. Thus, most potential users might be familiar with either the use of MT3DMS and/or PHREEQC-2.

Despite this apparent advantage, the successful application of the PHT3D model to geochemical transport modelling problems will, for most users, still require a significant initial effort.

### 1.3 What is new in PHT3D v2.10

The source code for version v2.10 of PHT3D has been largely rewritten compared to earlier versions. Data exchange between the two models is no longer achieved through external ASCII files, but through a tighter coupling of MT3DMS and PHREEQC-2. The tighter coupling ensures that now almost all of PHREEQC-2's original capabilities are also available in PHT3D v2.10. Perhaps most importantly this includes the option to simulate surface complexation reactions, a key feature for more realistically simulating the fate of metal(loid)s and radionuclides (e.g., arsenic, uranium).

For advanced users, PHT3D v2.10 provides now the possibility to prefix or append additional input information that uses PHREEQC-type input structure and keywords. This is a very powerful feature that allows users, for example, to easily and quickly include and trial additional or newly developed rate expressions, to define specific output information (e.g. through `SELECTED_OUTPUT`, `USER_PRINT` and `USER_PUNCH`) and to override default PHREEQC-2 and PHT3D behavior.

In PHT3D v2.10 the simulation of redox reactions has been modified compared to previous versions. As in PHREEQC-2, the total number of moles of hydrogen and oxygen in a solution are now transported and pH and pe are now calculated from the mole balances of these elements. Therefore, it is no longer necessary to transport all the different redox species (valence states) that exist of an element. Instead, it suffices in principle to transport a single element, which will be speciated to its proper redox state by PHREEQC depending on pH and pe. However, in most cases users may still want to separate the input and, perhaps more importantly, the output of the various redox states of an element. In other words, if for example Fe(2) and Fe(3) are treated as separate components, PHT3D will produce separate UCN concentration output files, whereas defining solely Fe as component will only provide UCN-type concentration output for Fe.

Previously, the reaction terms were not considered in the mass balance calculations of the transport simulator MT3DMS. This omission has now been fixed in PHT3D v2.10 and the mass balance information in the listing file and \*.MAS files now also includes the mass transfers due to chemical reaction.

PHT3D versions before version v2.10 included an option to select between

binary or ASCII output files. The option to generate ASCII output files has been retained but instead of replacing the binary output by ASCII output (as was previously the case), ASCII output files are now created in addition to binary output files. Binary output is written to files with extension \*.UCN, ASCII output is written to files with the extension \*.ACN.

From v2.10 on the concentration of ion exchange species are no longer defined in  $mol\ l_w^{-1}$  [ $M\ L^{-3}$ ] (with  $l_w$  referring to litre of pore water) but in  $mol\ l_v^{-1}$  [ $M\ L^{-3}$ ] (with  $l_v$  referring to litre of bulk volume). This change was introduced for consistency with the definitions of the other heterogeneous reactions, i.e., mineral dissolution/precipitation and surface complexation reactions.

PHT3D v2.10 is now also more versatile compared to older PHT3D versions with respect to defining initial concentrations. For example, when specifying the initial concentrations of the exchange species, an exchanger may be specified to be in equilibrium with a given solution composition. In this way, there is no longer a need to (i) explicitly calculate the equilibrium composition in PHREEQC a priori and (ii) to enter the calculated concentrations of the exchange species manually. Moreover, an unlimited number of exchangers can now be defined.

PHT3D v2.10 support all the options that are available in PHREEQC-2 to define input concentrations of aqueous species. For example, a concentration can be specified implicitly by equilibrating the solution with a pure phase or by enforcing a charge balance.

Two options for determining the length of a reaction time step are available in PHT3D v2.10. The first option is the same as in previous versions and involves a user-defined time step. This may be subdivided into multiple transport steps for which no reactions are calculated. In the second option, the reaction time steps coincide with the transport time steps. This means that for each transport time step, the reactions are calculated, which increases the computational load severely but may reduce operator splitting errors, where this is a problem.

The structure of the `pht3d_ph.dat` input file in PHT3D v2.10 has been changed slightly compared to the file structure in versions 1.47 and lower. Older input files are backward compatible and can be used without modification.

## 1.4 Limitations

Similarly as in the original MT3DMS code and other MT3DMS-based packages, PHT3D simulations are carried out on the base of a flow-field computed beforehand by a separate flow simulator, typically MODFLOW. Thus, it can't reproduce the potential impact of reactive processes on the groundwater flow field

and the model is not suitable to predict, for example, the impact of bioclogging or mineral precipitation on the hydraulic properties of an aquifer.

The simultaneous use of the MT3DMS chemical reaction package (RCT) and PHREEQC-2 (PHC) as reaction simulator(s) is possible. However, this should be done with appropriate care, i.e., control of potential operator-splitting errors.

## 1.5 Acknowledgments

Many people have over the years and in various ways helped to test and improve the PHT3D simulator.

**1.5.1 Funding support** The first versions of the model were developed as part of a self-funded PhD study at the University of Western Australia (UWA) and at CSIRO Australia Land and Water (Floreat Labs). Financial strain was reduced by a partial tuition fee waiver of the Centre for Water Research (CWR) at UWA and by financial support from the Centre for Groundwater Studies (CGS). The model was further developed (i) as part of a post-doctoral research project at the Contaminated Land Assessment and Remediation Research Centre (CLARRC) at the University of Edinburgh, funded by the Scottish Higher Education Funding Council (SHEFC) and (ii) during the 5<sup>th</sup> framework European Union project CORONA (Confidence in forecasting of natural attenuation).

Financial support that assisted the compilation of earlier versions of the software and its documentation was also provided by the Center for Applied Geoscience at the University of Tübingen, Delft University of Technology and the University of Alabama.

Recent model development and documentation activities for version v2.10 were supported by CSIRO Land and Water Australia, VU University Amsterdam and Flinders University/National Centre for Groundwater Research and Training (NC-GRT), Australia.

**1.5.2 Technical support** Wen-Hsing Chiang has provided significant support by adapting PMWIN/PMWIN Pro (Chiang and Kinzelbach, 2001) and Groundwater Explorer/3D Master for their use as GUI and visualisation software for PHT3D. This support was instrumental to efficiently test and apply the model. More recently PHT3D was also included in the Visual Modflow environment, which helped again to make PHT3D more accessible for users. In that process, Serguei Schmakov has contributed several code modifications. A very special thank goes to Janek Greskowiak who has provided the most significant

input with his assistance throughout the implementation and testing of the surface complexation modelling capabilities. Janek contributed **Example 12** to the manual and helped to test and improve many other new and old features and supported many PHT3D users.

Greg Davis, Tirtha Gautam, Michelle Grassi, Jasper Griffioen and Sabine Spiessl have reviewed earlier versions of this document and over the years a large number of users have provided valuable feedback and helped to test, debug and improve PHT3D.

Peter Engesgaard, John Molson, Tony Appelo, Yun-Wei Sun, Tirtha Gautam, Dominique Thiery and Gary Curtis have kindly provided data for the model evaluation. Andrew Barry, Chris Barber, Greg Davis, Peter Dillon, Peter Grathwohl, Chittaranjan Ray, Jasper Griffioen, Bob Kalin, Ruud Schotting, Georg Teutsch, Poul Bjerg, Boris van Breukelen, Massimo Rolle, Chunmiao Zheng and many others have initiated or supported modelling projects that included PHT3D model applications. Andrew Barry and Greg Davis who were both involved in the PHT3D development from the very beginning have collaborated in many scientific model applications at the University of Western Australia, at CSIRO Australia and at the University of Edinburgh. Chunmiao Zheng, David Parkhurst and Tony Appelo have always provided immediate and helpful technical (and moral) support.

## Model Concept

### 2.1 Hydrological Transport

The reactive transport equation (solved by MT3DMS) for the  $n^{\text{th}}$  (mobile) aqueous component is (in indicial notation):

$$\frac{\partial C_n}{\partial t} = \frac{\partial}{\partial x_\alpha} (D_{\alpha\beta} \frac{\partial C_n}{\partial x_\beta}) - \frac{\partial}{\partial x_\alpha} (v_\alpha C_n) + \frac{q_s C_n^s}{\theta} + r_{\text{reac},n} \quad (2.1.1)$$

and for immobile entities, e.g., minerals:

$$\frac{\partial C_n}{\partial t} = r_{\text{reac},n} \quad (2.1.2)$$

where  $v_\alpha$  is the pore-water velocity in direction  $x_\alpha$ ,  $D_{\alpha\beta}$  is the hydrodynamic dispersion coefficient tensor,  $q_s$  is a volumetric flow rate per unit volume of aquifer representing fluid sources (positive) and sinks (negative),  $\theta$  is the porosity of the subsurface medium,  $C_n^s$  is the concentration of the source or sink flux,  $r_{\text{reac},n}$  is a source/sink rate due to chemical reaction and  $C_n$  is the total aqueous component concentration of the  $n^{\text{th}}$  component (Yeh and Tripathi, 1989; Engesgaard and Kipp, 1992). There  $C_n$  is defined as:

$$C_n = c_n + \sum_{m=1, n_s} Y_m^s s_m \quad (2.1.3)$$

where  $c_n$  is the molar concentration of the (uncomplexed)  $n^{\text{th}}$  aqueous component,  $n_s$  is the number of species in dissolved form that have complexed with the aqueous component,  $Y_m^s$  is the stoichiometric coefficient of the aqueous component in the  $m^{\text{th}}$  complexed species and  $s_m$  is the molar concentration of the  $m^{\text{th}}$  complexed species.

Using a sequential operator-splitting technique (Herzer and Kinzelbach, 1989; Valocchi and Malmstead, 1992; Miller and Rabideau, 1993; Zysset, 1993; Zysset et al., 1994; Morshed and Kaluarachchi, 1995a,b; Barry et al., 1996, 1997; Steefel and MacQuarrie, 1996) the advection and dispersion terms within (2.1.1) are solved by the transport module MT3DMS for  $n_{\text{tot}}$  components and for each time step of a temporally discretised problem, with

$$n_{\text{tot}} = n_m + 3 \quad (2.1.4)$$

where  $n_m$  is the number of (mobile) chemical components (i.e., the entity that is defined as **SOLUTION\_MASTER\_SPECIES**) in PHREEQC-2). The 3 additional quantities that are included in the transport calculations are the total amounts of hydrogen and oxygen and the charge balance.

In contrast to the earlier version of PHT3D the total amounts of hydrogen and oxygen are now included in the solute transport simulations. This is because PHREEQC-2 is now used to calculate the  $pH$  and  $pe$  by solving the mass balance of these elements (H and O). The charge balance (or more precisely the charge imbalance) is now also a transported property. However, in critical cases more robust model results are obtained if all aqueous solutions that are applied in the simulations, either as initial water compositions or at model boundaries, are fully charge balanced.

## 2.2 Geochemical Reactions

In PHT3D all concentration changes of aqueous components and immobile entities that result from reactive processes are computed by PHREEQC-2. It is, in contrast to its precursor models PHREEQE (Parkhurst et al., 1980) and PHREEQC (Parkhurst, 1995), capable of simultaneously solving arbitrary, kinetically controlled reactions in addition to geochemical equilibrium problems. From PHT3D version v2.10 onwards, the full set of geochemical reactions that can be handled by PHREEQC-2 can be included in the simulations. This eliminates the limitations that existed with older versions of PHT3D, which included only a subset of reactions.

## 2.3 Coupling Procedure

Several options to couple transport and reactive processes through split-operator methods exist, e.g., sequential, alternating and iterative split-operator methods. Details of the different techniques have been discussed, e.g., by Herzer and Kinzelbach (1989), Valocchi and Malmstead (1992), Miller and Rabideau (1993), Zysset (1993), Zysset et al. (1994), Morshed and Kaluarachchi (1995a,b), Steefel and MacQuarrie (1996) and Barry et al. (1996, 1997, 2002). In PHT3D a slightly modified version of the 'standard' sequential split-operator method described by Walter et al. (1994) has been implemented. A time-discretised form of (2.1.1) for reactive transport of a component, as defined by (2.1.3) is:

$$C_n^{k+1} - C_n^k = L(C_n)^{k+1/2} \Delta t + R_{reac,n} \quad (2.3.1)$$

where  $L(C_n)^{k+1/2}$  ( $ML^{-3}$ ) is the spatial differential operator (central in time, i.e., time level  $k + 1/2$ ) and  $C_n^k$  and  $C_n^{k+1}$  ( $ML^{-3}$ ) are the total aqueous component concentrations of the  $n^{th}$  component at the old time level  $k$  and the new time level  $k + 1$ , respectively,  $\Delta t$  is the time step length, and  $R_{reac,n}$  ( $ML^{-3}$ ) is the difference in concentrations from before and after a reaction step. In the model presented by

Walter et al. (1994),  $R_{reac,n}$  represents the relative mass of a component generated or consumed instantaneously by an equilibration of the aqueous solution with a mineral assemblage at the time  $t^{equil}$  ( $t^k \leq t^{equil} \leq t^{k+1}$ ), compensating for the chemical perturbation arising from advective and dispersive transport during  $\Delta t$ . However, in PHT3D  $R_{reac,n}$  does not only represent concentration changes of aqueous components due to (equilibrium) precipitation/dissolution reactions, but also due to any other reactive process handled by PHREEQC-2, such as ion exchange, biodegradation, etc., depending on which reactions the  $n^{th}$  component participates in. The concentration change  $R_{reac,n}$  might occur as a result of equilibrium, kinetic or mixed equilibrium/kinetic reactions. In PHT3D, the (MT3DMS) advection and dispersion modules solve the concentrations  $C_n^{transp}$ , i.e., the concentrations at the new time level  $k + 1$  that result from physical transport only:

$$C_n^{transp} = L(C_n)^{k+1/2} \Delta t + C_n^k \quad (2.3.2)$$

for the  $n_{tot}$  compounds/components. Once  $C_n^{transp}$  is computed, the second step, which models the reaction(s), will be carried out in a sequential manner for each grid cell individually. The computation of the reaction step within a grid cell is independent from concentrations at neighbouring cells. This then leads to the concentrations  $C_n^{k+1}$  at the new time level  $k + 1$ , i.e.,

$$C_n^{k+1} = C_n^{transp} + R_{reac,n} \quad (2.3.3)$$

For the computation of the source/sink term  $R_{reac,n}$ , the concentrations  $C_n^{transp}$  from after the transport step(s) are used as initial concentrations for the chemistry calculation step.

In PHT3D, two options are available to determine the time step length  $\Delta t$ . In the first option the user defines the time step length. In this case, depending on the actual advection scheme selected for a simulation (FD, TVD, MOC, MMOC or HMOC), the transport simulator MT3DMS may sub-divide the user-defined time step length  $\Delta t$  into several transport steps that fulfill the relevant stability and/or accuracy criteria for physical transport (Courant number). Thus, sometimes several subsequent transport steps (without reactions) might be carried out by MT3DMS to compute  $C_n^{transp}$ . The time step length for the reaction simulation will correspond to the user-defined time step length  $\Delta t$  and not to the automatically selected transport step size, which depends on the actual advection scheme used for a simulation.

The first option helps to reduce model execution times, i.e., CPU-times by allowing the selection of a relatively-large time step length. This is often helpful,

particularly in the early, more conceptual stages of a modelling project, i.e., where (very high) solution accuracy is not a primary concern. Accuracy can be improved by reducing the size of  $\Delta t$ . For a small enough step size the numerical solution will become independent of  $\Delta t$  as a result of a negligible splitting error.

In the second option, the time step length  $\Delta t$  always corresponds to the length of the transport step length as determined automatically by MT3DMS. Thus, the number of time steps and the length of these will be variable for a simulation. Whereas the second option can significantly increase the computational load compared to the first option, operator splitting errors are reduced in this way.

For the computation of kinetic reactions PHREEQC-2 uses a 5<sup>th</sup> order integration scheme (Fehlberg, 1969) which, if a specified tolerance is not met for the error estimate of the integration, will automatically subdivide the user-defined time step length  $\Delta t$ . In that case, the user-defined time step will be numerically integrated over two or more subintervals, each of which is integrated with the 5<sup>th</sup> order integration scheme. Through this procedure the kinetic reactions are assured to be integrated accurately over  $\Delta t$ . Of course, an increased temporal splitting error will occur in the case of relatively large  $\Delta t$ .

In order to reduce computational load, a further optional modification of the 'standard' sequential split-operator technique was implemented in PHT3D. The modification allows the reaction step to be temporally omitted in cells where no reactive changes are expected. This modification exploits the fact that in many model applications there may exist zones, sometimes large, within the model domain where chemical gradients are negligible between neighbouring grid-cells and where the aqueous solution is in equilibrium with the mineral assemblage and the cation-exchange sites. In these zones the reaction term  $R_{reac}$  computed by PHREEQC-2 might be zero for significant portions of the total simulation time and thus the reaction step, in principle, can be omitted during these periods. A typical case where this applies is a steadily spreading point source contamination within an initially, chemically homogeneous, equilibrated multi-dimensional model domain, where in the early stages of the simulation geochemical changes occur in a very small portion of the aquifer. This concerns in particular cases where advection is the dominant transport mechanism. To decide whether the reaction step for the grid-cell in layer  $k$ , row  $i$  and column  $j$  can be omitted, the joint fulfillment of the two criteria (three-dimensional case):

$$\left| R_{reac_{k+a,i+a,j+a,n}} \right| < \epsilon_{aqu} \quad (2.3.4)$$

and

$$\left| R_{reac_{k+a,i+a,j+a,pH}} \right| < \epsilon_{pH} \quad (2.3.5)$$

$$\forall a \in \{-2, -1, 0, 1, 2\}$$

has been found to be an efficient test, where  $R_{\text{reac}_{k,i,j,n}}$  and  $R_{\text{reac}_{k,i,j,pH}}$  are the computed reaction term for the  $n^{\text{th}}$  component and computed pH change, respectively, in layer  $k$ , row  $i$  and column  $j$  and  $\epsilon_{\text{aqu}}$  and  $\epsilon_{\text{pH}}$  are user-defined criteria. The criteria (2.3.4) and (2.3.5) are tested for each grid-cell after a PHREEQC-2 reaction step. If both are fulfilled for a grid-cell, the execution of PHREEQC-2 (but not physical transport) is deactivated in this cell until it is reactivated during one of the subsequent reaction steps.

Reactivation occurs when either criterion (2.3.4) or (2.3.5) is not fulfilled, i.e., if reactive changes occur in neighbouring grid cells. Note, that (2.3.4) does not only include the directly adjacent cells but also cells that are two layers, two columns or two rows away. Grid-cells that receive external fluxes (e.g., through wells, rivers, recharge, ...) can not be deactivated and, furthermore, reaction simulations are always carried out for all grid-cells at the beginning of each new stress period, including the very first time step of the first stress period. For certain simulation problems, such as those where the initial aqueous solution and/or the inflow solution across model boundaries are not in equilibrium with the mineral assemblage and mineral reactions are kinetically controlled,  $r_{\text{reac}}$  might always be non-zero in most or all grid-cells.



## Model structure

### 3.1 Program design

In PHT3D v2.10 the coupling between MT3DMS and PHREEQC-2 is achieved by several new subroutines that enable the communication between the two programs and that call the appropriate PHREEQC functions to calculate the chemical transfers due to reactions. The MT3DMS code was used as the driver program, i.e., the main program. A package, called the PHREEQC-2 interface package (PHC), acts as the interface between MT3DMS and PHREEQC-2. The package is structured in the same way as other MT3DMS packages (e.g. advection, dispersion and reaction packages) and only small changes had to be made to the original MT3DMS source code. MT3DMS is written in Fortran 90 and PHREEQC-2 is written in the C programming language. The PHC package uses subroutines written in both Fortran 90 and C.

Despite the addition of those new subroutines, the original main model structures of both models, MT3DMS and PHREEQC-2 could be largely maintained. This bears the notable advantage that future, modified and improved versions of the two underlying models can be quickly implemented with a modest effort. In contrast to earlier PHT3D versions, all variables are kept in the computer's RAM. This ensures that data are transferred fast and efficiently between both codes. Both the original MT3DMS and PHREEQC data structures have been kept intact. This minimizes the amount of modifications needed for the coupling at the expense of increased memory usage.

Several subroutines have been written that are called during different stages of the execution of the MT3DMS main program loop (see figures 3.1 and 3.2). The subroutine *PHC1AL* allocates memory for the arrays used by the PHC package within MT3DMS. The subroutine *PHC1RP* initializes several variables and calls the function *MCRP*, which reads PHT3D specific input and prepares the input data for PHREEQC-2. It also calls the functions in PHREEQC-2 that calculate the initial composition of all solutions, phase assemblages, exchangers and surface. The subroutine *PHC1SS* ensures that for any solution defined through the MT3DMS SSM package, a speciation calculation in PHREEQC-2 is performed so that the amounts of `total_h` and `total_o` are known. The subroutine *PHC1RU* calls PHREEQC-2 to calculate the reactions for a reaction time step. It also determines if a cell must be activated or deactivated according to eqns. (2.3.4) and (2.3.5) in the subsequent reaction step. The subroutines *PHC1BD* calculates the contribution of chemical reaction transfers to the mass budget. Finally, the *PHC1OT*

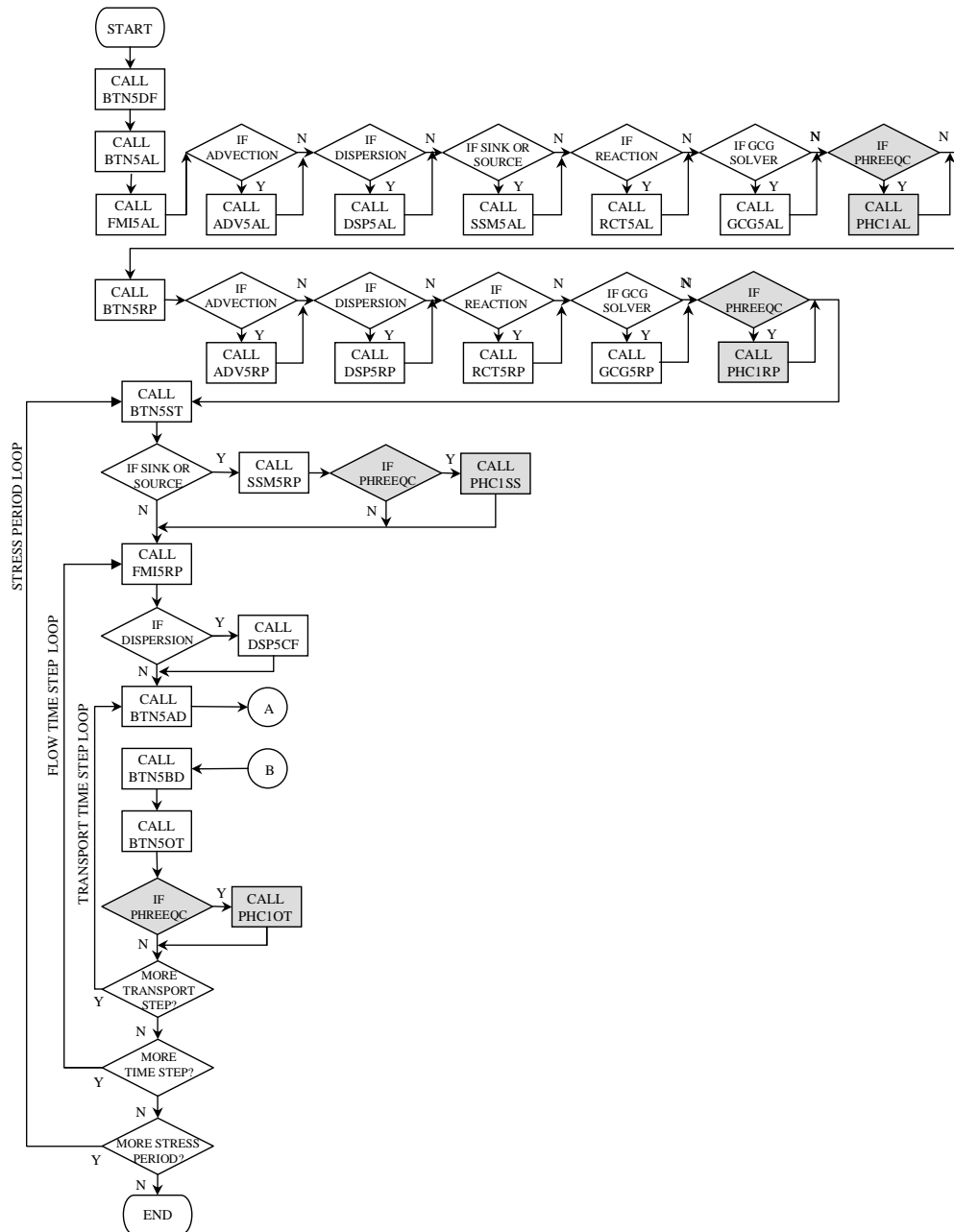


Figure 3.1: Flowchart for the main program of the PHT3D code (modified from (Zheng and Wang, 1999)). See the next page for the connections to and from A and B.

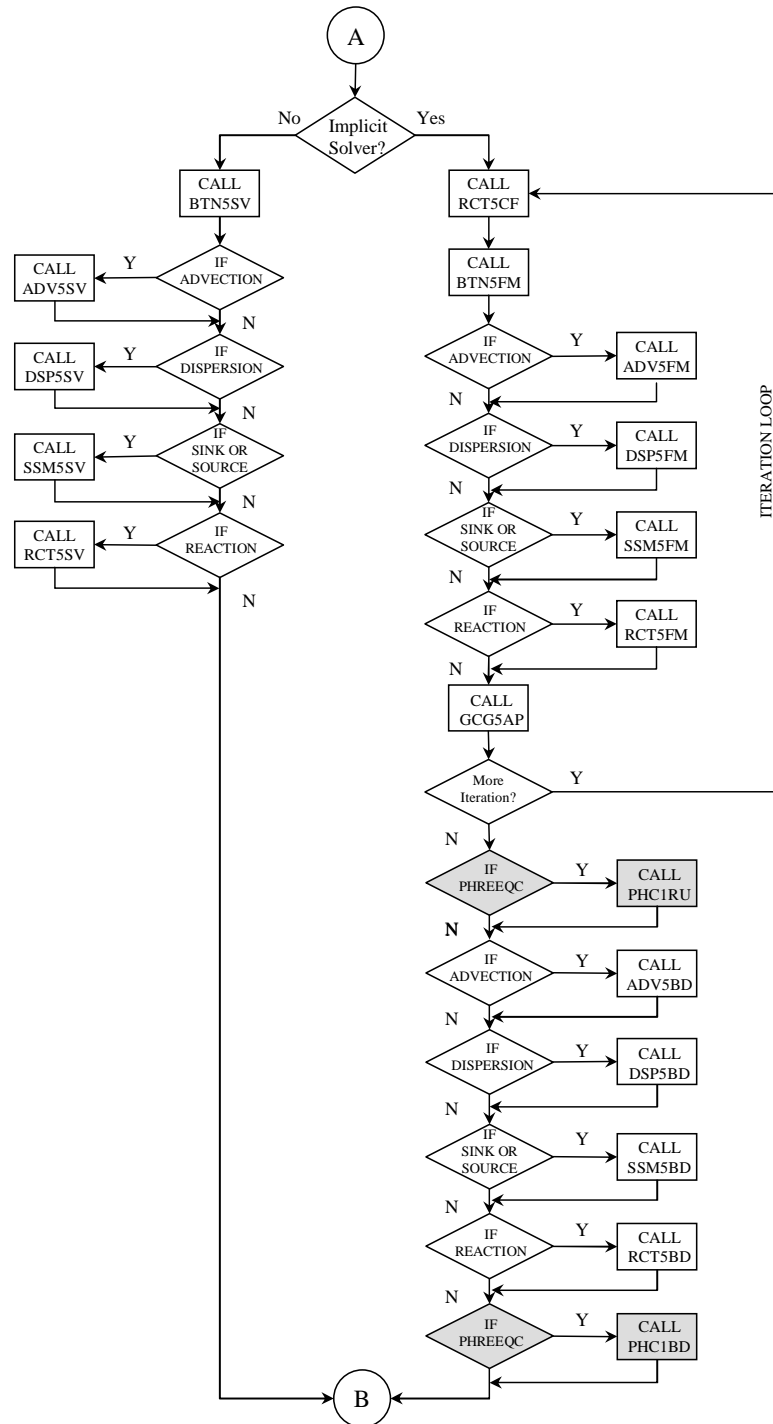


Figure 3.2: Flowchart for the main program of the PHT3D code (modified from (Zheng and Wang, 1999)). Continued from previous page.

routine controls the output that is written to unformatted binary (.UCN) and/or ASCII (.ACN) files.

### 3.2 Units

Units for time  $[T]$ , length  $[L]$  and mass  $[M]$  can be chosen freely in the original MT3DMS program and in the underlying MODFLOW program as long as they are used consistently throughout the data input. In contrast, time-dependent (kinetic) reactions in PHREEQC-2 need to be defined using *seconds* as time unit and the basic unit for concentration is *mol*. As a result of the combination of the two codes and for simplicity, concentration units in PHT3D can not be chosen freely in the present release. Concentrations of aqueous (mobile) chemicals need always to be provided in  $mol\ l_w^{-1}$  [ $M\ L^{-3}$ ] (with  $l_w$  referring to litre of pore water) while the model dimensions need to be defined in  $m$  [ $L$ ]. Mineral, exchanger and surface concentrations are defined in  $mol\ l_v^{-1}$  [ $M\ L^{-3}$ ] (with  $l_v$  referring to litre of bulk volume). It can be seen that some inconsistencies in the use of units (here length) are introduced to enable the use of more 'common' units, e.g.,  $mol\ l^{-1}$  instead of  $mol\ m^{-3}$ . All fixed units to be used for the data input for a PHT3D simulation are listed in Table 3.1.

Table 3.1: Units to be used for the data input of a PHT3D simulation

Concentrations of aqueous (mobile) chemicals	$mol\ l_w^{-1}$
Concentrations of other, user-defined immobile entities such as bacteria	$mol\ l_w^{-1}$
Concentrations of minerals	$mol\ l_v^{-1}$
Concentrations of exchangers and surfaces	$mol\ l_v^{-1}$

Time units can be used freely as in MODFLOW and MT3DMS. Care must be taken though that when kinetic reactions are included in the simulation, the appropriate value of **TUNIT** in the MT3DMS BTN file is selected. This ensures that the correct timestep length in seconds is passed on to PHREEQC. Also note that the user should carefully check that all kinetic rate parameters and expressions are consistent with the use of seconds as time units in PHREEQC.

### 3.3 Model output

The file PHT3D.OUT contains similar information as the standard formatted output file of the original MT3DMS program. This includes an overview of the

input files that were read, information on the progress of the simulation and summary mass balances.

Additionally, results of PHT3D simulations will be written to the UCN-files PHT3D001.UCN, ..., PHT3D**MCOMP**.UCN which contain the concentration results for all specified output times. The format of these files is identical to the format in the original MT3DMS package (binary files), which can be read by many existing pre/postprocessing packages. If the results are printed to ASCII files (\*.ACN), the format discussed in section 4.3 is used. The latter file-type might be used in conjunction with packages such as MATLAB<sup>®</sup>, Python or TECPLOT<sup>®</sup>.

The output to PHT3DXXX.MAS and PHT3DXXX.OBS files is the same as in MT3DMS. The mass balance information includes the mass transfers due to both transport and chemical reactions.

### 3.4 Temporal discretisation

The temporal discretisation procedure is largely based on the original time-stepping philosophy/strategy of MODFLOW/MT3DMS. This includes

- the user-defined subdivision of the total simulation time into periods of constant external stress parameters, so called **stress periods**
- the user-defined further subdivision of **stress periods** into **time steps**  $\Delta t$  in order to allow a sufficiently accurate approximation of transient processes
- the automatically invoked further subdivision of **time steps** into **transport steps** which satisfy the stability and/or accuracy constraints for the purely advective-dispersive transport.

As has been mentioned before (section 2.3), one PHREEQC-2 reaction step can be carried out for each **transport step** in PHT3D v2.10. This discretisation scheme is shown in Fig. 3.3a.

Alternatively, the integration of the reactive processes can be organised by using the user-defined time-step length  $\Delta t$  of the flow simulation as the time-step length for the reaction step. Therefore, kinetic reactions will be simulated and integrated over  $\Delta t$ , according to the temporal discretisation defined in the input files of both the MODFLOW basic flow package and the MT3DMS basic transport package. Only one reaction step is carried out per **time step**  $\Delta t$ , i.e., several transport steps might be carried out before a reaction step follows. The automatically selected **transport step** size can vary in dependence of the advection scheme used for a simulation (FD, TVD, ...) whereas the **reaction step** size (=

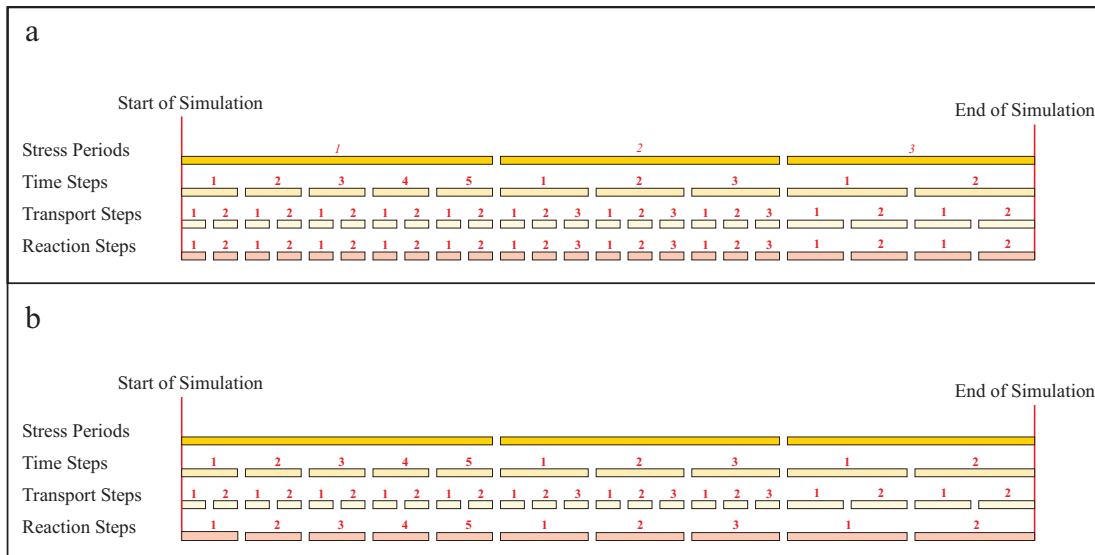


Figure 3.3: Temporal discretisation schemes in PHT3D

**time step** size) is not affected by the choice of the advection scheme/package. This discretisation scheme is shown in Fig. 3.3b.

Note that in the reporting of the mass balance, the mass transfers resulting from chemical reactions integrated over  $\Delta t$  are added to the transfers due to transport during the last **transport step**, which may have a duration that is smaller than  $\Delta t$ . Although mathematically this presents no problems, it is important to realize this from a conceptual point of view.

## Model input

### 4.1 PHT3D Input Files

As indicated before, the structure of the original MT3DMS model has been maintained largely. Therefore the format of existing MT3DMS model input data-files does not need any modifications. In PHT3D the data for the unmodified MT3DMS packages are read from the input files

- **pht3dbtn.dat** for the basic transport package
- **pht3dadv.dat** for the advection package input file
- **pht3ddsp.dat** for the dispersion package
- **pht3dssm.dat** for the source/sink mixing package
- **pht3dgcg.dat** for the GCG solver package
- **pht3drct.dat** for the original MT3DMS chemical reaction package

Older versions of PHT3D used a fixed naming convention as reflected by the file names above. Exactly like MT3DMS, PHT3D v2.10 reads the packages to be used and the corresponding names of the input files from a so-called name file (e.g., \*.NAM), thereby allowing flexibility in the names of the files. In addition to the above input files two additional files are needed for PHT3D, compared to a ‘standard’ MT3DMS simulation:

- **pht3d\_ph.dat** - a file that carries information about the number, names and types of chemicals included in a PHT3D simulation, reaction rate constants (and other reaction parameters) and
- **pht3d\_datab.dat** - a database file analogous to the original PHREEQC-2 database files

The input instructions for these two files is discussed in the next section.

Optionally, two additional files may be used by advanced users to control PHT3D input and simulations. These files have fixed names and are called **prefix.phrq** and **postfix.phrq**. The contents of these files should consist of PHREEQC-2 statements that are prefixed or appended to the PHREEQC-2 input file generated by PHT3D if both or either of these files are in the same directory as the PHT3D input files. Through this option, the user has access to less routinely used PHREEQC-2 capabilities for which the input can currently not be provided by the standard PHT3D input files.

## 4.2 Input instructions for the PHREEQC-2 database file

The input file **pht3d\_datab.dat** is essentially a PHREEQC-2 database file that defines both equilibrium and kinetic reactions. In the case of equilibrium reactions, all reaction parameters/constants must be included in this file while parameter values that are used in kinetic rate expressions can optionally be supplied outside the database file. The syntax for the definition of the reactions is identical with the original PHREEQC-2 syntax and as documented in the PHREEQC-2 manual by Parkhurst and Appelo (1999).

Before the creation of a 'new' user-defined reaction network for PHT3D is started, a basic knowledge of PHREEQC-2 must be obtained and, at least for more complex cases, it is strongly recommended to first test and debug reaction definitions in batch-mode, i.e., by setting up a PHREEQC-2 batch-type simulation.

The most important PHREEQC-2 keywords that might be used in PHT3D to create a reaction network are listed below, together with a brief description and examples. The full details for the keywords are given in the PHREEQC-2 manual.

**SOLUTION\_MASTER\_SPECIES** is the keyword that starts the data block

for the definition of aqueous master species, such as:

**Ca, Mg, Na, ...** i.e., elements that occur in only one redox state

**N(5), N(3), ..., S(6), S(-2), ...** i.e., elements that occur in multiple redox states

**Benzene, Tce, Tracer, ...** i.e., user-defined master species

For each **SOLUTION\_MASTER\_SPECIES** a line with the following entries is required:

**EL\_NAM** **MSPEC** **ALK** **GR\_FORM\_W** or **FORM** **GR\_FORM\_W\_EL**

**EL\_NAM** is the name of an element or element name followed by a valence state

**MSPEC** is the name/formula of an aqueous master species (including charge)

**ALK** is the alkalinity contribution

**GR\_FORM\_W** is the gram formula weight default value.

**FORM** is the chemical formula to calculate formula weight

**GR\_FORM\_W\_EL** is the gram formula weight for primary master species

**Example entries:**

Ca	Ca+2	0.0	Ca	40.08
Mg	Mg+2	0.0	Mg	24.312
Na	Na+	0.0	Na	22.9898
N	NO3-	0.0	N	14.0067
N(+5)	NO3-	0.0	N	
N(+3)	NO2-	0.0	N	
N(0)	N2	0.0	N	
N(-3)	NH4+	0.0	N	
Benzene	Benzene	0.0	Benzene	78.0
Tce	Tce	0.0	Tce	130.0
Tracer	Tracer	0.0	Tracer	1.0

**SOLUTION\_SPECIES** is the keyword that starts the data block for the definition of species, e.g.,  
**Na+, Cl-, Al+3, CO3-2, ...** identity reaction of "standard" master species  
**Benzene, Tce, Tracer, ...** identity reaction of user-defined master species  
**NaOH, NaCO3-, NaHCO3, ...** complexation products of master species

For each **SOLUTION\_SPECIES** the following entries are required:

**REAC** is the line describing the equilibrium association reaction  
**LOG\_K LOG\_K\_VAL** are the identifier and the Log K value at 25°C  
**DELTA\_H DELTA\_H\_VAL** are the identifier, the value and the unit, respectively, for the enthalpy of the reaction at 25°C  
**ANALYTICAL\_EXPRESSION A<sub>1</sub> A<sub>2</sub> A<sub>3</sub> A<sub>4</sub> A<sub>5</sub>** are the identifier and the 5 coefficients describing the temperature dependence of Log K  
**GAMMA DEBYE-HUECKEL\_A DEBYE-HUECKEL\_B** are the identifier for the use of the WATEQ activity equation and the two parameters used for its computation  
**NO\_CHECK** is an identifier that indicates that the reaction equation. It should not be checked for charge and elemental balance.  
**MOLE\_BALANCE FORMULA** is an identifier for the explicit definition of the stoichiometry of the species and the chemical formula to be used.

Example entries:

```

H+ = H+
log_k 0.000
-gamma 9.0000 0.0000
Ca+2 = Ca+2
log_k 0.000
-gamma 5.0000 0.1650
Tce = Tce
log_k 0.0
CO3-2 + H+ = HCO3-
log_k 10.329
delta_h -3.561 kcal
-analytic 107.8871 0.03252849 -5151.79 -38.92561
SO4-2 + 9 H+ + 8 e- = HS- + 4 H2O
log_k 33.65
delta_h -60.140 kcal
-gamma 3.5000 0.0000

```

**PHASES** for the definition of phases, e.g.,

Calcite, Fe(OH)<sub>3</sub>, Kaolinite, ...  
(Minerals)

For each of the **PHASES**  
the following entries are required:

**PHASE\_NAME** is the name of the phase

**REAC** is the line describing the (equilibrium) dissolution reaction

**LOG\_K LOG\_K\_VAL** are the identifier and the Log K value at 25°C

**DELTA\_H DELTA\_H\_VAL** are the identifier, the value and the unit,  
respectively, for the enthalpy of the reaction at 25°C

**ANALYTICAL\_EXPRESSION A<sub>1</sub> A<sub>2</sub> A<sub>3</sub> A<sub>4</sub> A<sub>5</sub>** are the identifier  
and the five coefficients describing the temperature dependence of Log K

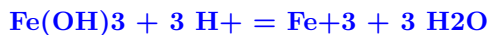
Example entries:

**Calcite**

log\_k -8.4789

delta\_h -2.297 kcal

-analytic -171.9065 -0.077993 2839.319 71.595

**Fe(OH)3(a)**

log\_k 4.891

**Kaolinite**

log\_k 7.435

delta\_h -35.300 kcal

**EXCHANGE\_MASTER\_SPECIES** for the definition of the exchange master species **X**

For the **EXCHANGE\_MASTER\_SPECIES**

a line with the following entries is required:

**EXCHANGE\_NAME EXCHANGE\_MASTER\_SPECIES** is the name of the exchange site and its chemical formula

The appropriate entry for the exchange master species needs to be:

**X X-**

**EXCHANGE\_SPECIES** for the definition of the

exchange species. The exchange species are complexes

between aqueous species and the exchange master species **X**,

i.e., the occupants of the exchanger.

For each **EXCHANGE\_SPECIES**

a line with the following entries is required:

**Example entries:**

**X- = X-**

```

log_k 0.0
Na+ + X- = NaX
log_k 0.0
-gamma 4.0 0.075
K+ + X- = KX
log_k 0.7
-gamma 3.5 0.015
delta_h -4.3
Li+ + X- = LiX
log_k -0.08
-gamma 6.0 0.0
delta_h 1.4

```

**RATES** for the definition of reaction rates.

The keyword **RATES** provides a powerful and easy way to define the rate expressions of kinetic reactions. For each rate expression a BASIC program consisting of a set of numbered BASIC statements must be written. Those statements will then be interpreted during PHREEQC-2 execution by a BASIC interpreter that is included as a subroutine within the PHREEQC-2 program (provided by David Gillespie, Synaptics, Inc., San Jose, CA).

Note, that in the present version of PHT3D, in contrast to the conventions in PHREEQC-2, the names of rate expressions need to be associated with either a **SOLUTION\_MASTER\_SPECIES** or a **PHASE**. If a rate is defined for a process, e.g., sulphate reduction, the introduction of a dummy **SOLUTION\_MASTER\_SPECIES** provides an easy, though slightly unelegant workaround.

For each kinetic expression entered into **RATES** a line with the following entries is required:

**NAME\_OF\_RATE\_EXPRESSION** is the name of a **SOLUTION\_MASTER\_SPECIES** or a **PHASE**

**START**, i.e., **-start** is an identifier that indicates the start of the BASIC program

**NUMBERED\_BASIC\_STATEMENT** are lines with BASIC instructions

**END**, i.e., **-end** is an identifier that indicates the end of the BASIC program

### 4.3 Input instructions for the PHREEQC-2 interface package file

The input data for this package, **pht3d\_ph.dat**, provide the necessary basic information required (i) to define which subset of the chemical entities defined in **pht3d\_datab.dat** participate in a reactive transport simulation, (ii) to allocate/link them to MT3DMS 1,...,**NCOMP** species/components (whereby the first **MCOMP** of them are mobile), and (iii) to optionally define the parameters of kinetically reacting chemicals.

Records PH1-PH8 are essential for all PHT3D simulations.

PH1 Record:

**OS TEMP ASBIN EPS\_AQU EPS\_PH**

**OS** is a flag for the operator-splitting scheme used:

1 = iterative operator-splitting scheme

2 = sequential operator-splitting scheme with reactions calculated after flow time steps only

3 = sequential operator-splitting scheme with reactions calculated after each transport step

**Note: In this release the first option is not implemented, only options 2 and 3 are available.**

**TEMP** is the temperature in °C used in chemical reactions for which a temperature dependence is defined in the database file. The default value is 25°C. Two options are available to specify the temperature. If a positive number is entered here, this value will be used as the temperature of all the cells in the model domain and for all the sources and sinks. If a negative integer number is entered, then the absolute value of this number refers to the species number that represents the temperature in a simulation that explicitly considers the transport of heat. This option is available in MT3DMS, readers are referred

to the supplemental documentation provided with MT3DMS to learn more about the usage of this option.

**ASBIN** is a flag that determines if ASCII output files (extension .ACN) that contain the computed concentrations for all grid-cells and for all output times that were defined in the BTN file. The concentrations contained herein are the same as those that are written to the MT3DMS unformatted concentration files, which are in binary format:

0 = Output to binary files only

1 = Output to both binary and ASCII files

**EPS\_AQU** is the PHREEQC-2 activation/deactivation criterion according to (2.3.4) as discussed in section 2.3. At the beginning of each reaction step, the PHC1RU subroutine checks for each cell by which amount the concentration of the mobile species have changed during the previous reaction step. If the change in a cell is smaller than **EPS\_AQU**, no reactions are calculated for that cell. In that way, the amount of computational effort can be limited because the time-consuming calls to PHREEQC-2 need not be made for all cells in the model domain. The user should always verify that the selected **EPS\_AQU** has negligible effect on the simulation outcome. If the value is set to 0, PHREEQC-2 will be executed for all grid-cells (except fixed concentration boundaries) in all reaction steps.

**EPS\_PH** is the PHREEQC-2 activation/deactivation criterion according to (2.3.5) as discussed in section 2.3. This value is only used when greater than zero and when **EPS\_AQU** is greater than zero.

PH2 Record:

**CB\_OFFSET** is a number that acts as a flag to indicate if the charge imbalance carried by a solution is to be transported. If **CB\_OFFSET** = 0, which is the recommended setting, then the charge imbalance is not transported. The user must take care in that case that all solutions in the simulation are charge balanced. If **CB\_OFFSET** > 0 then the charge imbalance of solutions is transported. This is achieved by adding **CB\_OFFSET** to the charge imbalance of all solution. The resulting values are used as the 'concentrations' in the transport equations to calculate the redistribution of the charge imbalance. Extreme care must be taken to use this option as the outcomes are highly-dependent on the advection scheme chosen and the numerical value of **CB\_OFFSET**.

PH3 Record:

**NR\_SOL\_MST\_SPEC\_EQU** (must be  $\geq 2$ )

**NR\_SOL\_MST\_SPEC\_EQU** defines the number of aqueous components that are assumed to be in chemical equilibrium and included in the simulation. **NR\_SOL\_MST\_SPEC\_EQU** must be  $\geq 2$  as pH and pe are included in all simulations. A transport simulation will be carried out for each of the included aqueous components, except for pH and pe, which are calculated from the mole balances of hydrogen and oxygen. If a component possibly occurs in different redox states, then there are two possible strategies:

- include all possible redox states as a separate component (e.g., S(6) and S(-2), Fe(2) and Fe(3), etc.). Note that in this case excluding a redox state of a component can potentially result in severe mass balance errors!
- include only the primary master species (e.g., Fe instead of both Fe(2) and Fe(3)). In practise the latter option is perhaps rather inconvenient as PHT3D will then during its UCN/ACN-type concentration output not discriminate between Fe(2) and Fe(3), but only provide results for Fe.

PH4 Record:

**NR\_MIN\_EQU**

**NR\_MIN\_EQU** defines the number of minerals included in the simulation and for which the local equilibrium assumption (LEA) is assumed to be valid. No transport step is carried out for minerals.

PH5 Record:

**NR\_ION\_EX**

**NR\_ION\_EX** defines the number of **EXCHANGE\_SPECIES** and/or **EXCHANGE\_MASTER\_SPECIES** for which cation-exchanging reactions with one or more exchangers should be considered.

PH6 Record:

**NR\_SURF**

**NR\_SURF** defines the number of surface master species.

PH7 Record:

**NR\_MOB\_KIN NR\_MIN\_KIN NR\_SURF\_KIN NR\_IMOB\_KIN**

**NR\_MOB\_KIN** defines the number of mobile reactants for which a rate expression is defined in the database-file **pht3d\_datab.dat** and the local equilibrium assumption is assumed to be invalid.

**NR\_MIN\_KIN** defines the number of minerals for which a rate expression is defined in the database-file **pht3d\_datab.dat** and the local equilibrium assumption is assumed to be invalid.

**NR\_SURF\_KIN** is reserved for kinetic surface-complexation reactions, which are not fully supported in this release. Therefore the input should be 0. If required, kinetic surface-complexation reactions can be defined via the **prefix.phrq** or the **postfix.phrq** files.

**NR\_IMOB\_KIN** defines the number of immobile reactants for which a rate expression is defined in the database-file **pht3d\_datab.dat** and the local equilibrium assumption is assumed to be invalid.

Example for the obligatory data blocks 1-7:

```
2 25 1E-10 0.001
0
4
0
2
0
5 0 0 1
```

The following data blocks need to be included optionally, depending on the data input for PH1-PH7.

PH8 Record:

If **NR\_MOB\_KIN** > 0

For each mobile kinetic reactant (1,...**NR\_MOB\_KIN**)

**NAME\_MOB\_KIN NR\_KIN\_PARM [M0]**

If **NR\_KIN\_PARM** > 0

**PARAMETER 1**

**PARAMETER 2**

**PARAMETER 3**

.....

**PARAMETER NR\_KIN\_PARM**

**FORMULA**

**NAME\_MOB\_KIN** defines the name of a mobile kinetic reactant.

**NR\_KIN\_PARM** defines the number of parameters needed by the kinetic rate expression that is defined in the database file **pht3d\_datab.dat** (using the PHREEQC-2 keyword **RATES**). Alternatively, the parameters can be defined directly in the database-file and **NR\_KIN\_PARM** is set to 0.

**M0** is an optional argument that defines the initial amount of the mobile kinetic reactant, expressed in moles. If no value is supplied, a default value of 1.0 moles is assumed.

**PARAMETER** is the numerical value of each of the **NR\_KIN\_PARM** parameters.

**FORMULA** is an equivalent to the PHREEQC-2 keyword and directly copied into the PHREEQC-2 input files: it defines the stoichiometric relationship between the computed change of mass of a kinetic reactant (for which the rate was defined by a **RATES** expression in the database-file **pht3d\_datab.dat**) and any other species/component that is included in this line together with its stoichiometric coefficient.

Example for **FORMULA**:

**-Formula Pce -1.0 H+ -1.0 Tce 1.0 Fe+2 1.0 Cl- 1.0**

For each mole computed by the rate defined for **NAME\_MOB\_KIN**, one mole of PCE (Perchloroethene), H<sup>+</sup> and Cl<sup>-</sup> will be irreversibly removed from the appropriate total mass of the reactant, as indicated by the negative stoichio-

metric factor (-1.0). On the other hand one mole of TCE (Trichloroethene) and Fe+2 will be produced. Note that in this way Fe<sup>2+</sup>, H<sup>+</sup> and Cl<sup>-</sup> are involved in kinetic reactions although they are not explicitly defined as kinetic reactants.

Example for data block 9:

```
Pce 2
1.0e-07
0.0001
-Formula Pce -1.0 H+ -1.0 Tce 1.0 Fe+2 1.0 Cl- 1.0
Tce 2
1.0e-08
0.0001
-Formula Tce -1.0 H+ -2.6 Dce 0.2 Ethe 0.8 Fe+2 2.6 Cl- 2.6
Dce 2
1.0e-07
0.0001
-Formula Dce -1.0 H+ -2.0 Ethe 1.0 Fe+2 2.0 Cl- 2.0
Ethe 2
1.0e-07
0.0001
-Formula Ethe -1.0 H+ 2.0 Etha 1.0
```

PH9 Record:

For all aqueous components 1,..., **NR\_SOL\_MST\_SPEC\_EQU** (remember **NR\_SOL\_MST\_SPEC\_EQU** must be  $\geq 2$ ) the names used and defined in the database files need to be listed here.

```
NAME_SOL_MST_SPEC_EQU 1 [ARG_SOL_MST_SPEC_EQU 1]
NAME_SOL_MST_SPEC_EQU 2 [ARG_SOL_MST_SPEC_EQU 2]
.....
pH [ARG_SOL_MST_SPEC_EQU NR_SOL_MST_SPEC_EQU - 1]
pe [ARG_SOL_MST_SPEC_EQU NR_SOL_MST_SPEC_EQU]
```

**ARG\_SOL\_MST\_SPEC\_EQU** is an optional argument that is passed to the PHREEQC-2 input file to take advantage of the numerous options in

PHREEQC to define concentration values. For example, the **charge** option can be invoked, or the option to calculate the input concentration of an element from equilibrium with a pure phase. See the PHREEQC-2 manual (under SOLUTION in the Description of data input section) for more details.

Example for data block 10 (**NR\_SOL\_MST\_SPEC\_EQU** = 8):

```
O(0)
C(4) CO2(g) -3.5 10
S(6)
S(-2)
Na
Cl charge
pH
pe
```

PH10 Record:

If **NR\_IMOB\_KIN** > 0

For each mobile kinetic reactant (1,...**NR\_IMOB\_KIN**)

**NAME\_IMOB\_KIN NR\_KIN\_PARM [M0]**

If **NR\_KIN\_PARM** > 0

**PARAMETER 1**

**PARAMETER 2**

**PARAMETER 3**

.....

**PARAMETER NR\_KIN\_PARM**

**FORMULA**

**NAME\_IMOB\_KIN** defines the name of an immobile kinetic reactant.

**NR\_KIN\_PARM** defines the number of parameters needed by the kinetic rate expression that is defined in the database file **pht3d\_datab.dat** (using the PHREEQC-2 keyword **RATES**). Alternatively, the parameters can be defined directly in the database-file and **NR\_KIN\_PARM** is set to 0.

**M0** is an optional argument that defines the initial amount of the immobile kinetic reactant, expressed in moles. If no value is supplied, a default value

of 1.0 moles is assumed.

**PARAMETER** is the numerical value of each of the **NR\_KIN\_PARM** parameters.

**FORMULA** is an equivalent to the PHREEQC-2 keyword and directly copied into the PHREEQC-2 input files: it defines the stoichiometric relationship between the computed change of mass of a kinetic reactant (for which the rate was defined by a **RATES** expression in the database-file **pht3d\_datab.dat**) and any other species/component that is included in this line together with its stoichiometric coefficient.

PH11 Record:

If **NR\_MIN\_EQU** > 0

**NAME\_MIN\_EQU 1 [SLMIN\_EQU 1]**

**NAME\_MIN\_EQU 2 [SLMIN\_EQU 2]**

.....

**NAME\_MIN\_EQU NR\_MIN\_EQU [SLMIN\_EQU NR\_MIN\_EQU]**

**NAME\_MIN\_EQU** has to be entered for each of the **NR\_MIN\_EQU** minerals that are included in a simulation. The mineral must be listed in the database-file **pht3d\_datab.dat** (**PHASES** keyword).

**SLMIN\_EQU** is an optional argument that can be entered for each of the **NR\_MIN\_EQU** minerals that are included in a simulation. This value represents the target Saturation Index (SI) for a pure phase in the aqueous phase. Example (**NAME\_MIN\_EQU = 3**) :

**Goethite**

**Pyrite**

**Fe(OH)3(a) -3.0**

PH12 Record:

If **NR\_ION\_EX** > 0

For each exchange master species or exchange species

**NAME\_EX 1 [STOICH 1] [NAME\_EMS 1]**

**NAME\_EX 2 [STOICH 2] [NAME\_EMS 2]**

.....

**NAME\_EX NR\_ION\_EX [STOICH NR\_ION\_EX] [NAME\_EMS NR\_ION\_EX]**

**NAME\_EX** has to be entered for each cation, exchange species or exchange master species to be included in the reaction network. If neither of the optional arguments **STOICH** or **NAME\_EMS** is defined, then the name defined here must be the name of an exchange species defined under the **EXCHANGE\_SPECIES** data block in the database-file **pht3d\_datab.dat**

**STOICH** is an optional argument that defines the stoichiometric coefficient of **NAME\_EMS** with the cation. For example, if the exchange master species is  $X^-$ , 2  $X^-$  are needed to balance  $Ca^{2+}$ . A negative value can be used to indicate that an exchange master species (defined through **NAME\_EX**) needs to be equilibrated with the solution that resides in the same cell as the exchange complex.

**NAME\_EMS** is an optional argument that defines the name of the exchange master species that forms part of the exchange species. Any name that is entered here must be defined under the **EXCHANGE\_MASTER\_SPECIES** data block in the database-file **pht3d\_datab.dat**. If no value is entered, it is assumed that the exchange master species is  $X^-$ .

Example for data block 13:

**CaX2**

**Na 1**

**Mg 2 X**

**Y -1**

In this example there are 2 exchangers, X and Y. The concentrations of species CaX2, NaX and MgX2 will be entered explicitly (by means of the initial concentrations specified in the BTN file), whereas the concentrations of the cations sorbed to Y will be calculated based on the composition of the water in the same cells as the exchanger. Note that the latter option has the advantage that the exchange composition does not have to be calculated

a priori (using PHREEQC for example). If, however, output of individual exchange species to UCN or ACN files is desired, this option can not be used and all exchange species have to be entered explicitly.

PH13 Record:

If **NR\_SURF** > 0

For surface master species

**NAME\_SURF 1 SURF\_AREA 1 MASS 1 [NAME 1] [SWITCH 1]**

**NAME\_SURF 2 SURF\_AREA 2 MASS 2 [NAME 2] [SWITCH 2]**

.....

**NAME\_SURF NR\_SURF [SURF\_AREA NR\_SURF] [MASS NR\_SURF]**

**[NAME NR\_SURF] [SWITCH NR\_SURF]**

**SURF\_CALC\_TYPE**

**NAME\_SURF** defines the name of a surface binding site or the surface binding site formula. PHREEQC-2 allows for various ways to define a surface, which are described in the PHREEQC-2 manual (under SURFACE in the Description of data input section).

**SURF\_AREA** defines the specific surface area of a surface, either in  $\text{m}^2/\text{g}$  (when the number of sites and mass of a surface are entered explicitly) or in  $\text{m}^2/\text{mol}$  (when the amount of surface sites is coupled to a pure phase or a kinetic reactant).

**MASS** defines the mass of solid and is used to calculate the surface area. Although a value must always be specified here, it is only used when the number of sites and mass are defined explicitly, i.e., when not coupled to a pure phase or kinetic reactant. In the latter case, the value entered here is ignored.

**NAME** is an optional argument to define a pure phase or kinetic reactant to which the surface binding site must be coupled. The number of moles of surface sites will be calculated from the number of moles of the phase/reactant.

**SWITCH** is an optional argument to define whether a pure phase is used (**SWITCH** = **equilibrium\_phase**) or a kinetic reactant (**SWITCH** = **kinetic\_reactant**). **SWITCH** only works in conjunction with **NAME**, that is, there is no need to specify it unless **NAME** is defined. If no value is specified the default is **equilibrium\_phase**.

**SURF\_CALC\_TYPE** is a line containing the information on which type of SCM calculation will be executed by PHREEQC. The most common options

include **-diffuse\_layer** and **-no\_edl**. An empty line indicates that none of the options is used.

Note that the number of sites or, when a surface is connected to a pure phase or kinetic reactant, the number of sites per mole, should be specified in the BTN file. Care should be taken when specifying the number of sites per mole in the case of the latter option is used because, by convention, PHT3D assumes that all the initial concentration values from the BTN file are expressed as moles per liter of bulk volume and hence divides these values by the porosity. Thus, when a surface is coupled to a pure phase or a kinetic reactant, the sites per mole that are entered through the BTN file must be multiplied by the porosity.

Here an example for data block 14.

```
Surfc_wOH 1e5 0.33 Fe(OH)3(a) equilibrium_phase  
-diffuse_layer
```

In this example a one surface (**Surfc\_wOH**) is defined and included as **SURFACE\_MASTER\_SPECIES**. **Surfc\_wOH** has a surface area (**SURF\_AREA**) of  $1 \times 10^{-5}$  and a **MASS** of 0.33. However, the latter value will not be used because the number of available sorption sites that is used in the simulation is instead dynamically linked to the simulated concentration of the mineral Fe(OH)3(a).

A second example, one in which electric double layer calculations are omitted, is:

```
S_aOH 0 0  
S_bOH 0 0  
S_cOH 0 0  
-no_edl
```

PH14 Record:

If **NR\_MIN\_KIN** > 0

For each mineral that is subject to a kinetic reaction:

**NAME\_MIN\_KIN NR\_KIN\_PARM**

If **NR\_KIN\_PARM** > 0

**PARAMETER 1**

**PARAMETER 2**

.....

**PARAMETER NR\_KIN\_PARM**

**NAME\_MIN\_KIN** defines the names of the **NR\_MIN\_KIN** minerals for which a kinetic rate expression describing precipitation and/or dissolution of this mineral is defined, and for which the local equilibrium assumption is not valid (or is expected not to be valid).

**NR\_KIN\_PARM** defines the number of parameters needed by the kinetic rate expressions that are defined in the database file **phtd3\_datab.dat** (using the PHREEQC-2 keyword **RATES**). Alternatively, the parameters can be defined directly in the database-file **pht3d\_datab.dat** and **NR\_KIN\_PARM** is set to 0.

**PARAMETER** is the numerical value of each of the **NR\_KIN\_PARM** parameters.

Example for data block 15:

**Siderite 1**

**1e-10**

**Fe(OH)3(a) 2**

**1**

**1e-09**

**Magnetite 2**

**1**

**1e-09**

## Benchmark problems and application examples

The following examples are meant to illustrate the use of PHT3D v2.10 for a range of reactive transport problems. Although the diversity of PHT3D model applications might become obvious in the following, it still only represents a fraction of the possibilities that arise from a PHREEQC-2 and MT3DMS-based model.

The examples discussed in this section were mostly selected from the peer-reviewed literature and thus simultaneously serve as benchmark problems for the evaluation of the numerical model. Generally, verification of reactive transport models by comparison with analytical solutions is limited to a few simple, often one-dimensional cases. Examples 1 and 7 represent such simulation problems. For more complex cases, the capability of the model to accurately approximate the governing equations needs to be verified by comparison with independently developed models. For the present version three new benchmark problems were included, both specifically evaluating the newly added surface complexation modelling capability and demonstrating modelling of isotope fractionation processes. As for any MT3DMS based model, the link file **mt3d.flo** (which is needed for the transport simulations) will be typically created by MODFLOW, as it has been the case in all of the examples described here. For most examples only a brief part is dedicated to describe the geochemistry and the dynamics of the geochemical changes. Users are encouraged to familiarise themselves with the simulation problems by studying the cited references. More examples are currently in preparation and will be added in updated versions of this document.

## 5.1 Example 1: Single Species Transport with Monod Kinetics

**5.1.1 Introduction** In this first example, the numerical solution obtained by PHT3D shall be compared with the analytical solution for a simple one-dimensional, purely advective transport coupled to kinetically controlled biodegradation. While obviously both transport and the reactive process in this exercise are very simple, it does include all the major steps that are involved in setting up a reactive transport model with PHT3D. The analytical solution was originally given by Parlange et al. (1984) as:

$$x = \frac{v_p}{v_{max}} [K \ln(\frac{C}{C_0}) + C_0 - C] \quad (5.1.1.1)$$

with

$$\frac{\partial C}{\partial x} = 0 \quad \text{at } x = 0, \quad (5.1.1.2)$$

where  $x$  is a length coordinate in a one-dimensional domain of the total length  $L$ ,  $C$  is the solute concentration and  $C_0$  is the concentration at the inflow boundary.  $K$ ,  $v_{max}$  and  $v_p$  are the half-saturation concentration, the maximum uptake rate and the pore-water velocity. For the comparison, a set of parameters that was previously used by Essaid and Bekins (1997) for the evaluation of the BIOMOC model was chosen (see Table 5.1).

For a PHT3D simulation of this particular problem, the input files

- **mt3d.flo**
- **pht3dbtn.dat**

Table 5.1: Parameters and chemical concentrations used in Example 1.

Flow simulation	steady state
Total simulation time ( <i>days</i> )	1826
Stress period	1
Time steps	200
Model length $L$ ( <i>m</i> )	150
Pore water velocity $v_p$ ( <i>m d</i> <sup>-1</sup> )	0.1
Porosity $n_e$	0.25
Dispersivity $\alpha_l$ ( <i>m</i> )	0
Maximum uptake rate $v_{max}$ <i>d</i> <sup>-1</sup>	$4.77 \times 10^{-3}$
Half-saturation concentration $K$ ( <i>mol L</i> <sub>w</sub> <sup>-1</sup> )	0.5
Inflow concentration (at $x = 0$ and for $t > 0$ ) ( <i>mol L</i> <sub>w</sub> <sup>-1</sup> )	1.0

- **pht3dadv.dat**
- **pht3dssm.dat**
- **pht3dgcg.dat**
- **pht3d\_datab.dat**
- **pht3d\_ph.dat**

need to be created. Only the latter two files are PHT3D-specific while all other files can be constructed by following the instructions in the MT3DMS manual. Consequently the contents of the non-PHT3D-specific files are not discussed here in great detail.

**5.1.2 Spatial discretisation and flow problem** In order to generate the one-dimensional flow field underlying the reactive transport problem a simple MODFLOW model needs to be set up. Of course, the desired pore-velocity of  $0.1 \text{ m d}^{-1}$  can be obtained through different combinations of boundary conditions and parameters. The subsequently described way represents only one of many different options. It is, however, a generally applicable way to rapidly generate a one-dimensional flow field of a particular pore-water velocity. A flow field comparable to the one used by Essaid and Bekins (1997) can be created by defining a domain of  $150 \text{ m}$  length,  $1 \text{ m}$  width and  $1 \text{ m}$  height which is then discretised into a model with 150 columns, 1 row and 1 layer. With a fixed head boundary at the downstream end (last column) and a given hydraulic conductivity, the desired pore-water velocity  $v_p$  can be obtained by placing an injection well into the first column. The flux in that well can be computed from:

$$Q_{well} = v_p n_e A \quad (5.1.2.1)$$

where  $Q_{well}$  is an injection rate for the well at the inflow boundary and  $A$  is the cross-sectional area of the model grid cell perpendicular to the flow direction, i.e.,  $1 \text{ m}^2$ . In **Example 1**,  $Q_{well}$  needs to be  $0.025 \text{ m}^3 \text{ d}^{-1}$ . Alternatively, if one chose to set  $n_e$  to 1,  $Q_{well}$  would be  $0.1 \text{ m}^3 \text{ d}^{-1}$ . Before a reactive transport simulation is set up in the next step, it is worthwhile to make sure that the simulated flow-field indeed agrees with the desired one. In the (likely) case that the MODFLOW model was set up with a preprocessing tool that offers a suite of other models, this can be either verified using a path-line-creating advective transport simulation or, alternatively, with a simple single-species transport simulation in which the breakthrough curve of a non-reactive chemical is used to evaluate the correct

travel times. To generate the flow-transport link file **mt3d.fl0**, which is needed by PHT3D, a MODFLOW version with an appropriate MT3D interface package needs to be used.

**5.1.3 Data input for the database file** To implement the kinetic biodegradation reaction for **Example 1**, the chemical reaction network needs to be prepared, i.e., the database-file **pht3d\_datab.dat** needs to be created or adapted. Although only a single species is involved in the present simulation problem, given the way PHREEQC-2 operates, the reaction network needs to include a basic set of **SOLUTION\_MASTER\_SPECIES** and **SOLUTION\_SPECIES**. The reactive species itself can be added to this basic set of equilibrium reactions. This involves the definition of the species

- as a component, i.e., as a **SOLUTION\_MASTER\_SPECIES**
- as a **SOLUTION\_SPECIES**, i.e., a complex of **SOLUTION\_MASTER\_SPECIES**.

The definition as a species is an identity reaction with  $\log_k = 0$ . In **Example 1** the name 'Species' was chosen for the reactive chemical. The choice for new names of chemicals must follow certain naming conventions, as outlined in the PHREEQC-2 manual. Finally, the rate expression for the kinetic biodegradation reaction must be defined in the form of BASIC instructions and added under the **RATES** keyword. Detailed instructions about the required syntax can also be found in the PHREEQC-2 manual. With the given set of instructions, kinetic reaction parameters can be either hard-coded into the rate expression or, alternatively, defined as parameter with the numeric value of the parameter provided in the file **pht3d\_ph.dat**.

Using the former option to include parameters, a minimal set of entries for the **pht3d\_datab.dat** file to simulate the reactive transport problem in **Example 1** is:

```
SOLUTION_MASTER_SPECIES
#
# element species alk gfw_formula element_gfw
#
```

H	H+	-1.	H	1.008
H(1)	H+	-1.	0.0	
E	e-	0.0	0.0	0.0
O	H2O	0.0	O	16.00
O(-2)	H2O	0.0	0.0	
Species	Species	0.0	Species	1.0

## SOLUTION\_SPECIES

H+ = H+

log\_k 0.0

e- = e-

log\_k 0.0

H2O = H2O

log\_k 0.0

Species = Species

log\_k 0.0

H2O = OH- + H+

log\_k -14.000

2 H2O = O2 + 4 H+ + 4 e-

log\_k -86.08

2 H+ + 2 e- = H2

log\_k -3.15

## RATES

Species

-start

10 mSpecies = tot("Species")

20 if (mSpecies &lt;= 1e-12) then goto 200

22 k\_mon = 0.5

24 v\_max = 4.77e-03 / 86400

30 rate = v\_max \* mSpecies / (k\_mon + mSpecies)

40 moles = rate \* time

50 if (moles &gt; m) then moles = m

200 SAVE moles

-end

END

The database file used for the simulation **Example 1** might include many more

chemicals. This has no effect on the result as long as **Species** and its rate expression is defined and as long as **Species** is not involved in other reactions. For example, **Species**, i.e., its entry into **SOLUTION\_MASTER\_SPECIES**, **SOLUTION\_SPECIES** and **RATES** could be simply added to the standard database file phreeqc.dat (which is distributed with PHREEQC-2) and the file renamed to **pht3d\_datab.dat**. As indicated before, the numeric values of parameters can also be defined in **pht3d\_ph.dat** rather than in the rate expression itself. A possible definition for the rate expression would then be:

```

RATES
Species
-start
10 mSpecies = tot("Species")
20 if (mSpecies <= 1e-12) then goto 200
22 k_mon = parm(1)
24 v_max = parm(2) / 86400
30 rate = v_max * mSpecies / (k_mon + mSpecies)
40 moles = rate * time
50 if (moles > m) then moles = m
200 SAVE moles
-end

```

**5.1.4 Data input for the PHREEQC interface package file** Based on a reaction network defined through the **pht3d\_datab.dat** file, the PHREEQC interface package file **pht3d\_ph.dat** needs to be set up. Essentially the information passed from this file to PHT3D is that there is one kinetically reacting mobile aqueous chemical of the name 'Species' and that the removal, i.e., biodegradation of 'Species' is linked to the computed rate for **Species** through a stoichiometric factor that is **-1.0**. The resulting entries into **pht3d\_ph.dat** for the case where hard-coded parameters were used in the rate expression for 'Species' are:

```

2 25 1 1E-10 .001 0
2
0
0 0
0
1 0 0 0
Species 0

```

**-formula Species -1.0**

**pH**

**pe**

For the alternative case, where parameters for  $k_{mon}$  and  $v_{max}$  were not hard-coded under **RATES**, the entries into **pht3d\_ph.dat** would be:

**2 25 1 1E-10 .001 0**

**2**

**0**

**0 0**

**0**

**1 0 0 0**

**Species 2**

**0.5**

**4.77e-03**

**-formula Species -1.0**

**pH**

**pe**

The **2** behind the name **Species** indicates that two numeric values for the parameters  $k_{mon}$  and  $v_{max}$  will follow in the proceeding two lines.

**5.1.5 Data input for the basic transport package file** The two above discussed files **pht3d\_datab.dat** and **pht3d\_ph.dat** define the reaction step. To activate their use i.e., the computation of concentration changes by PHREEQC-2, the sixth **TRNOP** entry for Record A5 needs to be set to **T** (= true) in the basic transport package file (**pht3dbtn.dat**). Furthermore, the entry for **NCOMP** needs to be 3 (for 'Species', 'pH', 'pe') and **MCOMP** needs to be 1 as only 'Species' is a mobile species/component. Apart from **TRNOP**, **NCOMP** and **MCOMP**, no further PHT3D-specific information is contained in the basic transport package file. The simulation time was set to 1826 days, divided into 200 time steps. After this time a steady state concentration profile has developed and the results can be compared with the analytical solution. The complete input for **pht3dbtn.dat** for **Example 1** becomes (note that the number of spaces between data entries are not shown exactly as required by the formatted input for this file):

**Example 1**

**Parlange et al (1984)**

**1 1 150 1 3 1**

**T L M**

```

T F T F T T
0
0 1 -1 A7. DELR(NCOL)
0 1 -1 A8. DELC(NROW)
0 1 -1 A9. HTOP(NCOL,NROW); Top of the first layer
0 1 -1 A10. Thickness of layer 1
0 1 -1 A11. Effective porosity of layer 1
0 1 -1 A12. ICBUND matrix of Layer 1
0 1 -1 A13. Start. conc. in layer 1 for spec. # 1 Species
0 0 0 A13. Start. conc. in layer 1 for spec. # 2 pH
0 0 0 A13. Start. conc. in layer 1 for spec. # 3 pe
1E+30 .05
0 0 0 0 T
1
1826
0 1
T 1
1826 200 1
0 50000 1 0

```

**5.1.6 Data input for the advection package file** No PHT3D-specific data input is required for **pht3dadv.dat**. The file entries for **pht3dadv.dat**, assuming the TVD scheme is used, are:

```
-1 .75 5000 0
```

**5.1.7 Data input for the source/sink mixing package file** The concentrations of mobile components need to be defined at any external source such as single injection wells, or for recharge water. In **Example 1**, the concentration of **Species** needs to be defined for the well in the first grid-cell which represents the upstream inflow boundary. The concentration of all immobile species remains 0. For **Example 1** the file **pht3dssm.dat** requires the following entries:

```

T F F F F F
2002

```

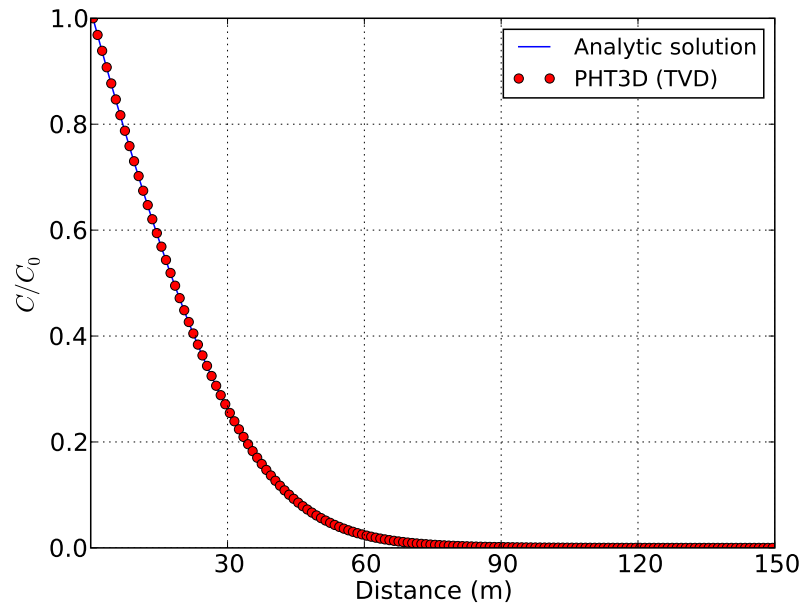


Figure 5.1: Single-species transport with Monod-type biodegradation.

1

1 1 1 0 2 1 7.0 4.0

**5.1.8 Simulation results** As can be seen in Figure 5.1, the numerical solution shows a very good agreement with the analytical solution developed by Parlange et al. (1984).

## 5.2 Example 2: Transport and mineral precipitation/dissolution

**5.2.1 Introduction** The simulation of mineral dissolution and precipitation reactions is one of the key features of PHT3D and one or more of them will be included in many typical model applications. The case described by **Example 2** was originally presented by Engesgaard and Kipp (1992) for a model verification of their MST1D code against the CHEMTRNS model by Noorishad et al. (1987). It involves a one-dimensional model domain in which an aqueous water composition that is in equilibrium with two minerals, calcite and dolomite, is successively replaced, i.e., flushed by water of a different chemical composition, leading to multiple precipitation-dissolution fronts. Dolomite is not present initially but is formed temporally.

**5.2.2 Spatial discretisation and flow problem** The flow simulation for the second reactive transport problem can be carried out in analogy to the previous example. In order to follow the discretisation chosen by Engesgaard and Kipp (1992), a model domain of 0.5  $m$  length is divided into 50 grid cells of 0.01  $m$  length, 1  $m$  width and 1  $m$  height (50 columns, 1 row and 1 layer). The total simulation time is 0.2430 days. It is divided into 210 time steps. A steady-state flow rate  $Q_{well}$  of  $0.259 m^3 d^{-1}$  is required to achieve a pore-velocity of  $0.083 m d^{-1}$  for the given porosity of 0.32. A summary of the parameters that define the flow field and non-reactive transport is given in Table 5.2.

**5.2.3 Data input for the database file** All of the aqueous species, components and minerals needed to simulate this LEA-based reactive transport problem are already included in the original PHREEQC-2 database. Thus, the file

Table 5.2: Flow and transport parameters used in Example 2.

Flow simulation	steady state
Total simulation time ( <i>days</i> )	0.24305
Stress period	1
Time steps	210
Grid spacing ( <i>m</i> )	0.01
Model length ( <i>m</i> )	0.50
Pore velocity ( <i>m d</i> <sup>-1</sup> )	0.083
Porosity	0.32
Dispersivity ( <i>m</i> )	0.0067

**pht3d\_datab.dat** could easily be created by copying the original PHREEQC-2 database file **Phreeqc.dat** and renaming it to **pht3d\_datab.dat**. However, the set of reactions would then not be identical with the one used for the solution published by Engesgaard and Kipp (1992). They have used a subset of the reaction network that is employed if the original PHREEQC-2 database is used. In both cases transport steps are carried out for the **SOLUTION\_MASTER\_SPECIES** Ca, C(4), Cl and Mg. If the original PHREEQC-2 database is used, the number of aqueous species is 21, whereas it is 15 for the subset employed by Engesgaard and Kipp (1992). Below are the entries for the database file that defines the reactions considered by Engesgaard and Kipp (1992).

#### SOLUTION\_MASTER\_SPECIES

```
#
# element species alk gfw_formula element_gfw
#
H      H+      -1.  H      1.008
H(1)   H+      -1.  0.0
E      e-      0.0  0.0    0.0
O      H2O     0.0  O      16.00
O(-2)  H2O     0.0  0.0
Ca     Ca+2    0.0  Ca     40.08
Mg     Mg+2    0.0  Mg     24.312
Cl     Cl-     0.0  Cl     35.453
C      CO3-2  2.0  HCO3   12.0111
C(+4)  CO3-2  2.0  HCO3
```

#### SOLUTION\_SPECIES

```
H+ = H+
  log_k 0.000
  -gamma 9.0000 0.0000
e- = e-
  log_k 0.000
H2O = H2O
  log_k 0.000
2 H+ + 2 e- = H2
  log_k -3.15
  delta_h -1.759
2 H2O = O2 + 4 H+ + 4 e-
  log_k -86.08
```

delta\_h 134.79 kcal

Ca+2 = Ca+2

log\_k 0.000

-gamma 5.0000 0.1650

Mg+2 = Mg+2

log\_k 0.000

-gamma 5.5000 0.2000

Cl- = Cl-

log\_k 0.000

-gamma 3.5000 0.0150

CO3-2 = CO3-2

log\_k 0.000

-gamma 5.4000 0.0000

H2O = OH- + H+

log\_k -14.010

delta\_h 13.362 kcal

-analytic -283.971 -0.05069842 13323.0 102.24447 -1119669.0

-gamma 3.5000 0.0000

CO3-2 + H+ = HCO3-

log\_k 10.31

delta\_h -3.561 kcal

-analytic 107.8871 0.03252849 -5151.79 -38.92561 563713.9

-gamma 5.4000 0.0000

CO3-2 + 2 H+ = CO2 + H2O

log\_k 16.71

delta\_h -5.738 kcal

-analytic 464.1965 0.09344813 -26986.16 -165.75951 2248628.9

Ca+2 + CO3-2 = CaCO3

log\_k 3.23

delta\_h 3.545 kcal

-analytic -1228.732 -0.299440 35512.75 485.818

Mg+2 + CO3-2 = MgCO3

log\_k 2.98

delta\_h 2.713 kcal

-analytic 0.9910 0.00667

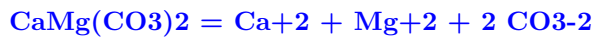
PHASES

**Calcite**

log\_k -8.470

delta\_h -2.297 kcal

-analytic -171.9065 -0.077993 2839.319 71.595

**Dolomite**

log\_k -17.170

delta\_h -9.436 kcal

**END**

**5.2.4 Data input for the PHREEQC interface package file** The file **pht3d\_ph.dat** contains the records which define that the reaction network contains 6 equilibrium aqueous components (including pH and pe) and two equilibrium minerals. The order in which the components are listed determines which species number will be allocated to each entity included in the simulation. For each of the first **MCOMP-2** (C(4)), Ca, Mg, Cl) of the **NCOMP** components advective-dispersive transport steps will be simulated by the appropriate MT3DMS routines. For component numbers **MCOMP-1** (pH) and **MCOMP** (pe) no transport step is carried out. Instead, pH and pe are computed from the balance for H and O during the reaction step.

Note that the present simulation problem does not involve redox changes. The entities **MCOMP+1,...,NCOMP** (here Calcite and Dolomite) are immobile and no transport simulation will be carried out for them.

The resulting input for **pht3d\_ph.dat** in **Example 2** is:

2 25 1 0 0

0

6

2

0 0

0

0 0 0 0

C(4)

Ca

Mg

Cl

pH

pe

Calcite

Dolomite

**5.2.5 Data input for the basic transport package file** The basic transport package file **pht3dbtn.dat** contains, among other information, the starting, i.e., initial concentrations (see Tables 5.3 and 5.4) for each of the **NCOMP** entities that are handled by the MT3DMS part of the simulator. Aqueous concentrations are always defined in units of  $mol L^{-1}$ .

**Note, that the unit for the initial concentrations of minerals is NOT mass per volume of water, i.e.,  $mol L^{-1}$ , but is defined as mass per bulk volume, i.e.,  $mol L_{volume}^{-1}$ .**

Engesgaard and Kipp (1992) defined their mineral concentrations as mass per mass of soil, i.e.,  $mol kg_{soil}^{-1}$  and provided the bulk density ( $1800 kg m^{-3}$ ) of the soil. Therefore, their initial concentrations for calcite of  $2.176 \times 10^{-5} mol kg_{soil}^{-1}$  translates to  $3.906 \times 10^{-5} mol l_{volume}^{-1}$ , which needs to be used in PHT3D.

If a simulation problem is a pure equilibrium problem, as the one here in **Example 2**, it is adequate that the initial water composition is in chemical equilibrium. If the aqueous solution is not in equilibrium, equilibrium conditions will be adjusted within the first reaction step at the end of the first time step. The file also contains the information about the number of stress periods, their length and the number of time steps (thus also the number of PHREEQC-2 steps) into which each stress period is subdivided. The entries for the basic transport package file for **Example 2** are:

**Example 2****Engesgaard and Kipp (1992)****1 1 50 1 8 4****T L M****T T T F T T****0****0 0.01 -1 A7. DELR(NCOL)**

```

0 1 -1 A8. DELC(NROW)
0 1 -1 A9. HTOP(NCOL,NROW); Top of the first layer
0 1 -1 A10. Thickness of layer 1
0 0.32 -1 A11. Effective porosity of layer 1
0 1 -1 A12. ICBUND matrix of Layer 1
0 1.227e-04 -1 A13. Start. conc. in layer 1 for spec. # 1 C(4)
0 1.227e-04 -1 A13. Start. conc. in layer 1 for spec. # 2 Ca
0 0 0 A13. Start. conc. in layer 1 for spec. # 3 Mg
0 0 0 A13. Start. conc. in layer 1 for spec. # 4 Cl
0 9.907196 -1 A13. Start. conc. in layer 1 for spec. # 5 pH
0 4 -1 A13. Start. conc. in layer 1 for spec. # 6 pe
0 3.906E-05 -1 A13. Start. conc. in layer 1 for spec. # 7 Calcite
0 0 0 A13. Start. conc. in layer 1 for spec. # 8 Dolomite
1E+30 .05
0 0 0 0 T
0
0 1
T 1
.243055 210 1
0 50000 1 0

```

The order of the component concentrations must follow the order that is pre-defined in **pht3d\_ph.dat**.

Table 5.3: Aqueous concentrations used in Example 2.

Aqueous component	$C_{init}$ ( $mol L_w^{-1}$ )	$C_{inflow}$ ( $mol L_w^{-1}$ )
pH	9.91	7.0
pe	4.00	4.0
C(4)	$1.23 \times 10^{-4}$	0.0
Ca	$1.23 \times 10^{-4}$	0.0
Mg	0.0	$1.0 \times 10^{-3}$
Cl	0.0	$2.0 \times 10^{-3}$

**5.2.6 Data input for the advection package file** The file entries for **pht3dadv.dat**, assuming the TVD scheme is used, are:

-1 .75 5000 0

**5.2.7 Data input for the dispersion package file** A dispersivity of 0.0067  $m$  was used by Engesgaard and Kipp (1992). The data input for the dispersion package **pht3ddsp.dat** file is thus:

0 .0067(20G14.0) -1 C1. Longit. disp. of layer 1  
 0 0.1(1G14.0) -1 C2. TRPT=(horiz. transv. disp.) / (Longit. disp.)  
 0 0.1(1G14.0) -1 C3. TRPV=(vert. transv. disp.) / (Longit. disp.)  
 0 0(1G14.0) -1 C4. effective molecular diffusion coefficient [ $L^2/T$ ]

**5.2.8 Data input for the source/sink mixing package file** The inlet (inflow) water composition is defined by providing the component concentrations for the injection well located at the first cell. In **Example 2**, the inlet water contains 0.001  $mol L^{-1}$  of Mg and 0.002  $mol L^{-1}$  of Cl. In contrast to the initial water composition, no C(4) and no Ca is contained in the inflow water.

T F F F F F  
 2002  
 1  
 1 1 1 0 2 0 0 .001 .002 7.0 4.0 0 0

**5.2.9 Simulation results** As can be seen in Figure 5.2, the numerical solution obtained by PHT3D, the concentration profiles after 21000  $s$  (0.2403 *days*), of most aqueous components and minerals agrees closely with the one given by Engesgaard and Kipp (1992). In particular, the positions of the mineral fronts

Table 5.4: Mineral concentrations used in Example 2.

Mineral	$C_{init}$ ( $mol L_v^{-1}$ )
Calcite ( $CaCO_3$ )	$3.906 \times 10^{-5}$
Dolomite ( $CaMg(CO_3)_2$ )	0.0

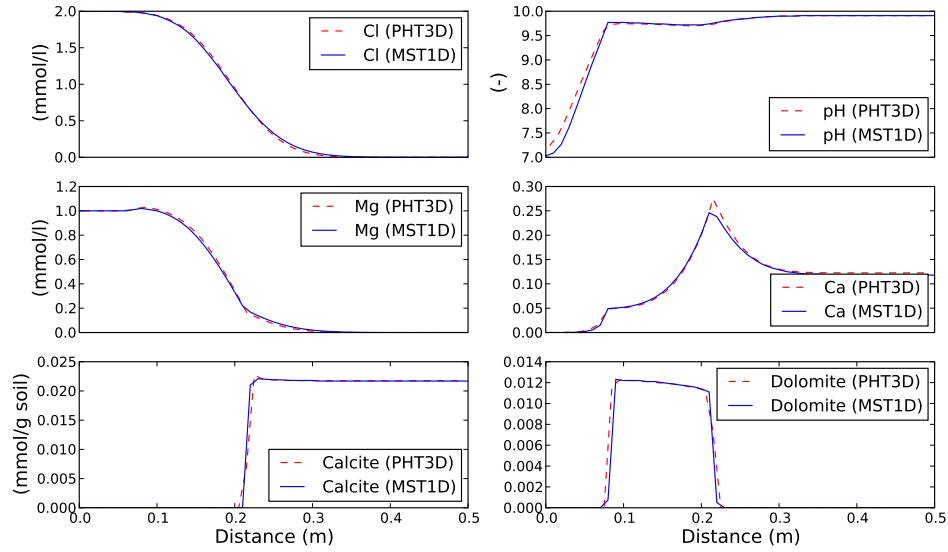


Figure 5.2: Simulation results for PHT3D and MST1D: Aqueous and mineral concentrations after 21000 s.

agree very well, whereas the PHT3D-simulated pH near the inflow end of the model domain lies slightly above the pH simulated by MST1D.

### 5.3 Example 3: Migration of precipitation/dissolution fronts

**5.3.1 Introduction** The third test problem is a one-dimensional, purely inorganic redox problem that was first presented by Walter et al. (1994). It was subsequently used as a benchmark problem by Guerin and Zheng (1998). It demonstrates the evolution of some important geochemical processes that occur when acidic mine tailings leach into an anaerobic carbonate aquifer. Aqueous complexation and dissolution/precipitation are all considered as equilibrium reactions. If the reaction network defined by Walter et al. (1994) is used, the simulation includes 17 aqueous components, 15 of which are transported, 54 aqueous species and six minerals. The initial and inflow source/sink concentrations are shown in Table 5.6 for the aqueous components, while the initial concentrations of the minerals are given in Table 5.7. The parameters describing the model domain and physical transport parameters are listed in Table 5.5.

**5.3.2 Spatial discretisation and flow problem** The MODFLOW model underlying the reactive transport problem can be generated in a similar fashion to the one described for **Example 1**. Following the spatial discretisation chosen by Walter et al. (1994), the model of 0.4  $m$  length is divided into 80 grid cells of 0.005  $m$  length and a cross-sectional area of 1  $m^2$  (80 columns, 1 row and 1 layer). The pore-velocity in the present problem is 0.02  $m d^{-1}$  and the porosity is 0.35. For an arbitrarily chosen conductivity of 1  $m d^{-1}$ , the appropriate flow rate  $Q_{well}$  at the upstream inflow boundary cell becomes then 0.007  $m^3 d^{-1}$ . As in the previous examples a fixed head boundary is assigned to the the downstream boundary.

**5.3.3 Data input for the database file** The present simulation problem, like the previous example, contains only components, species and minerals that are defined in the original PHREEQC-2 database file **Phreeqc.dat**. Again, the input file **pht3d\_datab.dat** could be simply created by copying it from **Phreeqc.dat**.

Table 5.5: Flow and transport parameters used in Example 3.

Grid spacing ( $m$ )	0.05
Model length ( $m$ )	0.40
Pore velocity ( $m d^{-1}$ )	0.02
Porosity	0.35
Dispersivity ( $m$ )	0.005

However, in order to define and reproduce the results presented by Walter et al. (1994) as closely as possible, some minor modifications of the database file are required, including the modification of equilibrium constants and the removal of some aqueous complexation reactions, i.e., species.

**5.3.4 Data input for the PHREEQC interface package file** The number of aqueous components (**NR\_INORG\_COMP\_EQU** = 14) and minerals (**NR\_MIN\_EQU** = 6) that form the reaction network in this particular problem and the names of these components and minerals need to be defined in the PHT3D-specific file **pht3d\_ph.dat** according to the input instructions given in Chapter 3. The present problem includes four elements, **C**, **S**, **Fe** and **Mn**, which could occur in multiple redox-states. Generally, in such a case, it is recommended to include all possible valence states of those elements, i.e., **C(4)/C(-4)**, **C(6)/C(-2)**, **Fe(2)/Fe(3)** and **Mn(2)/Mn(3)**, respectively. However, if an element is not initially present in a particular valence state and it can be foreseen that it will definitively not be produced during the course of the simulation, it might not be included in the simulation. In the present example (**Example 3**), this has been done for **S(-6)** and **C(-4)**. The order at which the first 14 aqueous components are listed is free except for pH and pe, which have to be the last 2 aqueous components, then followed by the 6 minerals. Again, the order of the minerals can be freely chosen by the user. However, the defined order of both aqueous components and minerals must correspond with the order used in **pht3dbtn.dat** and in **pht3dssm.dat**.

```

2 25 1 0 0
0
14
6
0 0 0 0 0 0
0
0 0 0 0
C(4)
S(6)
Fe(2)
Fe(3)
Mn(2)
Ca
Mg

```

Na  
 K  
 Cl  
 Al  
 Si  
 pH  
 pe  
 Calcite  
 Siderite  
 Gibbsite  
 Fe(OH)<sub>3</sub>(a)  
 Gypsum  
 SiO<sub>2</sub>(a)

**5.3.5 Data input for the basic transport package file** The basic transport package file **pht3dbtn.dat** contains, besides information regarding the model geometry and the temporal discretisation, the starting concentrations for all aqueous components and minerals (in MT3DMS all equally termed species). As mentioned above, the order at which the concentrations are entered must comply with the definition in **pht3d\_ph.dat**. The initial concentrations of the aqueous components and minerals to be entered into **pht3dbtn.dat**, and as given by Walter et al. (1994), are listed in Tables 5.6 and 5.7. The data input for the file **pht3dbtn.dat** for the simulation of Example 3 is:

### Example 3

Walter et al (1994)

1 1 80 1 20 12

T L M

T T T F T T

0

0 0.005(20G14.0) -1 A7. DELR(NCOL)

0 1(1G14.0) -1 A8. DELC(NROW)

0 1(20G14.0) -1 A9. HTOP(NCOL,NROW); Top of the first layer

0 1(20G14.0) -1 A10. Thickness of layer 1

0 .35(20G14.0) -1 A11. Effective porosity of layer 1

0 1(20I3) -1 A12. ICBUND matrix of Layer 1

0 .00394(20G14.0) -1 A13. Start. conc. in layer 1 for spec. # 1 C(4)

Table 5.6: Aqueous concentrations used in Example 3.

Aqueous component	$C_{init}$ ( $mol L_w^{-1}$ )	$C_{inflow}$ ( $mol L_w^{-1}$ )
pH	6.96	3.99
pe	1.67	7.69
C(4)	$3.94 \times 10^{-3}$	$4.92 \times 10^{-4}$
S(6)	$7.48 \times 10^{-3}$	$5.00 \times 10^{-2}$
S(-2)	-	-
Fe(2)	$5.39 \times 10^{-5}$	$3.06 \times 10^{-2}$
Fe(3)	$2.32 \times 10^{-8}$	$1.99 \times 10^{-7}$
Mn(2)	$4.73 \times 10^{-5}$	$9.83 \times 10^{-6}$
Ca	$6.92 \times 10^{-3}$	$1.08 \times 10^{-2}$
Mg	$1.96 \times 10^{-3}$	$9.69 \times 10^{-4}$
Na	$1.30 \times 10^{-3}$	$1.39 \times 10^{-3}$
K	$6.65 \times 10^{-5}$	$7.93 \times 10^{-4}$
Cl	$1.03 \times 10^{-3}$	$1.19 \times 10^{-4}$
Al	$1.27 \times 10^{-7}$	$4.30 \times 10^{-3}$
Si	$1.94 \times 10^{-3}$	$2.08 \times 10^{-3}$

Table 5.7: Mineral concentrations used in Example 3.

Mineral	$C_{init}$ ( $mol L_v^{-1}$ )
Calcite ( $CaCO_3$ )	$1.95 \times 10^{-2}$
Siderite ( $FeCO_3$ )	$4.22 \times 10^{-3}$
Gibbsite ( $Al(OH)_3$ )	$2.51 \times 10^{-3}$
amorphous $Fe(OH)_3$	$1.86 \times 10^{-3}$
Gypsum ( $CaSO_4 \cdot 2H_2O$ )	0.0
amorphous $SiO_2$	$4.07 \times 10^{-1}$

```

0 .00692(20G14.0) -1 A13. Start. conc. in layer 1 for spec. # 2 Ca
0 .00103(20G14.0) -1 A13. Start. conc. in layer 1 for spec. # 3 Cl
0 .00196(20G14.0) -1 A13. Start. conc. in layer 1 for spec. # 4 Mg
0 .00130(20G14.0) -1 A13. Start. conc. in layer 1 for spec. # 5 Na
0 .0000665(20G14.0) -1 A13. Start. conc. in layer 1 for spec. # 6 K
0 .0000539(20G14.0) -1 A13. Start. conc. in layer 1 for spec. # 7 Fe(2)
0 2.32E-08(20G14.0) -1 A13. Start. conc. in layer 1 for spec. # 8 Fe(3)
0 .0000473(20G14.0) -1 A13. Start. conc. in layer 1 for spec. # 9 Mn(2)
0 1.27E-07(20G14.0) -1 A13. Start. conc. in layer 1 for spec. # 10 Al
0 .00194(20G14.0) -1 A13. Start. conc. in layer 1 for spec. # 11 Si
0 .00748(20G14.0) -1 A13. Start. conc. in layer 1 for spec. # 12 S(6)
0 6.96(20G14.0) -1 A13. Start. conc. in layer 1 for spec. # 13 pH
0 1.67(20G14.0) -1 A13. Start. conc. in layer 1 for spec. # 14 pe
0 .0063(20G14.0) -1 A13. Start. conc. in layer 1 for spec. # 15 Calcite
0 .0018161(20G14.0) -1 A13. Start. conc. in layer 1 for spec. # 16 Siderite
0 0(20G14.0) -1 A13. Start. conc. in layer 1 for spec. # 17 Gypsum
0 .14245(20G14.0) -1 A13. Start. conc. in layer 1 for spec. # 18 SiO2(a)
0 .0008812(20G14.0) -1 A13. Start. conc. in layer 1 for spec. # 19 Gibbsite
0 .000651(20G14.0) -1 A13. Start. conc. in layer 1 for spec. # 20 Fe(OH)3(a)
1E+30 .05
0 0 0 0 T
3
6 12 24
0 1
T 1
24 192 1
0 50000 1 0

```

As mentioned previously, the only PHT3D-specific information included in the above input data set is contained in line 4, where the PHREEQC reaction step is activated (**T T T F F T** instead of **T T T F F F**), requiring the existence and appropriate data input in **pht3d\_ph.dat**.

**5.3.6 Data input for the advection package file** The data input needed for the advective transport simulation are provided by **pht3dadv.dat**. As already shown for the previous examples, if the MMOC advection scheme is applied the file entries are:

```
2 .1 100000 0
```

3 .5

1 0 15

**5.3.7 Data input for the dispersion package file** The longitudinal dispersivity, as given by Walter et al. (1994), is entered into the **pht3ddsp.dat** file:

```
0 0.005(20G14.0) -1 C1. Longitudinal disp. of layer 1
0 0.1(1G14.0) -1 C2. TRPT=(horiz. transv. disp.) / (Longit. disp.)
0 0.1(1G14.0) -1 C3. TRPV=(vert. transv. disp.) / (Longit. disp.)
0 0(1G14.0) -1 C4. effective molecular diffusion coefficient [ $L^2/T$ ]
```

Note, that the file also includes information about transverse dispersion, which in the present, one-dimensional case is not used for the computation of the results.

**5.3.8 Data input for the source/sink mixing package file** The data input of the **pht3dssm.dat** file defines the concentration for each of the mobile chemicals (termed species in MT3DMS). Source concentrations of immobile chemicals and for the mobile aqueous components **pH** and **pe** need to be set to 0. Like in **pht3dbtn.dat** the order at which concentrations are entered must comply with the definition from **pht3d\_ph.dat**. The equilibrated water composition of the acidic inflow water, as listed in Table 5.6, forms the base for the following data input of the **pht3dssm.dat** file:

T F F F F F

2002

1

```
1 1 1 0 2 .000492 .0108 .000119 .000969 .00139 .000793 .0306 1.99E-07 ... same line
... 9.83E-06 .0043 .00208 .05 3.99 7.69 0 0 0 0 0
```

**5.3.9 Simulation results** Only a few aspects of the geochemical evolution observed in the model simulation are described in the following. For a detailed description see Walter et al. (1994).

As shown in Figure 5.3, the acidic inflow solution is initially buffered by calcite ( $CaCO_3$ ), maintaining the  $pH$  at an almost neutral level (6.5 - 7). In this zone, gypsum ( $CaSO_4 \cdot 2H_2O$ ) is formed from calcium released during calcite dissolution and sulphate ( $S(6)$ ) from the inflow solution ( $C_{in,S(6)} > C_{backgr,S(6)}$ ). Similarly, siderite ( $FeCO_3$ ) can form from  $C(4)$  ( $CO_3$ ) released during dissolution

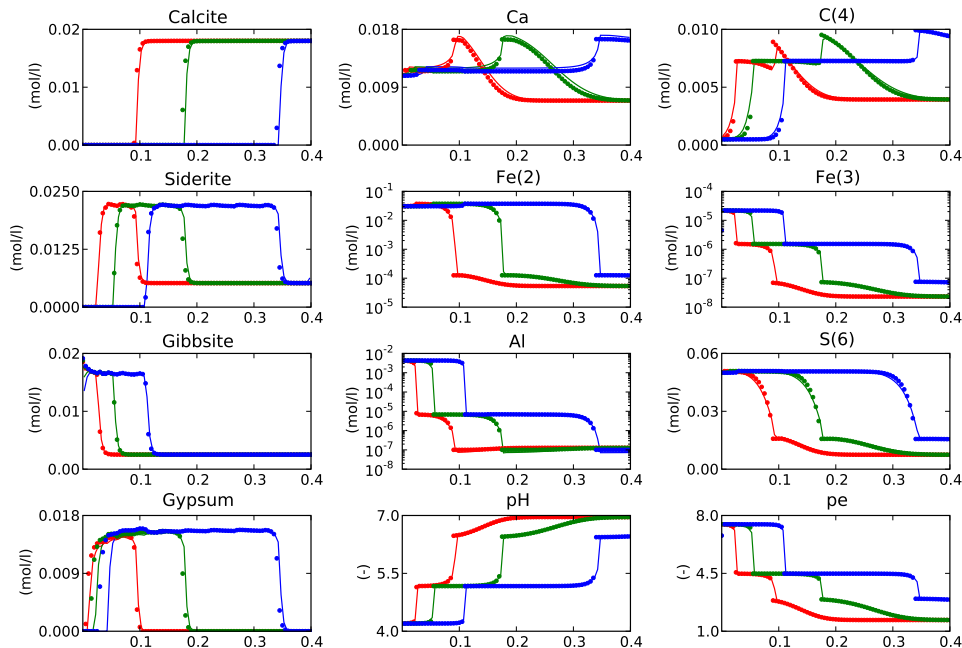


Figure 5.3: Selected aqueous component and mineral concentrations for PHT3D (solid lines) and MINTRAN (dotted lines) at  $t = 6, 12$  and  $24$  days.

and the  $Fe(2)$ -rich inflow solution. At locations where calcite is completely dissolved, siderite becomes the buffering mineral, dissolving until it is also entirely removed. Finally, gibbsite ( $Al(OH)_3$ ) precipitation is the buffer mechanism at locations where both calcite and siderite are completely removed. The three different buffering mechanisms lead to three distinct levels of  $pH$ , with sharp fronts in between. As for  $pe$ , three distinct levels evolve with fronts from more reduced to more oxidised water. The fronts have the same positions as those in the  $pH$  plot. As the  $pe$  of the solution is completely controlled by the redox couple  $Fe(2)/Fe(3)$ , the  $pe$  changes reflect the changes in their concentration ratio. Both  $Fe(2)$  and  $Fe(3)$  concentrations are strongly controlled by the  $pH$  of the solution. Generally, their solubility increases with a decreasing  $pH$ . However, as the increase of their solubilities is not proportional, the  $Fe(2)/Fe(3)$  ratio can change and so does the  $pe$ .

Simulation results of PHT3D in comparison with the finite-element model MINTRAN (Walter et al., 1994) are shown in Figure 5.3 for concentrations of selected components and minerals after 6, 12 and 24 days. The modelling results for both models are derived from simulations in sequential operator-splitting mode.

As can be seen, the models compare very well. The remaining differences are most likely due to small differences in the databases of the geochemical equilibrium models used.

## 5.4 Example 4: Cation exchange - flushing of a sodium-potassium nitrate solution with calcium chloride

**5.4.1 Introduction** This modelling example is the first among several examples that include and demonstrate ion-exchanging reactions in flow-through systems. The example was originally used as PHREEQM (Nienhuis et al., 1994) test case, and is also included in the PHREEQC-2 documentation (Parkhurst and Appelo, 1999) as Example 11. Further discussion can be found in (Appelo and Postma, 1993), where it forms Example 10.13, and in (Appelo, 1994). The one-dimensional simulation problem describes a hypothetical column experiment where porewater containing sodium ( $Na^+$ ), potassium ( $K^+$ ) and nitrate ( $NO_3^-$ ) in equilibrium with exchangeable cations is flushed by a calcium chloride ( $CaCl_2$ ) solution.

**5.4.2 Spatial discretisation and flow problem** The underlying flow model can be set up comparably to the previous one-dimensional examples with an upstream inflow boundary, e.g., an injection well, and a fixed head boundary at the downstream end of the column. The length of the column is 0.08 *m*. It is discretised into 40 grid-cells of 0.002 *m* length, following the "refined" run described in Appelo and Postma (1993).

Table 5.8: Flow and transport parameters used in Example 4.

Flow simulation	steady state
Total simulation time ( <i>days</i> )	0.24
Stress period	1
Time steps	120
Grid spacing ( <i>m</i> )	0.002
Model length ( <i>m</i> )	0.08
Pore velocity ( <i>m d</i> <sup>-1</sup> )	1.0
Porosity	1.0
Dispersivity ( <i>m</i> )	0.002

To obtain a cross-sectional area of 1 *m*<sup>2</sup>, the aquifer bottom can be set to an elevation of 0 *m*, the top to 1 *m* and the width of the row to 1 *m*. With a porosity of 1.0, a hydraulic conductivity of 1.0 *m d*<sup>-1</sup> and a flux of 1 *m*<sup>3</sup> *d*<sup>-1</sup> at the upstream boundary, the time for one pore volume to pass through the column would be 0.08 *d*. All relevant features of the cation breakthrough curves can be

captured with a total simulation time of 0.24 *d* (or 3 pore volumes). The essential parameters used in the flow simulation for **Example 4** are listed in Table 5.8.

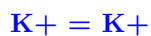
**5.4.3 Data input for the database file** Either the contents of the original PHREEQC-2 database file or a consistent subset, such as the one given below, can be used to define the relevant chemicals and reactions in **pht3d\_datab.dat** that are involved in this problem.

#### SOLUTION\_MASTER\_SPECIES

```
#
# element species alk gfw_formula element_gfw
#
H      H+      -1.  H      1.008
H(0)   H2       0.0  H
H(1)   H+       -1.  0.0
E      e-       0.0  0.0  0.0
O      H2O     0.0  O      16.00
O(0)   O2       0.0  O
O(-2)  H2O     0.0  0.0          IIII
Ca     Ca+2    0.0  Ca     40.08
Na     Na+     0.0  Na    22.9898
K      K+      0.0  K     39.102
Cl     Cl-     0.0  Cl    35.453
N      NO3-   0.0  N     14.0067
N(+5) NO3-     0.0  N
```

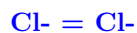
#### SOLUTION\_SPECIES

```
H+ = H+
  log_k 0.000
  -gamma 9.0000 0.0000
e- = e-
  log_k 0.000
H2O = H2O
  log_k 0.000
Ca+2 = Ca+2
  log_k 0.000
  -gamma 5.0000 0.1650
Na+ = Na+
  log_k 0.000
  -gamma 4.0000 0.0750
```



log\_k 0.000

-gamma 3.5000 0.0150



log\_k 0.000

-gamma 3.5000 0.0150



log\_k 0.000

-gamma 3.0000 0.0000



log\_k -14.000

delta\_h 13.362 kcal

-analytic -283.971 -0.05069842 13323.0 102.24447 -1119669.0 -gamma 3.5000



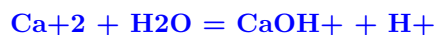
log\_k -86.08

delta\_h 134.79 kcal



log\_k -3.15

delta\_h -1.759



log\_k -12.780



log\_k -14.180



log\_k -14.460

## PHASES



$\text{O}_2 = \text{O}_2$

log\_k -2.960

delta\_h -1.844 kcal



$\text{H}_2 = \text{H}_2$

log\_k -3.150

delta\_h -1.759 kcal

## EXCHANGE\_MASTER\_SPECIES

```

X X-
EXCHANGE_SPECIES
X- = X-
    log_k 0.0
Na+ + X- = NaX
    log_k 0.0
K+ + X- = KX
    log_k 0.7
    -gamma 3.5 0.015
    delta_h -4.3 # Jardine & Sparks, 1984
Ca+2 + 2X- = CaX2
    log_k 0.8
    -gamma 5.0 0.165
    delta_h 7.2 # Van Bladel & Gheyl, 1980
END

```

**5.4.4 Data input for the PHREEQC interface package file** The interface package file for this example carries the information that (i) in total 7 aqueous components (all assumed to be in chemical equilibrium) are included in the simulation and (ii) exchange reactions occur for the three cations. Remember that care must be taken that all cations that are included as aqueous components and for which an exchange reaction is defined in the database file **pht3d\_datab.dat** must be included here (see also Chapter 3). The input data set for **Example 4** is:

```

2 25.0 1 0 0
0
7
0
3 0
0
0 0 0 0
Ca
Cl
K
Na
N(5)

```

pH  
 pe  
 Ca 2  
 Na 1  
 K 1

**5.4.5 Data input for the basic transport package file** Most parts of the relevant data input of the **pht3dbtn.dat** file can be constructed as explained for the previous examples, with appropriate adaptations to the geometry selected for this example. As described by Appelo and Postma (1993) and by Parkhurst and Appelo (1999), the water that is initially present in the column contains the two cations potassium (*K*) and sodium (*Na*) as well as chloride and nitrate. *K* and *Na* are also initially present as exchangeable cations, i.e., sorbed to sediments. The actual concentration which represents equilibrium conditions with the given aqueous phase (dissolved) concentrations depends on the cation exchange capacity (CEC) of the sediments and can be determined through a simple PHREEQC batch-simulation. Note, that the CEC itself is not defined explicitly within PHT3D. The equilibrated initial aqueous concentrations as well as the appropriate initial exchanger compositions are listed in Tables 5.9 and 5.10, respectively. Based on this information, the **pht3dbtn.dat** file might look as follows:

**Example 4**

Appelo (1993,1994), Parkhurst and Appelo (1999)

1 1 40 1 10 5

Table 5.9: Aqueous concentrations used in Example 4.

Aqueous component	$C_{init}$ ( $mol L_w^{-1}$ )	$C_{inflow}$ ( $mol L_w^{-1}$ )
pH	7.0	7.0
pe	12.5	12.5
Ca	0	$0.6 \times 10^{-3}$
Cl	0	$1.2 \times 10^{-3}$
K	$2.0 \times 10^{-4}$	0
Na	$1.0 \times 10^{-3}$	0
N(5)	$1.2 \times 10^{-3}$	0

Table 5.10: Initial exchanger concentrations used in Example 4.

	$C_{init}$ ( $mol L^{-1w}$ )
Ca-X2	0
Na-X	$5.493 \times 10^{-4}$
K-X	$5.507 \times 10^{-4}$

```

T L M
T T T F T T
0
0 0.002(20G14.0) -1 A7. DELR(NCOL)
0 1(1G14.0) -1 A8. DELC(NROW)
0 1(20G14.0) -1 A9. HTOP(NCOL,NROW); Top of the first layer
0 1(20G14.0) -1 A10. Thickness of layer 1
0 1(20G14.0) -1 A11. Effective porosity of layer 1
0 1(20I3) -1 A12. ICBUND matrix of Layer 1
0 0 0 A13. Start. conc. in layer 1 for spec. # 1 Ca
0 0 0 A13. Start. conc. in layer 1 for spec. # 2 Cl
100 .0002(20G14.0) -1 A13. Start. conc. in layer 1 for spec. # 3 K
100 .001(20G14.0) -1 A13. Start. conc. in layer 1 for spec. # 4 Na
100 .0012(20G14.0) -1 A13. Start. conc. in layer 1 for spec. # 5 N(5)
100 7(20G14.0) -1 A13. Start. conc. in layer 1 for spec. # 6 pH
0 12.5 0 A13. Start. conc. in layer 1 for spec. # 7 pe
0 0 0 A13. Start. conc. in layer 1 for spec. # 8 Ca_ex
100 .0005493(20G14.0) -1 A13. Start. conc. in layer 1 for spec. # 9 Na_ex
100 .0005507(20G14.0) -1 A13. Start. conc. in layer 1 for spec. # 10 K_ex
1E+30 .05
0 0 0 0 T
201
0 .0012 .0024 .0036 .0048 .006 .0072 .0084
.0096 .0108 .012 .0132 .0144 .0156 .0168 .018
...
... (timesteps for which concentrations are printed to PHT3D...UCN files)
...
.2304004 .2316004 .2328004 .2340004 .2352004 .2364004 .2376004 .2388005

```

```
.24
0 1
T 1
.24 120 1
0 50000 1 0
```

**5.4.6 Data input for the advection package file** The TVD scheme was used in this modelling example, defined by the following data input for the **pht3dadv.dat** file:

```
-1 .75 100000 0
```

**5.4.7 Data input for the dispersion package file** As shown in Parkhurst and Appelo (1999), the inclusion of dispersive transport might change significantly the shape of the cation breakthrough curves, compared to the solution for purely advective transport with reactions. While in the advection-only case no data file **pht3ddsp.dat** is required, for the advection-dispersion-reaction case described in Parkhurst and Appelo (1999), using a longitudinal dispersivity of 0.002 *m*, the following input is required:

```
0 0.002(20G14.0) -1 C1. Longitudinal disp. of layer 1
0 0.1(1G14.0) -1 C2. TRPT=(horiz. transv. disp.) / (Longit. disp.)
0 0.1(1G14.0) -1 C3. TRPV=(vert. transv. disp.) / (Longit. disp.)
0 0(1G14.0) -1 C4. effective molecular diffusion coefficient [ $L^2/T$ ]
```

**5.4.8 Data input for the source sink/mixing package file** The water that resides initially in the model column is flushed with a  $CaCl_2$  solution (see Table 5.9). The input data needed to define this inlet water composition are:

```
T F F F F F
2002
1
1 1 1 0 2 .0006 .0012 0 0 0 7.0 12.5 0 0 0
```

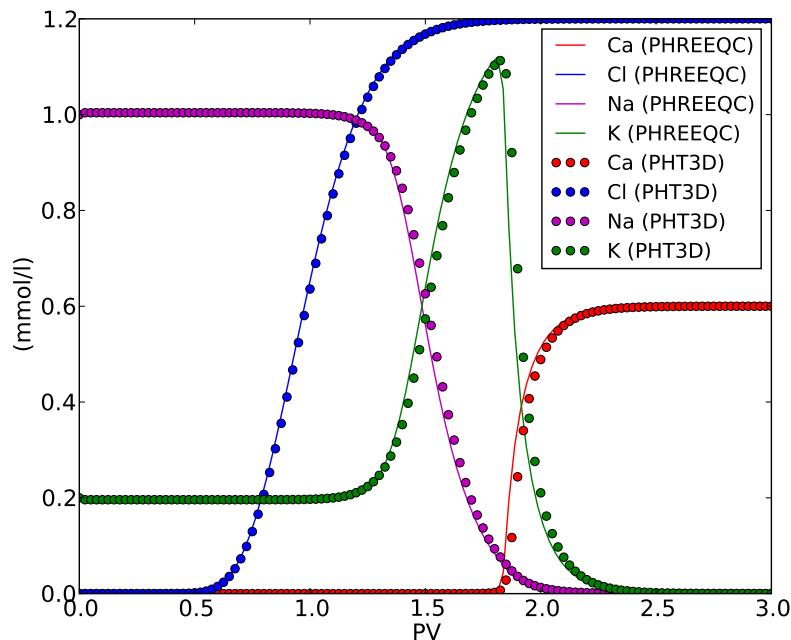


Figure 5.4: Comparison of simulated cation concentrations.

**5.4.9 Simulation results** Resulting from the inflow of the  $CaCl_2$  solution, sorbed potassium and sodium ions are successively replaced by calcium, starting at the inflow end. Per definition, the breakthrough concentrations of the non-reactive chloride increases from the initial concentration ( $0 \text{ mmol}$ ) to  $1 \text{ mmol}$  (inflow concentration) after around one pore-volume. In contrast, the elution of calcium is retarded and takes significantly longer due to the exchange-reactions. Calcium from the inflow solution first replaces exchangeable sodium and, thereafter, potassium. The PHT3D simulation results are shown in Figure 5.4 in comparison with the results obtained from a PHREEQC-2 simulation. As stated in the introduction to this example, more detailed discussions of the results of this particular test case can be found in, e.g., Appelo and Postma (1993); Parkhurst (1995); Parkhurst and Appelo (1999). A very good, more general discussion on multi-component ion exchange and, e.g., the resulting chromatographic effects, can be found in Appelo (1996).

## 5.5 Example 5: Cation exchange during artificial recharge

**5.5.1 Introduction** This example, as the previous one, serves to evaluate the PHT3D model's capability of correctly handling cation-exchange reactions. The case, including field observations and modelling, was originally published by Valocchi et al. (1981). Since then it has served as a benchmark problem for several other models (Appelo and Postma, 1993; Walter et al., 1994; Zysset, 1993). The modelling problem describes a field injection experiment where freshwater (pre-treated municipal effluent) was injected into an alluvial brackish aquifer in the Palo Alto Baylands region. It involves non-reactive transport of chloride and the transport of three exchangeable heterovalent cations ( $Mg^{2+}$ ,  $Ca^{2+}$ ,  $Na^{+}$ ) undergoing surface reactions.

**5.5.2 Spatial discretisation and flow problem** As described in more detail by Valocchi et al. (1981), the injection of the municipal effluent water at a rate of approximately  $21 \text{ m}^3\text{h}^{-1}$  created an essentially two-dimensional, radial flow-field around the injection point *I1*. Valocchi et al. (1981) simulated the resulting advective-dispersive transport using a modified (Valocchi, 1980) one-dimensional model based on a solution provided by Rubin and James (1973). Zysset (1993) derived the relevant effective parameters of flow velocity and longitudinal dispersivity by fitting the analytical, one-dimensional model of van Genuchten (1980) to the observed breakthrough curve for chloride ( $Cl^{-}$ ) at the borehole *S23*, located in  $16 \text{ m}$  distance from the injection point. Zysset (1993) so found an average flow velocity of  $27.024 \text{ m d}^{-1}$  and a longitudinal dispersivity  $\alpha_l$  of  $1.737 \text{ m}$ . These values, which differ from the ones given by Valocchi et al. (1981), were used in the current example. To simulate the breakthrough curves of the cations at borehole *S23*, the flow path between *I1* and *S23*, i.e., a one-dimensional model of  $16 \text{ m}$  length, can be discretised into 16 grid-cells of equal length and water added through a well to the first grid-cell at the inflow boundary at a rate of

$$27.024 \text{ m d}^{-1} \times 0.35 \text{ (porosity)} = 9.458 \text{ m}^{-3} \text{ d}^{-1} \quad (5.5.2.1)$$

to produce the flow velocity as determined by Zysset (1993).

**5.5.3 Data input for the database file** The simulation problem involves two types of waters, the initially present brackish water type with high sodium and magnesium concentrations, and the injected fresh water which is dominated by sodium and calcium (Appelo, 1996). A reaction network that is suitable for this problem can be built based on the one for the previous **Example 4**. However, the aqueous components  $Mg$ ,  $C(4)$  and  $O(0)$  have been included whereas  $K$  has now

Table 5.11: Flow and transport parameters used in Example 5.

Flow simulation	steady state
Total simulation time ( <i>days</i> )	83.33
Stress period	1
Time steps	120
Grid spacing ( <i>m</i> )	1.0
Model length ( <i>m</i> )	16.0
Pore velocity ( <i>m d</i> <sup>-1</sup> )	27.024
Porosity	0.35
Dispersivity ( <i>m</i> )	1.737

been removed, compared to the previous example. Similarly, exchange reactions for  $Mg - X2$  have now been included whereas  $KX$  was removed.

**5.5.4 Data input for the PHREEQC interface package file** The reaction network of this example includes 8 aqueous components, two of them are  $pH$  and  $pe$ , and 3 immobile exchange species (cations), all in chemical equilibrium with each other.

```

2 25.0 1 0 0
0
8
0
3 0
0
0 0 0 0
O(0)
C(4)
Ca
Cl
Na
Mg
pH
pe
Ca 2
Na 1

```

Table 5.12: Aqueous concentrations used in Example 5.

Aqueous component	$C_{init}$ ( $mol L_w^{-1}$ )	$C_{inflow}$ ( $mol L_w^{-1}$ )
pH	7.286	
pe	-1.555	
C(4)	$2.588 \times 10^{-3}$	$3.610 \times 10^{-3}$
Ca	$1.120 \times 10^{-1}$	$2.130 \times 10^{-3}$
Na	$8.650 \times 10^{-2}$	$1.466 \times 10^{-2}$
Mg	$1.820 \times 10^{-2}$	$9.400 \times 10^{-3}$
Cl	$1.600 \times 10^{-1}$	$5.000 \times 10^{-4}$

Table 5.13: Initial exchanger concentrations used in Example 5.

	$C_{init}$ ( $mol L_w^{-1}$ )
Ca-X2	$1.526 \times 10^{-1}$
Na-X	$1.593 \times 10^{-1}$
Mg-X2	$1.427 \times 10^{-1}$

**Mg 2**

**5.5.5 Data input for the basic transport package file** The initial brackish water composition is defined in the file **pht3dbtn.dat** and is listed in Table 5.12. Like in the previous case, a batch PHREEQC-2 simulation can be used to determine the initial exchanger composition for the given cation exchange capacity of  $750 meq l^{-1}$  of this silty sand aquifer.

**Example 5****Valocchi et al (1981)****1 1 17 1 11 6****T L M****T T T F T T****0****0 1 -1 A7. DELR(NCOL)****0 1 -1 A8. DELC(NROW)**

```

0 1 -1 A9. HTOP(NCOL,NROW); Top of the first layer
0 1 -1 A10. Thickness of layer 1
0 .350 -1 A11. Effective porosity of layer 1
0 1 -1 A12. ICBUND matrix of Layer 1
0 0 -1 A13. Start. conc. in layer 1 for spec. # 1O(0)
0 .002588 -1 A13. Start. conc. in layer 1 for spec. # 2C(4)
0 .0112 -1 A13. Start. conc. in layer 1 for spec. # 3Ca
0 .16 -1 A13. Start. conc. in layer 1 for spec. # 4Cl
0 .0865 -1 A13. Start. conc. in layer 1 for spec. # 5Na
0 .0182 -1 A13. Start. conc. in layer 1 for spec. # 6Mg
0 7.286 -1 A13. Start. conc. in layer 1 for spec. # 7pH
0 -1.5554 -1 A13. Start. conc. in layer 1 for spec. # 8pe
0 .0534 -1 A13. Start. conc. in layer 1 for spec. # 9Ca_ex
0 .0558 -1 A13. Start. conc. in layer 1 for spec. # 10Na_ex
0 .0499 -1 A13. Start. conc. in layer 1 for spec. # 11Mg_ex
1E+30 .05 0 0 0 0 T 835 0 .1 .2 .3 .4 .5 .6 .7
.8000001 .9000001 1 1.1 1.2 1.3 1.4 1.5
1.6 1.7 1.8 1.9 2 2.1 2.2 2.3
2.4 2.5 2.6 2.7 2.799999 2.899999 2.999999 3.099999
80.79934 80.89934 80.99934 81.09933 81.19933 81.29933 81.39933 81.49933
...
...
...
81.59933 81.69933 81.79932 81.89932 81.99932 82.09932 82.19932 82.29932
82.39931 82.49931 82.59931 82.69931 82.79931 82.89931 82.99931 83.0993
83.1993 83.2993 83.3333
0 1
T 1
83.3333 1000 1
0 50000 1 0

```

**5.5.6 Data input for the advection package file** The TVD scheme was used for the present example. The advection package file **pht3dadv.dat** has the following entries:

```
-1 .75 5000 0
```

**5.5.7 Data input for the dispersion package file** The longitudinal dispersivity, as given by Table 5.11, is entered into the **pht3ddsp.dat** file:

```
0 1.737(17G14.0) -1 C1. Longitudinal disp. of layer 1
0 0.1(1G14.0) -1 C2. TRPT=(horiz. transv. disp.) / (Longit. disp.)
0 0.1(1G14.0) -1 C3. TRPV=(vert. transv. disp.) / (Longit. disp.)
0 0.1(1G14.0) -1 C4. effective molecular diffusion coefficient [ $L^2/T$ ]
```

**5.5.8 Data input for the source/sink mixing package file** The composition of the injected fresh water, as listed in Table 5.12, needs to be defined in the **pht3dssm.dat** file. Data input is also needed for pH, pe and immobile entities. However, the input values need to be set to 0. For **Example 5**, the **pht3dssm.dat** file has the following entries.

```
T F F F F F
2002
1
1 1 1 0 2 0 .003651 .00213 .01466 .0094 .0005 0 0 0 0 0 0 0
```

**5.5.9 Simulation results** The breakthrough of the injected concentrations at neighboring wells exhibits the chromatographic effects that result from the nonlinear ion-exchange processes. In Figure 5.5, breakthrough curves simulated with PHT3D for chloride and for the cations are plotted in comparison with results from a corresponding PHREEQC-2 simulation. Results agree very well, despite the different approaches taken with respect to modelling the flow field.

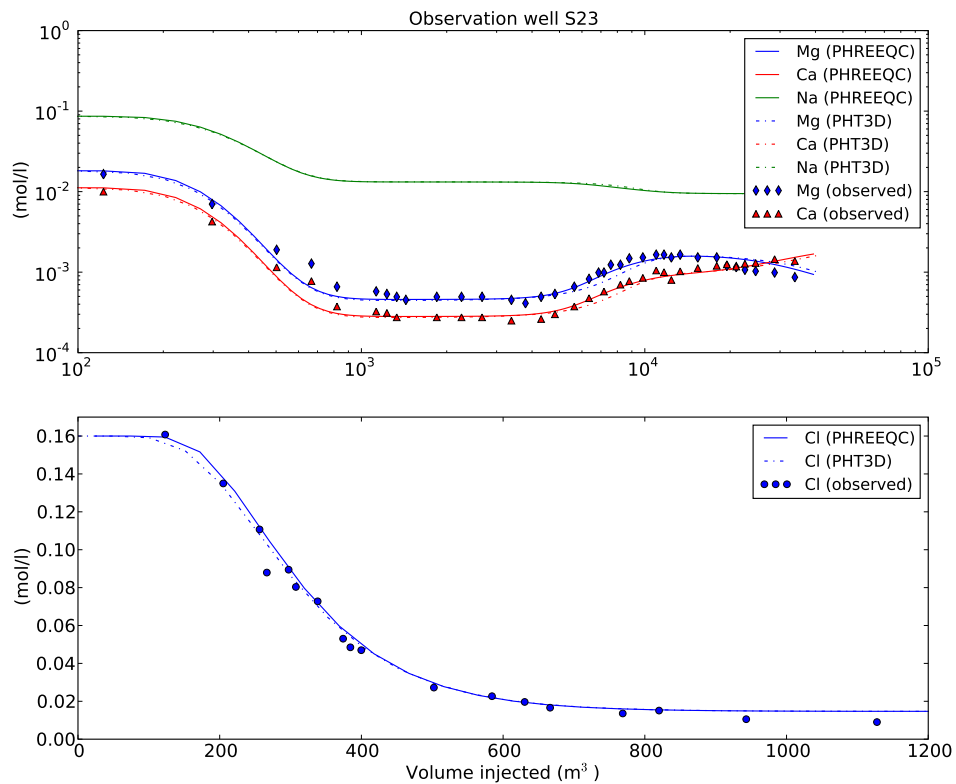


Figure 5.5: Comparison of simulated chloride and cation concentrations 16  $m$  from the injection point.

## 5.6 Example 6: Cation exchange and precipitation/dissolution during tenside injection

**5.6.1 Introduction** In this modelling example multi-component transport with simultaneous dissolution/precipitation and ion-exchanging reactions is demonstrated through a case, initially presented by Sardin et al. (1986), featuring the transport and reactions of an anionic tenside (alkylbenzenesulfonates of sodium).

The process of tenside injection is used for enhanced oil recovery in (i) oilfields and (ii) at oil-product contaminated sites. The understanding and quantification of the physico-chemical processes involved thus has important applications. Sardin et al. (1986) carried out a range of batch and column experiments and analysed the results using a one-dimensional reactive multi-species transport model.

**5.6.2 Spatial discretisation and flow problem** The length and diameter of the column used in the experiments were 0.2 *m* and 0.0254 *m*, respectively (Sardin et al., 1986). The water flux through the column was maintained at a constant rate of 1.0 *cm min*<sup>-3</sup>. The porosity (pore-volume) and the longitudinal dispersivity were determined separately by analysing the breakthrough curve from a *CaCl*<sub>2</sub> injection experiment within the same column (see Table 5.14). The resulting flow velocity in the column is 6.696 (*m d*<sup>-1</sup>). The setup of the flow model is similar to the flow models in the previous examples (e.g., boundary conditions, cross-sectional area) The spatial discretisation chosen for the numerical model

Table 5.14: Flow and transport parameters used in Example 6.

Flow simulation	steady state
Total simulation time ( <i>days</i> )	0.2083
Length stress period 1	0.5944
Length stress period 2	0.1489
Stress periods	2
Time steps (stress period 1)	250
Time steps (stress period 2)	600
Grid spacing ( <i>m</i> )	0.00111
Model length ( <i>m</i> )	0.2
Pore velocity ( <i>m d</i> <sup>-1</sup> )	6.696
Porosity	0.424
Dispersivity ( <i>m</i> )	0.05755

(180 grid-cells of  $0.00111 \text{ m d}^{-1}$  length) replicates the discretisation chosen by Zysset (1993).

**5.6.3 Data input for the database file** Sardin et al. (1986) proposed an LEA-based reaction network for the simulation of the experiments and identified

- Sorption, i.e., ion-exchanging reactions of sodium ( $Na^+$ ) and calcium ( $Ca^{2+}$ )
- Aqueous complexation reactions of calcium-carbonate species
- Precipitation of calcium tenside ( $T_2Ca$ )

as the most important reactions to be considered. A database file that is adapted for this simulation problem is needed here to accommodate the reactions involving tenside and to supply/modify reaction constants to those identified experimentally by Sardin et al. (1986). The ion-exchanging reactions of sodium ( $Na^+$ ) and calcium ( $Ca^{2+}$ ) were modelled by Sardin et al. (1986) using:

$$\overline{N_e} = 2[sur_2Ca] + [surNa] \quad (5.6.3.1)$$

and

$$K_{(Ca/Na)} = \frac{[Na^+]^2[sur_2Ca]}{[surNa]^2[Ca^{2+}]} \quad (5.6.3.2)$$

where  $N_e$  is the cation exchange capacity (CEC),  $K_{(Ca/Na)}$  is a selectivity constant,  $[Na^+]$  and  $[Ca^{2+}]$  are the concentrations of sodium and calcium in the aqueous phase, respectively and  $[sur_2Ca]$  and  $[surNa]$  are the concentrations of calcium and sodium on the exchanger, respectively. Values for  $N_e$  and  $K_{(Ca/Na)}$  were determined experimentally by Sardin et al. (1986). The above model can be replicated with the PHREEQC-2 ion-exchange model if the equilibrium constants for the ion-exchanging reactions are adapted accordingly. The reaction definition which has been used for the simulation of the benchmark problems is listed below:

#### **SOLUTION\_MASTER\_SPECIES**

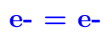
```
#
# element species alk gfw_formula element_gfw
#
```

H	H+	-1.	H	1.008	
H(1)	H+	-1.	0.0		
E	e-	0.0	0.0	0.0	
O	H2O	0.0	O	16.00	
O(0)	O2	0.0	O		
O(-2)	H2O	0.0	0.0		IIII
Ca	Ca+2	0.0	Ca	40.08	
Na	Na+	0.0	Na	22.9898	
Cl	Cl-	0.0	Cl	35.453	
C	CO3-2	2.0	HCO3	12.0111	
C(+4)	CO3-2	2.0	HCO3		
T	T-	0.0	T	50.	

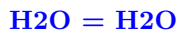
## SOLUTION\_SPECIES



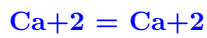
log\_k 0.000



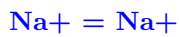
log\_k 0.000



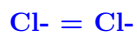
log\_k 0.000



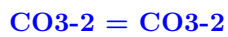
log\_k 0.000



log\_k 0.000



log\_k 0.000



log\_k 0.000



log\_k 0.000



log\_k -13.998



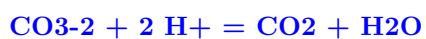
log\_k -86.08



log\_k -3.15



log\_k 10.329



```
log_k 16.681
Na+ + H2O = NaOH + H+
log_k -14.179142

EXCHANGE_MASTER_SPECIES
X X-
EXCHANGE_SPECIES
X- = X-
    log_k 0.0

Na+ + X- = NaX
    log_k 3.83 # Zysset (1993)

Ca+2 + 2X- = CaX2
    log_k 10.0 # Zysset (1993)

PHASES

CO2(g)
    CO2 = CO2
    log_k -1.468
Calcite
    CaCO3 = CO3-2 + Ca+2
    log_k -8.1432711 # Zysset (1993)
Calciumtenside
    CaT2 = 2 T- + Ca+2
    log_k -9.05 # Zysset (1993)
END
```

**5.6.4 Data input for the PHREEQC interface package file** In the input file **pht3d\_ph.dat**, the number of equilibrium aqueous components, (7), cations undergoing exchange-reactions (2) and minerals (2) included in the reaction network proposed by Sardin et al. (1986) needs to be defined and their names listed. The order of the entities (here aqueous components, minerals, ion-exchanging cations) is important whereas within each group the order is unimportant (except for pH and pe) as long as the order complies with the one chosen within the **pht3dbtn.dat** and **pht3dssm.dat** files, respectively. The entries for

the **pht3d\_ph.dat** file for **Example 6** might look as follows:

```

2 25.0 1 0 0
0
7
2
2 0
0
0 0 0 0
C(4)
Ca
Cl
Na
T
pH
pe
Calcite
Calciumtenside
Ca 2
Na 1

```

**5.6.5 Data input for the basic transport package file** The basic transport package file **pht3dbtn.dat** contains the information regarding the spatial and temporal discretisation of the transport model and defines all initial concen-

Table 5.15: Aqueous concentrations used in Example 6.

Aqueous component	$C_{init}$ ( $mol L_v^{-1}$ )	$C_{inflow 1}$ ( $mol L_v^{-1}$ )	$C_{inflow 2}$ ( $mol L_v^{-1}$ )
pH	8.56		
pe	9.37		
C(4)	$1.420 \times 10^{-5}$	$1.420 \times 10^{-5}$	$1.420 \times 10^{-5}$
Ca	0.0	0.0	
Na	0.0	$5.00 \times 10^{-2}$	$5.00 \times 10^{-2}$
Cl	0.0	0.0	$5.00 \times 10^{-2}$
Tenside	0.0	$5.00 \times 10^{-4}$	0.0

trations. Aqueous concentrations, in cases such as the one described here, represent concentrations that are in thermodynamic equilibrium with other phases participating in the simulation. The initial water composition in the example here is a demineralised water in equilibrium with atmospheric  $CO_2$  (Sardin et al., 1986). Therefore **C(4)** is the only aqueous component with an initial concentration  $> 0$ . Next, as the column was flushed with a  $CaCl_2$  solution, the exchanger sites are assumed to all being occupied by  $Ca$  ions. The concentration of  $Ca - X_2$  thus equals the cation exchange capacity.

**Example 6**

**Sardin et al (1986)**

**1 1 180 2 14 8**

**T L**

**T T T F T T**

**0 0.001111 0 A7. DELR(NCOL)**

**0 1 0 A8. DELC(NROW)**

**0 1 0 A9. HTOP(NCOL,NROW); Top of the first layer**

**0 1 0 A10. Thickness of layer 1**

**0 .4240 0 A11. Effective porosity of layer 1**

**0 1 0 A12. ICBUND matrix of Layer 1**

**0 0.000142 0 A13. Start. conc. in layer 1 for spec. # 1C(4)**

**0 0 0 A13. Start. conc. in layer 1 for spec. # 2Ca**

**0 0 0 A13. Start. conc. in layer 1 for spec. # 3Cl**

**0 0 0 A13. Start. conc. in layer 1 for spec. # 4Na**

**0 0 0 A13. Start. conc. in layer 1 for spec. # 5T**

**0 0 0 A13. Start. conc. in layer 1 for spec. # 6T**

**0 0 0 A13. Start. conc. in layer 1 for spec. # 7T**

Table 5.16: Initial mineral and exchanger concentrations used in Example 6.

	$C_{init}$ ( $mol L_v^{-1}$ )
Calcite	$1.444 \times 10^{-1}$
Calcium-tenside	0.0
Ca-X2	$2.43 \times 10^{-2}$
Na-X	0.0

```

0 0 0 A13. Start. conc. in layer 1 for spec. # 8T
0 9.91 0 A13. Start. conc. in layer 1 for spec. # 9pH
0 9.36 0 A13. Start. conc. in layer 1 for spec. # 10pe
0 .144492 0 A13. Start. conc. in layer 1 for spec. # 11Calcite
0 0 0 A13. Start. conc. in layer 1 for spec. # 12Calciumtenside
0 0.0243 0 A13. Start. conc. in layer 1 for spec. # 13Ca_ex
0 0 0 A13. Start. conc. in layer 1 for spec. # 14Na_ex
1E+30 .05
0 0 0 0 T
101
0 2.083E-03 4.167E-03 6.250E-03 8.333E-03 1.042E-02 .0125 1.458E-02
1.667E-02 .01875 2.083E-02 2.292E-02 .025 2.708E-02 2.917E-02 .03125
3.333E-02 3.542E-02 3.750E-02 3.958E-02 4.167E-02 4.375E-02 4.583E-02 4.792E-
02
5.000E-02 5.208E-02 5.417E-02 5.625E-02 5.833E-02 6.042E-02 6.250E-02 6.458E-
02
6.667E-02 6.875E-02 7.083E-02 7.292E-02 7.500E-02 7.708E-02 7.917E-02 .08125
8.333E-02 8.542E-02 .0875 8.958E-02 9.167E-02 9.375E-02 9.583E-02 9.792E-02
1.000E-01 .1020833 .1041666 .10625 .1083333 .1104166 .1125 .1145833
.1166666 .11875 .1208333 .1229166 .125 .1270833 .1291666 .13125
.1333333 .1354166 .1375 .1395833 .1416666 .14375 .1458333 .1479166
.1499999 .1520833 .1541666 .1562499 .1583333 .1604166 .1624999 .1645833
.1666666 .1687499 .1708333 .1729166 .1749999 .1770833 .1791666 .1812499
.1833332 .1854166 .1874999 .1895832 .1916666 .1937499 .1958332 .1979166
.1999999 .2020832 .2041666 .2062499 .2083332
0 1
T 1
5.944E-02 250 1
0 50000 1 0
.1488889 600 1
0 50000 1 0

```

**5.6.6 Data input for the advection package file** The TVD package was used for the simulation results presented in Figure 5.6. Standard parameters were used, as defined in the file **pht3dadv.dat**.

```
-1 .75 5000 0
```

**5.6.7 Data input for the dispersion package file** As mentioned in 5.6.2, the longitudinal dispersivity in the column was determined in a separate experiment. Fitting of the breakthrough curve of this experiment delivers a value of  $5.76 \times 10^{-4} m$ .

```
0 .000576(20G14.0) -1 C1. Longitudinal disp. of layer 1
0 0.1(1G14.0) -1 C2. TRPT=(horiz. transv. disp.) / (Longit. disp.)
0 0.1(1G14.0) -1 C3. TRPV=(vert. transv. disp.) / (Longit. disp.)
0 0(1G14.0) -1 C4. effective molecular diffusion coefficient [ $L^2/T$ ]
```

**5.6.8 Data input for the source/sink mixing package file** In the initial stage of the experiment water in chemical equilibria with atmospheric  $CO_2$  was added to the column. The resulting equilibrium conditions define the initial concentrations in the numerical model, as pointed out in 5.6.5. After this initial equilibration phase a slug of two pore-volumes of sodium and tenside-containing inflow water was added. This second phase of the flow-through experiment represents the first stress-period of the simulation. In the following and final stage of the experiment approximately five pore-volumes of a sodium chloride solution were added to the column as feedstock solution. The sodium chloride solution defines the input for the second stress-period within the **pht3dssm.dat** file.

```
T F F F F F
2002
1
1 1 1 0 2 .0000142 0 0 .005 .005 7 4 0 0 0 0
1
1 1 1 0 2 .0000142 0 .005 .005 0 7 4 0 0 0 0
```

**5.6.9 Simulation results** As shown in Figure 5.6, the comparison of the simulated breakthrough curves for tenside,  $Ca$  and  $Mg$  with the experimental data from Sardin et al. (1986) exhibits a good agreement. The model replicates qualitatively quite well the complexities of these curves that form as a result of the water-sediment interactions. Generally, the model-predicted curves are steeper and more pronounced. As Zysset (1993) points out, effects that could be responsible for the deviations are (i) kinetic effects, in particular with respect to the

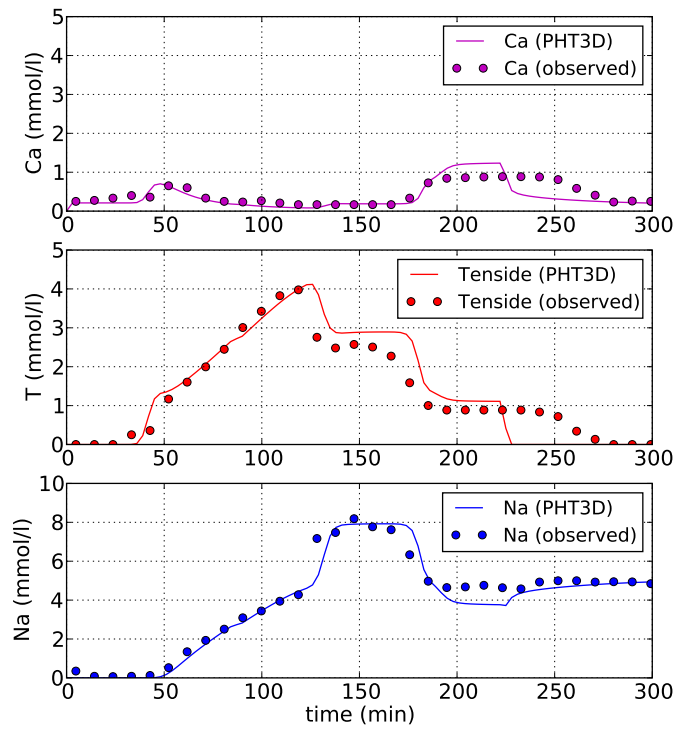


Figure 5.6: Comparison of simulated tenside and cation concentrations.

dissolution of  $T_2Ca$  (ii) differences in the dispersivities between the tracer experiment and the reactive transport experiment and (iii) heterogeneity of chemical properties and factors that affect adsorption and precipitation.

## 5.7 Example 7: Kinetic, sequential/parallel degradation of multiple species

**5.7.1 Introduction** Sun et al. (1999), and, in a more generalised form Clement (2001), presented an analytical solution for one-dimensional advective-dispersive transport coupled to arbitrary multi-species series and/or parallel first-order reactions. In contrast to previously published analytical solutions for this type of problem, the solution is suitable of handling reactions with stoichiometric yields other than unity. Sun et al. (1999) applied their solution technique for a test case involving 5 biodegrading species and compared the results with a numerical solution computed with RT3D. Figure 5.7 shows the reaction network of their test case. It includes three possible reaction chains  $A \rightarrow B \rightarrow C_1$ ,  $A \rightarrow B \rightarrow C_2$  and  $A \rightarrow B \rightarrow C_3$ . The governing equations for this reaction network are (Sun et al., 1999):

$$\frac{\partial C_A}{\partial t} - D \frac{\partial^2 C_A}{\partial x^2} + v \frac{\partial C_A}{\partial x} = -k_A C_A \quad (5.7.1.1)$$

$$\frac{\partial C_B}{\partial t} - D \frac{\partial^2 C_B}{\partial x^2} + v \frac{\partial C_B}{\partial x} = y_B k_A C_A - k_B C_B \quad (5.7.1.2)$$

$$\frac{\partial C_{C1}}{\partial t} - D \frac{\partial^2 C_{C1}}{\partial x^2} + v \frac{\partial C_{C1}}{\partial x} = y_{C1} k_B C_B - k_{C1} C_{C1} \quad (5.7.1.3)$$

$$\frac{\partial C_{C2}}{\partial t} - D \frac{\partial^2 C_{C2}}{\partial x^2} + v \frac{\partial C_{C2}}{\partial x} = y_{C2} k_B C_B - k_{C2} C_{C2} \quad (5.7.1.4)$$

$$\frac{\partial C_{C3}}{\partial t} - D \frac{\partial^2 C_{C3}}{\partial x^2} + v \frac{\partial C_{C3}}{\partial x} = y_{C3} k_B C_B - k_{C3} C_{C3} \quad (5.7.1.5)$$

where  $C_A$ ,  $C_B$ ,  $C_{C1}$ ,  $C_{C2}$  and  $C_{C3}$  are the concentrations of the five species  $A$ ,  $B$ ,  $C1$ ,  $C2$  and  $C3$ , respectively, whereas  $y_A$ ,  $y_B$ ,  $y_{C1}$ ,  $y_{C2}$  and  $y_{C3}$  are the appropriate stoichiometric coefficients and  $k_A$ ,  $k_B$ ,  $k_{C1}$ ,  $k_{C2}$  and  $k_{C3}$  are the appropriate first-order reaction rate constants. This test case forms the base for **Example 7**.

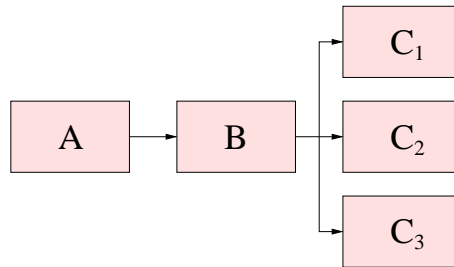


Figure 5.7: Reaction network used in Example 7

**5.7.2 Spatial discretisation and flow problem** The flow model can again be constructed similarly to the ones in **Examples 1-6**. The one-dimensional model-domain of 40  $m$  length is subdivided into 40 grid-cells in analogy to the discretisation of the RT3D simulation by Sun et al. (1999). The pore velocity in the example is  $1 m d^{-1}$ , requiring a flux (injection rate) of  $0.4 m^3 d^{-1}$  at the inflow end of the model given the cross-sectional area of  $1 m^2$  and a porosity of 1.0 (no porous media, see also Table 5.17).

**5.7.3 Data input for the database file** The right-hand sides of equations (5.7.1.1) - (5.7.1.5) describe the reaction term, i.e., the kinetics to be solved within the PHREEQC-2 step. Appropriate **RATES** expression must be formulated for each of the 5 species and, together with their definition as **SOLUTION\_MASTER\_SPECIES** and as **SOLUTION\_SPECIES** be included in the database file **pht3d\_datab.dat**. All **RATES** expressions have a similar form. The reaction rate constants  $k_A$ ,  $k_B$ , etc. are included as parameters **parm(1)** and thus their numerical values need to be defined separately in **pht3d\_ph.dat**. Alternatively, the rate constants could also be hard-coded within the **RATES** expressions. The information about the reaction stoichiometry will also be included in **pht3d\_ph.dat** and is not a part of the **RATES** expressions. Besides the definition of the kinetic species needed to solve this particular reactive problem, a basic set of **SOLUTION\_MASTER\_SPECIES** and of **SOLUTION\_SPECIES** for water must additionally be defined in the database in order to allow PHREEQC-2 to work properly. The species named  $A$ ,  $B$ ,  $C1$ ,  $C2$  and  $C3$  by Sun et al. (1999) were renamed  $S_a$ ,  $S_b$ ,  $S_c$ ,  $S_{cc}$  and  $S_{ccc}$ , respectively. The appropriate entries into the database file **pht3d\_datab.dat** for **Example 7** are:

Table 5.17: Flow and transport parameters used in Example 7.

Flow simulation	steady state
Total simulation time ( <i>days</i> )	40
Stress periods	1
Time steps	120
Grid spacing ( <i>m</i> )	1
Model length ( <i>m</i> )	40
Pore velocity ( $m d^{-1}$ )	0.40
Porosity	1.0
Dispersivity ( <i>m</i> )	10

## SOLUTION\_MASTER\_SPECIES

```

#
# element species alk gfw_formula element_gfw
#
H      H+      -1.  H      1.008
H(1)   H+      -1.  0.0
E      e-      0.0  0.0   0.0
O      H2O     0.0  O      16.00
O(-2)  H2O     0.0  0.0
S_a    S_a     0.0  S_a    1
S_b    S_b     0.0  S_b    1
S_c    S_c     0.0  S_c    1
S_cc   S_cc    0.0  S_cc   1
S_ccc  S_ccc   0.0  S_ccc  1

```

## SOLUTION\_SPECIES

```

H+ = H+
    log_k 0.000
e- = e-
    log_k 0.000
H2O = H2O
    log_k 0.000
S_a = S_a
    log_k 0.0
S_b = S_b
    log_k 0.0
S_c = S_c
    log_k 0.0
S_cc = S_cc
    log_k 0.0
S_ccc = S_ccc
    log_k 0.0
H2O = OH- + H+
    log_k -14.000
2 H2O = O2 + 4 H+ + 4 e-
    log_k -86.08
2 H+ + 2 e- = H2
    log_k -3.15

```

**RATES**

S\_a

**-start**

10 mS\_a = tot("S\_a")

20 if (mS\_a &lt;= 0) then goto 200

30 rate = parm(1) \* mS\_a

40 moles = rate \* time

200 SAVE moles

**-end**

S\_b -start

10 mS\_b = tot("S\_b")

20 if (mS\_b &lt;= 0) then goto 200

30 rate = parm(1) \* mS\_b

40 moles = rate \* time

200 SAVE moles

**-end**

S\_c

**-start**

10 mS\_c = tot("S\_c")

20 if (mS\_c &lt;= 0) then goto 200

30 rate = parm(1) \* mS\_c

40 moles = rate \* time

200 SAVE moles

**-end**

S\_cc

**-start**

10 mS\_cc = tot("S\_cc")

20 if (mS\_cc &lt;= 0) then goto 200

30 rate = parm(1) \* mS\_cc

40 moles = rate \* time

200 SAVE moles

**-end**

```

S_ccc
-start
10 mS_ccc = tot("S_ccc")
20 if (mS_ccc <= 0) then goto 200
30 rate = parm(1) * mS_ccc
40 moles = rate * time
200 SAVE moles
-end
END

```

**5.7.4 Data input for the PHREEQC interface package file** As discussed above, the input of the reaction rate constants and the information about the reaction stoichiometries need to be defined in the file `pht3d_ph.dat`. The appropriate values given by Sun et al. (1999) are listed in Table 5.18. Data input for each kinetic species requires three lines in `pht3d_ph.dat`. The first line contains the name and the number of parameters that are used in the **RATES** expression. In the present example the only parameter to be defined here is `parm(1)`, the first-order rate constant, e.g.,  $k_A = 0.2 \text{ d}^{-1}$  for the degradation of  $S_a$ . The value of this constant forms the second line dedicated to this species. **Note, that the time unit used by PHREEQC-2 is fixed to seconds, so the values given by Sun et al. (1999) must be converted.** Alternatively, the conversion could be a part of the BASIC routine within the **RATES** definition, for example, for  $S_a$ , using a conversion factor of 1/86400 in

```

S_a
-start
10 mS_a = tot("S_a")
20 if (mS_a <= 0) then goto 200
30 rate = parm(1)/86400 * mS_a
40 moles = rate * time
200 SAVE moles
-end

```

would allow the input in `pht3d_ph.dat` to define the rate constants in  $\text{d}^{-1}$  rather than  $\text{s}^{-1}$ . The third line, starting with **-formula**, defines which species are produced or removed at a rate proportional to the one computed for this **RATES** expression, here  $S_a$ . For the rate termed  $S_a$  the mother product is  $S_a$  itself. The entry `S_a -1.0` indicates a stoichiometric factor (yield) of -1.0, which will lead to a removal of  $S_a$  at the magnitude of the computed rate. The second part of

the line, **S\_b 0.5** indicates that  $S_b$  is produced at a rate that is 50 % of the removal rate of  $S_a$ . From the degraded mass of species  $S_b$ , 30 % is converted to species  $S_c$ , 20 % is converted to species  $S_{cc}$ , 10 % is converted to species  $S_{ccc}$  and the remaining 40 % are degrading to unspecified daughter products. The degradation of the species  $S_c$ ,  $S_{cc}$  and  $S_{ccc}$  is not linked to the production of any new species. The complete data entry for the **pht3d\_ph.dat** file in **Example 7** is:

```

2 25.0 1 0 0
0
2
0
0 0
0
5 0 0 0
S_a 1
2.314814E-06
-formula S_a -1.0 S_b 0.5
S_b 1
1.1574E-06
-formula S_b -1.0 S_c 0.3 S_cc 0.2 S_ccc 0.1
S_c 1
2.314814E-07
-formula S_c -1.0
S_cc 1
2.314814E-07
-formula S_cc -1.0
S_ccc 1
2.314814E-07
pH
pe

```

**5.7.5 Data input for the basic transport package file** The basic transport file **pht3dbtn.dat** contains most of the relevant information to define the transport problem, including the geometry of the problem, boundary conditions and the initial water composition. For the PHT3D simulation sodium pH and pe were included in addition to the five reactive species ( $S_a$ ,  $S_b$ ,  $S_c$ ,  $S_{cc}$  and

Table 5.18: Reaction rate constants and stoichiometric yields used in Example 7.

Parameter	Value
First-order rate constant $k_A$ ( $d^{-1}$ )	0.2
First-order rate constant $k_B$ ( $d^{-1}$ )	0.1
First-order rate constant $k_{C1}$ ( $d^{-1}$ )	0.02
First-order rate constant $k_{C2}$ ( $d^{-1}$ )	0.02
First-order rate constant $k_{C3}$ ( $d^{-1}$ )	0.02
Stoichiometric yield $A \rightarrow B$ $y_B$	0.5
Stoichiometric yield $B \rightarrow C1$ $y_{C1}$	0.3
Stoichiometric yield $B \rightarrow C2$ $y_{C2}$	0.2
Stoichiometric yield $B \rightarrow C3$ $y_{C3}$	0.1

Table 5.19: Aqueous concentrations used in Example 7.

Aqueous component	$C_{init}$ ( $mol L_w^{-1}$ )
pH	7
pe	4
S_a (first grid-cell)	0.001
S_a (all other grid-cells)	0
S_b	0
S_c	0
S_cc	0
S_ccc	0

S\_ccc). However, the pH and pe results are meaningless.

Note, that in contrast to some of the previously discussed one-dimensional problems, the inflow water composition is not defined/determined through the source/sink mixing package, but instead through the fixed concentration boundary. While in some cases the choice of the boundary conditions might not affect the results (i.e., the resulting concentration profiles) very strongly, in the present case the choice has a significant influence.

### Example 7

Sun et al. (1999)



**5.7.7 Data input for the dispersion package file** Sun et al. (1999) chose a relatively large longitudinal dispersivity of 10  $m$  for their application example. Dispersive transport thus plays a much bigger role than in the previous examples. The data entries for the dispersion package file **pht3ddsp.dat** are:

```
0 10 -1 C1. Longitudinal disp. of layer 1
0 0.1 -1 C2. TRPT=(horiz. transv. disp.) / (Longit. disp.)
0 0.1 -1 C3. TRPV=(vert. transv. disp.) / (Longit. disp.)
0 0 -1 C4. effective molecular diffusion coefficient [ $L^2/T$ ]
```

**5.7.8 Data input for the source/sink mixing package file** The water at the inflow end of the column contains only the mother product, i.e., species  $S_a$ . The other species, i.e.,  $S_a$ ,  $S_b$ ,  $S_c$ ,  $S_{cc}$ , and  $S_{ccc}$ , form only downstream within the column. The influent water composition is already defined through the fixed concentration boundary. Therefore, the water composition defined and assigned through the **pht3dssm.dat** file has essentially no influence on the result.

**5.7.9 Simulation results** The PHT3D simulation results were compared with the analytical solution of Sun et al. (1999), and numerical solutions computed with PHREEQC-2 and RT3D, respectively. The results for solutions and all 5 species coincide very closely, except for the effluent end of the column, between 35  $m$  and 40  $m$ , where slight differences occur for species  $S_c$ ,  $S_{ccc}$  and  $S_{ccc}$ . There, the numerical results of the numerical model (PHT3D, RT3D and PHREEQC-2) deviate slightly from the analytical solution whereas they still coincide with each other.

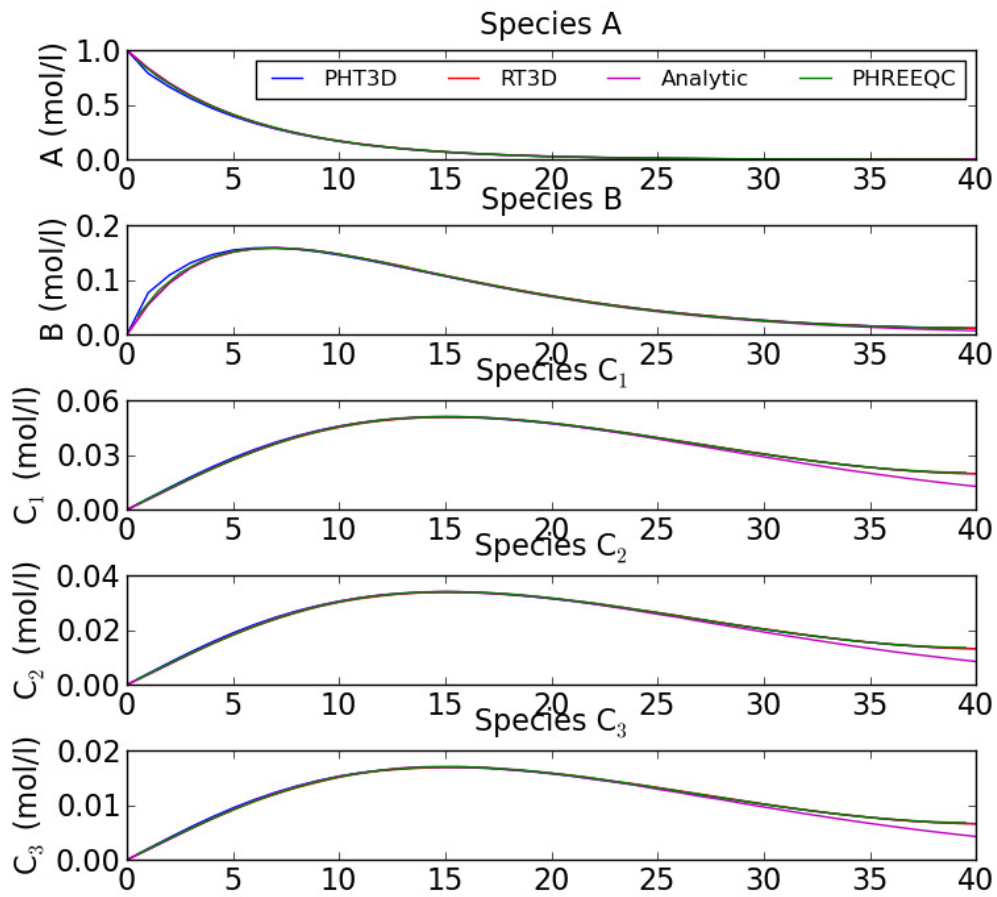


Figure 5.8: Comparison of simulated concentrations after 40 days simulation time.

## 5.8 Example 8: Kinetic, sequential degradation of chlorinated hydrocarbons

**5.8.1 Introduction** Simulation of transport and reactions of chemicals that undergo biodegradation might be dealt with at different levels of process detail, starting with formulations where the reaction kinetics are independent of the concentrations of other chemicals. One example of such a formulation is the previously described single-species biodegradation model of **Example 1**. More complex formulations incorporate the dependency of the reaction kinetics on the concentrations of other solutes (Clement, 1997), explicitly model growth and decay of bacteria (Prommer et al., 2002a) or even take into account the pH-dependency of bacterial growth (Brun and Engesgaard, 2002). For the purpose of model evaluation, two 2D simulation problems presented by Clement (1997) were used to verify kinetic multi-species biodegradation reactions. The first case models the sequential first-order degradation of PCE (RT3D reaction module 6), whereas the second case models a Monod-type BTEX degradation that uses sequentially a series of electron-acceptors ( $O_2$ ,  $NO_3^-$ ,  $Fe^{3+}$ ,  $SO_4^{2-}$ ,  $CO_2$ ). The PCE case forms the present example (**Example 8**) whereas the BTEX case forms **Example 9** and will be discussed thereafter. Two additional model applications that illustrate alternative modelling approaches for biodegradation reactions are given by **Example 10** and **Example 11**. The main purpose of presenting **Example 8** and **Example 9** is to verify PHT3D's capability to accurately simulate kinetically controlled reactions by comparing simulation results with those from other codes. However, it is noteworthy that the fully kinetic simulation problems described in these particular two examples are solved at much lower computational cost by RT3D. Applying PHT3D for such simple, fully kinetic cases may still make sense, in those cases where

- simple reaction kinetics are modified (regularly) to adapt them to changing conceptual models that typically evolve during a modelling study
- the simple model serves as a starting point for more complex formulations (e.g., inclusion of isotope fractionation) and particularly in cases where the simulations consider dependencies/feedback between the aquifer's geochemical behaviour (pH, redox conditions, ...) and reaction rate kinetics.

In both cases the reaction models can be simply changed by changing the **RATES** expressions in the database file **pht3d\_datab.dat**

Table 5.20: Flow and transport parameters used in Examples 8 and 9.

Flow simulation	steady state
Total simulation time ( <i>days</i> )	350
Stress period	1
Time steps	30
Grid spacing ( <i>m</i> )	$10 \times 10$
Model length ( <i>m</i> )	510
Model width ( <i>m</i> )	310
Aquifer type	confined
Horizontal hydraulic conductivity ( $m d^{-1}$ )	50
Height datum aquifer (bottom) ( <i>m</i> )	0
Height datum aquifer (top) ( <i>m</i> )	10
Prescribed head influent boundary ( <i>m</i> )	100
Prescribed head effluent boundary ( <i>m</i> )	99
Porosity	0.30
Longitudinal dispersivity ( <i>m</i> )	10.0
Transversal horizontal dispersivity ( <i>m</i> )	3.0

**5.8.2 Spatial discretisation and flow problem** The flow field underlying the reactive transport simulation is characterised by a parallel groundwater flow within a 10 *m* thick homogeneous aquifer. Following Clement (1997), the model domain of 510 *m* length and 310 *m* width is subdivided into 51 and 31 grid-cells, respectively. Fixed head boundary conditions were assigned to the inflow and the outflow boundaries. A well with a small flux of 2  $m d^{-1}$  is positioned 155 *m* downstream of the influent boundary. It will be used to inject a specific PCE mass per time in order to simulate in a rather simplistic way the contaminant source (zone). Using a horizontal hydraulic conductivity of 50  $m d^{-1}$  and a porosity of 0.3, the head difference of 1 *m* between the upstream boundary and the effluent boundary results in a pore velocity of 0.33  $m d^{-1}$ . Figure 5.9 shows the setup of the model and the relevant parameters needed to build the flow model are summarised in Table 5.22.

**5.8.3 Data input for the database file** The reaction network that describes the dechlorination consists of a decay chain that includes the sequential degradation steps from *PCE* (perchloroethylene) to *TCE* (trichloroethylene)



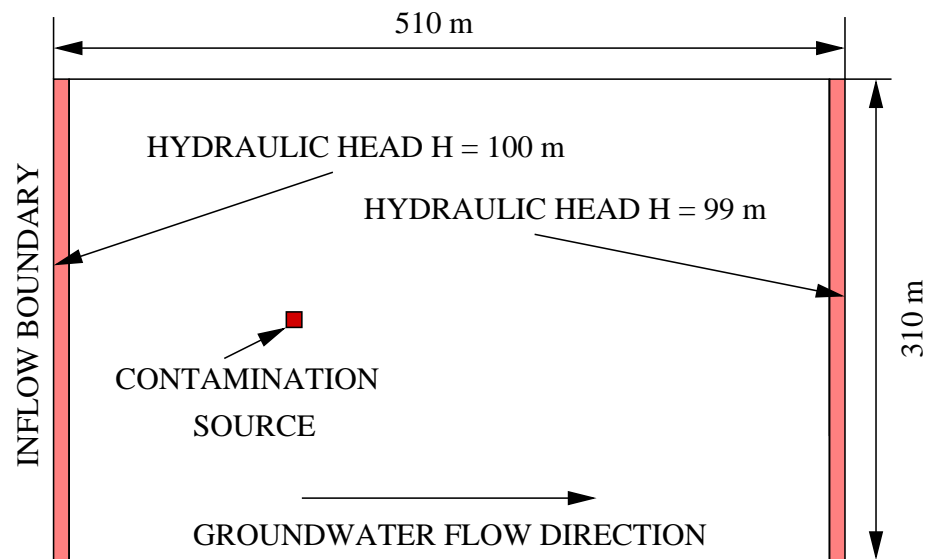


Figure 5.9: Model grid and location of the contaminant source

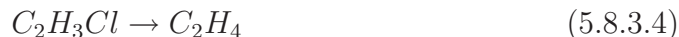
from *TCE* to *DCE* (dichloroethylene)



from *DCE* to *VC* (vinyl chloride)



and from *VC* to ethylene



*Cl* is successively removed until the nontoxic end product ethylene is formed. Note, that the intermediate product vinyl chloride is the most hazardous chemical within the decay chain. Following Clement (1997), each of the degradation/dechlorination steps is modelled as a kinetically controlled first order reaction. For simplicity, the degradation rates are assumed to be independent of the redox-chemistry of the aquifer. The required reaction definition within the database file **pht3d\_datab.dat** is very similar to the previous case **Example 7**. The entries for this file are:

#### SOLUTION\_MASTER\_SPECIES

```
#
# element species alk gfw_formula element_gfw
#
H      H+      -1.  H      1.008
H(1)   H+      -1.  0.0
E      e-      0.0  0.0  0.0
O      H2O     0.0  O      16.00
O(0)   O2      0.0  O
O(-2)  H2O     0.0  0.0
Na      Na+     0.0  Na      22.9898  llll
Cl      Cl-     0.0  Cl      35.453
Pce     Pce     0.0  Pce     164.0
Tce     Tce     0.0  Tce     130.0
Dce     Dce     0.0  Dce     100.0
Vc      Vc      0.0  Vc      50.0
Ethe    Ethe    0.0  Ethe    26.0
SOLUTION_SPECIES
```

```
H+ = H+
```

```
log_k 0.000
```

```
-gamma 9.0000 0.0000
```

e- = e-

log\_k 0.000

H2O = H2O

log\_k 0.000

Na+ = Na+

log\_k 0.000

Cl- = Cl-

log\_k 0.000

Pce = Pce

log\_k 0.0

Tce = Tce

log\_k 0.0

Dce = Dce

log\_k 0.0

Vc = Vc

log\_k 0.0

Ethe = Ethe

log\_k 0.0

H2O = OH- + H+

log\_k -14.000

delta\_h 13.362 kcal

-analytic -283.971 -0.05069842 13323.0 102.24447 -1119669.0

-gamma 3.5000 0.0000

2 H2O = O2 + 4 H+ + 4 e-

log\_k -86.08

delta\_h 134.79 kcal

2 H+ + 2 e- = H2

log\_k -3.15

delta\_h -1.759 kcal

Na+ + H2O = NaOH + H+

log\_k -14.180

RATES

Pce

-start

10 mPce = tot("Pce")

20 if (mPce ≤ 1e-10) then goto 200

```
30 rate = parm(1) * mPce
40 moles = rate * time
200 SAVE moles
-end
Tce
-start
10 mTce = tot("Tce")
20 if (mTce ≤ 1e-10) then goto 200
30 rate = parm(1) * mTce
40 moles = rate * time
200 SAVE moles
-end
Dce
-start
10 mDce = tot("Dce")
20 if (mDce ≤ 1e-10) then goto 200
30 rate = parm(1) * mDce
40 moles = rate * time
200 SAVE moles
-end
Vc
-start
10 mVc = tot("Vc")
20 if (mVc ≤ 1e-10) then goto 200
30 rate = parm(1) * mVc
40 moles = rate * time
200 SAVE moles
-end
Ethe
-start
10 mEthe = tot("Ethe")
20 if (mEthe ≤ 1e-10) then goto 200
30 rate = parm(1) * mEthe
40 moles = rate * time
200 SAVE moles
-end
END
```

The first order rate constants for the kinetic species are represented through the parameter(s) (**parm(1)**). Thus, the appropriate values, i.e., rate constants, can and need to be defined in the **pht3d\_ph.dat** file.

**5.8.4 Data input for the PHREEQC interface package file** The four chlorinated compounds (PCE, TCE, DCE, VC), ethylene, Na and Cl form the reaction network that is defined in the PHREEQC-2 interface package file. The reaction constants, i.e., the first order rate constants are also defined within the **pht3d\_ph.dat** file. The entries for this file are:

```

2 25 0 1E-10 0.001
0
4
0
0 0
0
4 0 0 0
Pce 1
5.787037E-08
-formula Pce -1.0 Tce 1.0 Cl- 1.0
Tce 1
3.472222E-08
-formula Tce -1.0 Dce 1.0 Cl- 1.0
Dce 1
2.314815E-08
-formula Dce -1.0 Vc 1.0 Cl- 1.0
Vc 1
1.157407E-08
-formula Vc -1.0 Ethc 1.0 Cl- 1.0
Cl
Na
pH
pe

```

As discussed earlier, PHREEQC-2 expects **seconds** as time unit and the constants given by Clement (1997) require an appropriate conversion. As the unit for mass in PHT3D consistently is **mol**, the stoichiometric coefficients differ as well from those given by Clement (1997). Using **mol** as mass unit, the transformation

of one PCE molecule results in the production of one molecule of TCE, adds one  $Cl^-$  ion to and removes one hydrogen ( $H^+$ ) from the aqueous solution. Apart from the changes in  $Cl$  concentration the reaction network used in this example neglects the hydrochemical interactions between the dechlorination reactions and the background chemistry, including the removal of hydrogen.

**5.8.5 Data input for the basic transport package file** The construction of the basic transport package file **pht3dbtn.dat** does not differ significantly from the previously described examples and is not discussed in much detail here. The entries for this file are:

**Example 8**

PCE->TCE->DCE->VC after Clement (1997)

1 31 51 1 8 6

T L M

T T T F T T

0

0 10(20G14.0) -1 A7. DELR(NCOL)

0 10(20G14.0) -1 A8. DELC(NROW)

0 10(20G14.0) -1 A9. HTOP(NCOL,NROW); Top of the first layer

0 10(20G14.0) -1 A10. Thickn. of layer 1

0 0.3(20G14.0) -1 A11. Effective porosity of layer 1

100 1(20I3) -1 A12. ICBUND matrix of Layer 1

-1 1

1 1

1 1

-1 1

1 1 1 1 1 1 1 ...

...

... for all 31 rows ...

...

-1 1

1 1

1 1

0 0 0 A13. Start. conc. in layer 1 for spec. # 1Pce

0 0 0 A13. Start. conc. in layer 1 for spec. # 2Tce

0 0 0 A13. Start. conc. in layer 1 for spec. # 3Dce

0 0 0 A13. Start. conc. in layer 1 for spec. # 4Vc

```

0 0.001 -1 A13. Start. conc. in layer 1 for spec. # 5Cl
0 0.001 -1 A13. Start. conc. in layer 1 for spec. # 6Na
0 7 0 A13. Start. conc. in layer 1 for spec. # 7pH
0 14 0 A13. Start. conc. in layer 1 for spec. # 8pe
1E+30 .05
0 0 0 0 T
56
0 20 40 60 80 100 120 140
160 180 200 220 240 260 280 300
320 340 360 380 400 420 440 460
480 500 520 540 560 580 600 620
640 660 680 700 720 740 760 780
800 820 840 860 880 900 920 940
960 980 1000 1020 1040 1060 1080 1100
0 1
T 1
1100 55 1
0 50000 1 0

```

The important PHT3D specific information are the **T** (logical) flag which activates/includes the PHREEQC-2 interface and reactions in a simulation, the definition of **NCOMP**, i.e., the total number of chemical entities (in MT3DMS always termed **species**) of **MCOMP**, the number of entities that require hydrological transport (advection and dispersion) and of the initial concentrations for all **NCOMP** entities.

**5.8.6 Data input for the advection package file** The TVD scheme is used for the simulation of advective transport in this example and the input for the **pht3dadv.dat** file might have the following entries:

```
-1 .75 5000 0
```

Detailed information regarding the meaning of those entries/parameters should be obtained from the original MT3DMS manual.

**5.8.7 Data input for the dispersion package file** The longitudinal and transversal dispersivities of 10 m and 3 m, respectively, are entered through the file **pht3ddsp.dat**, which consequently has the following entries:

```

0 10(20G14.0) -1 C1. Longitudinal dispersivity of layer 1
0 0.3(1G14.0) -1 C2. TRPT=(horiz. transv. disp.) / (Long. disp.)
0 0.3(1G14.0) -1 C3. TRPV=(vert. transv. disp.) / (Long. disp.)
0 0(1G14.0) -1 C4. eff. molec. diffusion coeff. [ $L^2/T$ ]

```

Note, that the transversal dispersivities are defined relative to the longitudinal dispersivity, i.e., in the present case through the factor 0.3.

**5.8.8 Data input for the source/sink mixing package file** The concentrations of external fluxes to the model domain, e.g, through wells and recharge, need to be defined in the file **pht3dssm.dat**. In the present example, the contaminant source is simulated through a well with a flux of  $2 \text{ m d}^{-1}$ . However, only the PCE concentration is 0. The input for source/sink mixing package file becomes:

```

T F F F F F
2063
1
1 16 16 0 2 .006031 0 0 0 0 7 4

```

**5.8.9 Simulation results** The injection of PCE leads to the formation of a considerable plume of dissolved PCE which, as a result, reaches a steady state size before the end of the simulation time. Plumes of TCE, DCE and VC form as a result of the sequential dechlorination reaction. The PCE concentration are highest at the point source whereas the concentration of the daughter products peak downstream of the contamination source zone. The PHT3D results are compared with those obtained from a RT3D simulation as described in Clement (1997). Figure 5.10 shows the concentration contours after three years simulation time for the mother product PCE and for VC, one of the transformation intermediates. Both solutions agree well considering the different solution techniques for the chemistry step being used by PHT3D/PHREEQC-2 and RT3D, respectively.

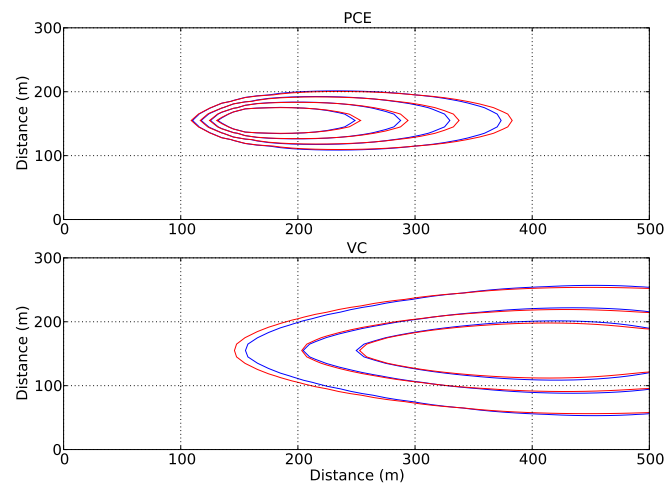


Figure 5.10: Simulated PCE and VC concentrations after 3 years (PHT3D = dashed lines, RT3D = solid lines).

## 5.9 Example 9: Kinetic degradation of BTEX using multiple electron acceptors

**5.9.1 Background** A second model comparison with the RT3D model forms the here-described **Example 9**. The case is based on the same principle (hydrogeological) model setup as the previous case. However, the simulated contamination scenario now involves the degradation of BTEX-type hydrocarbons under sequential consumption of electron acceptors. The reaction network of this case forms reaction module 3 in the RT3D model by Clement (1997). The model considers a rate-dependency on electron donor and electron acceptor concentrations. It is assumed that all hydrocarbon compounds have similar physical and chemical properties, which implies, e.g., that all compounds (bio)degrade at the same rate. Based on (2.1.1), the transport equation for the hydrocarbon compound is

$$\frac{\partial C_{hc}}{\partial t} = \frac{\partial}{\partial x_j} \left( D_{jk} \frac{\partial C_{hc}}{\partial x_k} \right) - \frac{\partial}{\partial x_j} (v_j C_{hc}) + r_{\text{reac},hc} \quad (5.9.1.1)$$

where  $C_{hc}$  is the hydrocarbon concentration. The reaction rate in (5.9.1.1), i.e.,  $(r_{\text{reac},hc})$  consists of the sum of several degradation terms, each representing a degradation process associated with a particular electron acceptor:

$$r_{\text{reac},hc} = r_{O_2} + r_{NO_3^-} + r_{Fe^{2+}} + r_{SO_4^{2-}} + r_{CH_4} \quad (5.9.1.2)$$

where  $r_{O_2}$ ,  $r_{NO_3^-}$ ,  $r_{Fe^{2+}}$ ,  $r_{SO_4^{2-}}$  and  $r_{CH_4}$  represent the contributions from aerobic degradation, denitrification, iron reduction, sulfate reduction and methanogenesis, respectively. For example, the term for hydrocarbon degradation under aerobic conditions is:

$$r_{O_2} = -k_{O_2} C_{hc} \frac{C_{O_2}}{K_{O_2} + C_{O_2}} \quad (5.9.1.3)$$

where  $k_{O_2}$  is a rate constant,  $C_{O_2}$  is the concentration of oxygen and  $K_{O_2}$  is the half-saturation constant for oxygen. As long as oxygen is present, degradation involving other electron acceptors is typically inhibited and consequently all other terms in 5.9.1.2 should be negligible. The rate expressions for less favourable electron acceptors thus need to contain additional terms that guarantee that the computed rates for those degradation processes do not differ significantly from 0 while a degradation process involving a more favourable electron acceptor is ongoing. For example, hydrocarbon degradation due to denitrification in the (occasional) presence of oxygen is then modelled as (Clement, 1997; Lu et al., 1999):

$$r_{NO_3^-} = -k_{NO_3^-} C_{hc} \frac{K_{inh,O_2}}{K_{inh,O_2} + C_{O_2}} \frac{C_{NO_3^-}}{K_{NO_3^-} + C_{NO_3^-}} \quad (5.9.1.4)$$

where  $k_{NO_3^-}$  is the rate constant for denitrification and  $K_{inh,O_2}$  is an inhibition constant for oxygen. For the other, thermodynamically even less favourable degradation processes modified forms of 5.9.1.4 exist. They include additional inhibition terms, one for each more favourable electron accepting process, i.e., the rate of hydrocarbon removal resulting iron reduction is computed from

$$r_{Fe^{2+}} = -k_{Fe^{2+}} C_{hc} \frac{K_{inh,O_2}}{K_{inh,O_2} + C_{O_2}} \frac{K_{inh,NO_3^-}}{K_{inh,NO_3^-} + C_{NO_3^-}} \frac{C_{Fe^{3+}}}{K_{Fe^{3+}} + C_{Fe^{3+}}} \quad (5.9.1.5)$$

the appropriate removal rate resulting from sulfate reduction is

$$r_{SO_4^{2-}} = -k_{SO_4^{2-}} C_{hc} \frac{K_{inh,O_2}}{K_{inh,O_2} + C_{O_2}} \frac{K_{inh,NO_3^-}}{K_{inh,NO_3^-} + C_{NO_3^-}} \frac{K_{inh,Fe^{3+}}}{K_{inh,Fe^{3+}} + C_{Fe^{3+}}} \frac{C_{SO_4^{2-}}}{K_{SO_4^{2-}} + C_{SO_4^{2-}}} \quad (5.9.1.6)$$

Finally, the hydrocarbon removal rate resulting from methanogenesis is

$$r_{CH_4} = -k_{CH_4} C_{hc} \frac{K_{inh,O_2}}{K_{inh,O_2} + C_{O_2}} \frac{K_{inh,NO_3^-}}{K_{inh,NO_3^-} + C_{NO_3^-}} \frac{K_{inh,Fe^{3+}}}{K_{inh,Fe^{3+}} + C_{Fe^{3+}}} \frac{K_{inh,SO_4^{2-}}}{K_{inh,SO_4^{2-}} + C_{SO_4^{2-}}} \frac{C_{CO_2}}{K_{CH_4} + C_{CO_2}} \quad (5.9.1.7)$$

where  $C_{Fe^{3+}}$ ,  $C_{SO_4^{2-}}$ ,  $C_{CO_2}$  and  $C_{CH_4}$  are the concentrations of iron(III), sulphate, carbondioxide and methane, respectively,  $k_{Fe^{3+}}$ ,  $k_{SO_4^{2-}}$  and  $k_{CH_4}$  are rate constants for iron reduction, sulphate reduction and methanogenesis, respectively,  $K_{Fe^{3+}}$ ,  $K_{SO_4^{2-}}$  and  $K_{CH_4}$  are the half saturation constant for iron(III), sulfate and methane, respectively, and  $K_{inh,NO_3^-}$ ,  $K_{inh,Fe^{3+}}$ , and  $K_{inh,SO_4^{2-}}$  are inhibition constants for nitrate, iron and sulphate, respectively. Note, that the concentrations of  $Fe^{3+}$  and  $CO_2$  are not directly tracked in the model but rather computed indirectly under the assumptions that

$$C_{Fe^{3+}} = C_{Fe_m^{2+}ax} - C_{Fe^{2+}} \quad (5.9.1.8)$$

and

$$C_{CO_2} = C_{CH_4,max} - C_{CH_4} \quad (5.9.1.9)$$

where  $C_{Fe_m^{2+}ax}$  and  $C_{CH_4,max}$  are user defined values representing the site-specific aquifer capacity for iron reduction and methanogenesis. Full details on the reaction module and the description of a field-scale application for the module can be found in Lu et al. (1999).

**5.9.2 Spatial discretisation and flow problem** The model discretisation and the flow in this example are similar to the previous case (**Example 8**) and are not repeated here.

**5.9.3 Data input for the database file** The reaction network of the RT3D reaction module 3 was translated into a PHREEQC-2 database file, i.e., new species/components were defined, where needed, and rate expressions formulated as BASIC programs. The reaction network in the RT3D module includes one organic compound and five inorganic species. Three of the inorganic species are electron acceptors ( $O_2$ ,  $NO_3^-$ ,  $SO_4^{2-}$ ) and two are degradation end products, i.e., the reduced forms of electron acceptors ( $Fe^{2+}$ ,  $CH_4$ ). For the simulation with PHT3D, kinetic rate expressions were formulated only for the five inorganic species whereas no rate formulation is needed for the hydrocarbon species **Hy\_carb**. In the chosen model formulation the kinetically controlled (reactive) changes of the hydrocarbon concentration result from the superposition of the concentration changes that result from the stoichiometric linking of the hydrocarbon removal to electron acceptor consumption, as defined in **pht3d\_ph.dat**. The database file **pht3d\_datab.dat** for **Example 9** is:

#### SOLUTION\_MASTER\_SPECIES

```
#
# element species alk gfw_formula element_gfw
#
H      H+      -1.  H      1.008
H(1)   H+      -1.  0.0
E      e-      0.0  0.0    0.0
O      H2O     0.0  O      16.00
Na     Na+     0.0  Na     22.9898
Cl     Cl-     0.0  Cl     35.453
N      NO3-   0.0  N      14.0067
N(5)   NO3-   0.0  N
S      SO4-2  0.0  SO4    32.064
S(6)   SO4-2  0.0  SO4
Fe     Fe+2    0.0  Fe     55.847
Fe(+2) Fe+2    0.0  Fe
Hy_carb Hy_carb  0.0  Hy_carb  92.
Meth   Meth    0.0  Meth    16.
```

#### SOLUTION\_SPECIES

```
H+ = H+
    log_k 0.000
    -gamma 9.0000 0.0000
e- = e-
    log_k 0.000
H2O = H2O
```

```

log_k 0.000
Na+ = Na+
log_k 0.000
Cl- = Cl-
log_k 0.000
Fe+2 = Fe+2
log_k 0.000
-gamma 6.0000 0.0000
SO4-2 = SO4-2
log_k 0.000
-gamma 5.0000 -0.0400
NO3- = NO3-
log_k 0.000
-gamma 3.0000 0.0000
Hy_carb = Hy_carb
log_k 0.0
Meth = Meth
log_k 0.0
H2O = OH- + H+
log_k -14.000
delta_h 13.362 kcal
-analytic -283.971 -0.05069842 13323.0 102.24447 -1119669.0
-gamma 3.5000 0.0000
2 H2O = O2 + 4 H+ + 4 e-
log_k -86.08
delta_h 134.79 kcal
2 H+ + 2 e- = H2
log_k -3.15
delta_h -1.759 kcal
Na+ + H2O = NaOH + H+
log_k -14.180

```

#### RATES

```

#-----
# Oxygen
# Y_O2/HC = (9 * 32) / 92 = 3.14 (mg/mg)
# (using mol. weight of toluene)

```

```

# C7H8 + 9 O2 + 3 H2O = 7 HCO3- + 7 H+
# -> Y_O2/HC = 9 (mol/mol)
#-----
O(0)
-start
10 mHy_carb = tot("Hy_carb")
20 mO2 = mol("O2")
30 if (mHy_carb ≤ 1e-08) then goto 200
40 if (mO2 ≤ 1e-08) then goto 200
90 monod_ox = mO2 / (0.5/1000/32 + mO2)
120 rate = parm(1) * 86400 * mHy_carb * monod_ox
180 moles = rate * time
200 SAVE moles
-end
#-----
# Nitrate
# Y_NO3/HC = (7.2 * 62) / 92 = 4.90 (mg/mg)
# (using mol. weight of toluene)
# C7H8 + 7.2 NO3- + 0.2 H+ = 7 HCO3- + 3.6 N2 + 0.6 H2O
# -> Y_NO3/HC = 7.2 (mol/mol)
#-----
N(5)
-start
10 mHy_carb = tot("Hy_carb")
20 mO2 = mol("O2")
30 mNO3 = tot("N(5)")
40 if (mHy_carb ≤ 1e-08) then goto 200
50 if (mNO3 ≤ 1e-08) then goto 200
90 inhib_ox = 0.001/1000/32 / (0.001/1000/32 + mO2)
100 monod_no3 = mNO3 / (0.5/1000/62 + mNO3)
120 rate = parm(1) / 86400 * mHy_carb * inhib_ox
130 rate = rate * monod_no3
180 moles = rate * time
200 SAVE moles
-end
#-----
# Fe(2)

```

```

# Y_Fe/HC = (36*55.847) / 92 = 21.80 (mg/mg)
# (using mol. weight of toluene)
# C7H8 + 36 Fe+3 + 21 H2O = 7 HCO3- + 36 Fe+2 + 43 H+
# -> Y_Fe/HC = 36 (mol/mol)
#-----
Fe(2)
-start
5 mFE3_max = 25/1000/55.847
10 mHy_carb = tot("Hy_carb")
20 mO2 = mol("O2")
30 mNO3 = tot("N(5)")
40 mSO4 = tot("S(6)")
50 mFE2 = tot("Fe(2)")
60 mFE3 = mFE3_max - mFE2
70 if (mHy_carb ≤ 1e-08) then goto 200
80 if (mFE3 ≤ 1e-08) then goto 200
90 inhib_ox = 0.001/1000/32 / (0.001/1000/32 + mO2)
100 inhib_no3 = 0.001/1000/62 / (0.001/1000/62 + mNO3)
110 monod_fe3 = mFE3 / (0.5/1000/55.847 + mFE3)
120 rate = parm(1) / 86400 * mHy_carb * inhib_ox
130 rate = rate * inhib_no3 * monod_fe3
180 moles = rate * time
200 SAVE moles
-end
#-----
# Sulfate # Y_SO4/HC = (4.5 * 96) / 92 (mg/mg)
# (using mol. weight of toluene)
# C7H8 + 4.5 SO4-2 + 3 H2O + 2 H+ = 7 HCO3- +4.5 HS-
# -> Y_SO4/HC = 4.5 (mol/mol)
#-----
S(6)
-start
5 mFE3_max = 25/55.847/1000
10 mHy_carb = tot("Hy_carb")
20 mO2 = mol("O2")
30 mNO3 = tot("N(5)")
40 mFE2 = tot("Fe(2)")

```

```

50 mSO4 = tot("S(6)")
60 mFE3 = mFE3_max - mFE2
70 if (mHy_carb ≤ 1e-08) then goto 200
80 if (mSO4 ≤ 1e-08) then goto 200
90 inhib_ox = 0.001/1000/32 / (0.001/1000/32 + mO2)
100 inhib_no3 = 0.001/1000/62 / (0.001/1000/62 + mNO3)
110 inhib_fe3 = 0.001/1000/55.847 / (0.001/1000/55.847 + mFE3)
120 monod_so4 = mSO4 / (0.5/1000/96 + mSO4)
130 rate = parm(1) / 86400 * mHy_carb * inhib_ox
140 rate = rate * inhib_no3 * inhib_fe3
150 rate = rate * monod_so4
170 moles = rate * time
200 SAVE moles
-end
#-----
# Methane
# Y_Meth/HC (4.5 * 16) / 92 = 0.78 (mg/mg)
# (using mol. weight of toluene)
# C7H8 + 7.5 H2O = 2.5 HCO3- + 2.5 H+ 4.5CH4
# -> Y_Meth/HC = - 4.5 (mol/mol)
#-----
Meth
-start
1 mMeth_max = 30/16/1000
5 mFE3_max = 25/55.847/1000
10 mHy_carb = tot("Hy_carb")
15 mO2 = mol("O2")
20 mNO3 = tot("N(5)")
25 mSO4 = tot("S(6)")
30 mFE2 = tot("Fe(2)")
40 mMETH = tot("Meth")
50 mCO2 = mMeth_max - mMETH
60 mFE3 = mFE3_max - mFE2
70 if (mHy_carb ≤ 1e-08) then goto 200
80 if (mMETH ≤ 1e-08) then goto 200
90 inhib_ox = 0.001/1000/32 / (0.001/1000/32 + mO2)
100 inhib_no3 = 0.001/1000/62 / (0.001/1000/62 + mNO3)

```

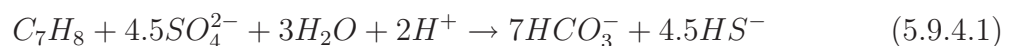
```

110 inhib_fe3 = 0.001/1000/55.847/ (0.001/1000/55.847 + mFE3)
120 inhib_so4 = 0.001/1000/96 / (0.001/1000/96 + mSO4)
130 monod_co2 = mCO2 / (0.5/1000/16 + mCO2)
140 rate = parm(1) / 86400 * mHy_carb * inhib_ox
150 rate = rate * inhib_no3 * inhib_fe3
160 rate = rate * inhib_so4 * monod_co2
180 moles = rate * time
200 SAVE moles
-end
END

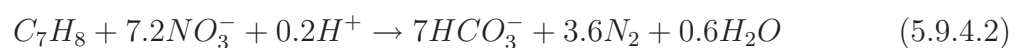
```

Note, as the main purpose of this example is the PHT3D model evaluation, the above rate expressions include many hard-coded reaction parameters such as half saturation and inhibition constants as given in Clement (1997). They might be unsuitable for other site-specific applications. Modifications of those parameters can be done either directly in the database file or, alternatively, and more elegantly, the values can be replaced by `parm(2)`, `parm(3)`, etc and defined separately in `pht3d_ph.dat` (see also **Example 1**). For demonstration purposes the necessary conversions of parameter values due to different units ( $mg L^{-1}$  vs.  $mol L_w^{-1}$ ) are explicitly included in the individual rate expressions. The time unit used for the definition of reaction constants in `pht3d_ph.dat` is **days**, as in Clement (1997). However, a conversion to **seconds** is included as part of the **RATES** definition in the `pht3d_datab.dat` file.

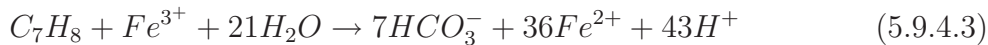
**5.9.4 Data input for the PHREEQC interface package file** As mentioned above, the PHREEQC-2 interface package file for the present example holds the reaction parameters and the information that determines the reaction stoichiometry, i.e, the factors at which species/components are destroyed or produced relative to the computed rate as defined in the **RATES** section of the `pht3d_datab.dat` file. The correct stoichiometry can be extracted from the balanced mineralisation reactions. For toluene, which is used by Clement (1997) as a representative compound for the BTEX mixture, this is in the case of aerobic conditions



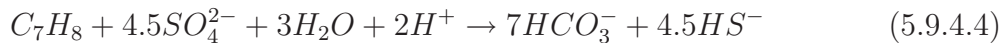
for denitrifying conditions



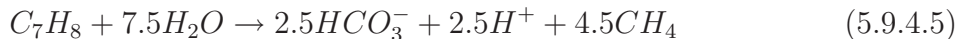
for iron-reducing conditions



for sulphate-reducing conditions



and for methanogenic conditions



As can be seen, for example from reaction (5.9.4.4), the removal of one mol of toluene consumes 4.5 mol of sulphate. These and the other appropriate values need to be incorporated into the **pht3d\_ph.dat** file. The complete entries for this file are

```

2 25 0 1E-10 0.001
0
5
0
0 0
0
5 0 0 0
O(0) 1
.1
-formula O2 -9.0 Hy_carb -1.0
N(5)
1
.008
-formula NO3- -7.2 Hy_carb -1.0
Fe(2)
1
.0005
-formula Fe+2 36.0 Hy_carb -1.0
S(6)
1
.00025
-formula SO4-2 -4.5 Hy_carb -1.0
Meth 1

```

.0001

-formula Meth 4.5 Hy\_carb -1.0

Cl

Na

Hy\_carb

pH

pe

Sodium (*Na*) and chloride (*Cl*) were only included to simultaneously (and optionally) track the fate of non-reactive species/components.

**5.9.5 Data input for the basic transport package file** The basic transport package file **pht3dbtn.dat** for this example is very similar to the appropriate file for **Example 8**. The main difference is the different number of components, their different initial concentrations and the different temporal discretisation. The initial molar concentrations are listed in Table 5.21,

Table 5.21: Aqueous concentrations used in Example 9.

Aqueous component	$C_{init}$ ( $mol L_w^{-1}$ )	$C_{well}$ ( $mol L_w^{-1}$ )
pH	7.0	7.0
pe	14.0	14.0
Hy_carb	0.0	$1.087 \times 10^{-2}$
O(0)	$2.5 \times 10^{-4}$	0.0
N(5)	$3.226 \times 10^{-4}$	0.0
Fe(2)	0.0	0.0
S(6)	$1.041 \times 10^{-4}$	0.0
Meth	0.0	0.0
Na	$1.0 \times 10^{-3}$	$1.0 \times 10^{-3}$
Cl	$1.0 \times 10^{-3}$	$1.0 \times 10^{-3}$

The entries for the basic transport package file are:

**Example 9**

**Kinetically controlled BTEX concentration after Clement (1997)**

**1 31 51 1 10 8**

**T L M**

```

T T T F T T
0
0 10(20G14.0) -1 A7. DELR(NCOL)
0 10(20G14.0) -1 A8. DELC(NROW)
0 10(20G14.0) -1 A9. HTOP(NCOL,NROW); Top of the first layer
0 10(20G14.0) -1 A10. Thickn. of layer 1
0 0.3(20G14.0) -1 A11. Effective porosity of layer 1
100 1(20I3) -1 A12. ICBUND matrix of Layer 1
-1 1 1 1 1 1 1 1 1 1 1 1 1 1 1 1 1 1 1 1 1 1 1 1 1 1 1 1 1 1 1 1
1 1 1 1 1 1 1 1 1 1 1 1 1 1 1 1 1 1 1 1 1 1 1 1 1 1 1 1 1 1 1 1
1 1 1 1 1 1 1 1 1 1 1
-1 1 1 1 1 1 1 1 1 1 1 1 1 1 1 1 1 1 1 1 1 1 1 1 1 1 1 1 1 1 1 1
1 1 1 1 1 1 ....
...
... for all 31 rows ...
...
-1 1 1 1 1 1 1 1 1 1 1 1 1 1 1 1 1 1 1 1 1 1 1 1 1 1 1 1 1 1 1 1
1 1 1 1 1 1 1 1 1 1 1 1 1 1 1 1 1 1 1 1 1 1 1 1 1 1 1 1 1 1 1 1
1 1 1 1 1 1 1 1 1 1 1
0 .00025 0 A13. Start. conc. in layer 1 for spec. # 1O(0)
0 3.226E-04 0 A13. Start. conc. in layer 1 for spec. # 2N(5)
0 0 0 A13. Start. conc. in layer 1 for spec. # 3Fe(2)
0 .0001041 0 A13. Start. conc. in layer 1 for spec. # 4S(6)
0 0 0 A13. Start. conc. in layer 1 for spec. # 5Meth
0 0.001 0 A13. Start. conc. in layer 1 for spec. # 6Na
0 0.001 0 A13. Start. conc. in layer 1 for spec. # 7Cl
0 0 0 A13. Start. conc. in layer 1 for spec. # 8Hy_carb
0 7 0 A13. Start. conc. in layer 1 for spec. # 9pH
0 14 0 A13. Start. conc. in layer 1 for spec. #10pe
1E+30 .05
0 0 0 0 T
41
0 10 20 30 40 50 60 70
80 90 100 110 120 130 140 150
160 170 180 190 200 210 220 230
240 250 260 270 280 290 300 310
320 330 340 350 360 370 380 390

```

```

400
0 1
T 1
400 40 1
0 50000 1 0

```

**5.9.6 Data input for the advection package file** The input for the advection package is similar to the input for **Example 8**.

**5.9.7 Data input for the dispersion package file** The input for the dispersion package is similar to the input for **Example 8**.

**5.9.8 Data input for the source/sink mixing package file** Like in **Example 8**, the contamination source zone is simulated via injection of the contaminant, i.e., toluene. Concentrations of other species/components are set to 0 (see Table 5.21). The entries for the source sink/mixing file **pht3dssm.dat** are:

```

T F F F F F
2063
1 16 16 0 2 0 0 0 0 .002 .002 .0108696 7 4

```

**5.9.9 Simulation results** The injection, transport and degradation of the hydrocarbon contaminant successively consumes the electron acceptors near and downstream of the hypothetical source zone. As a result of the model approach used in the simulation, they are consumed in the pre-defined order, i.e., redox sequence. The simulation results of PHT3D and RT3D were compared for a simulation time of one year. The contour plots shown in Fig. 5.11 for hydrocarbon, oxygen, and nitrate concentrations compare extremely well, however, some slight differences exist for  $Fe^{2+}$ .

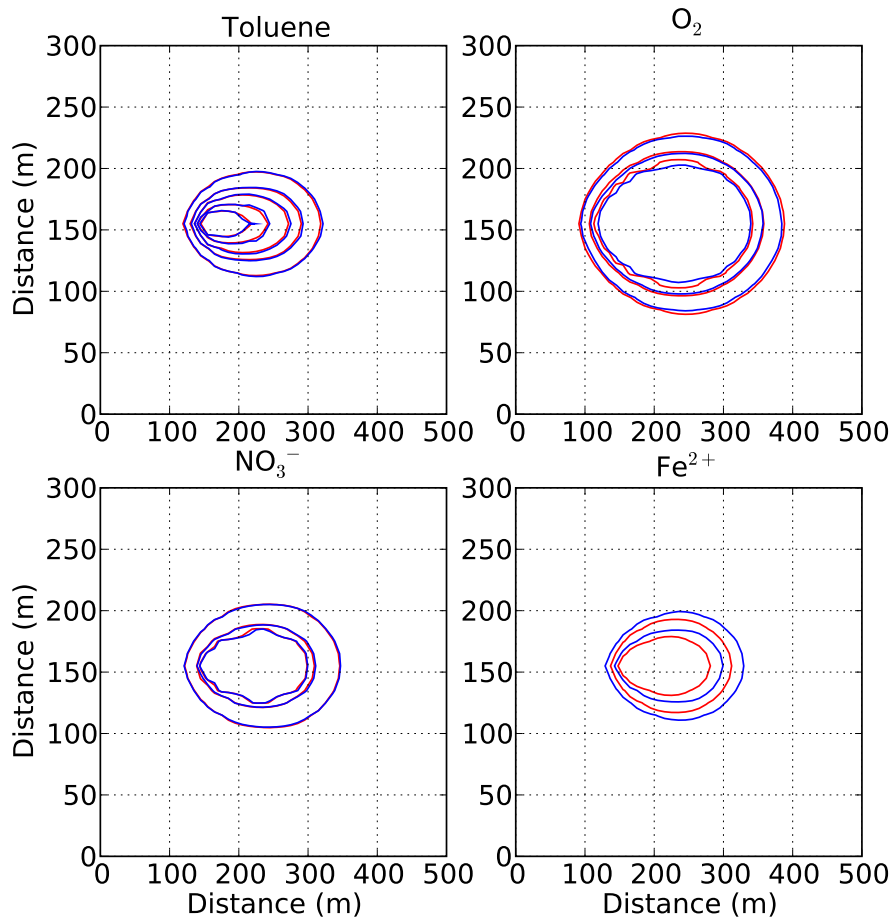


Figure 5.11: Comparison of concentration contours between PHT3D (dashed lines) and RT3D (solid lines) simulations for hydrocarbon (toluene, 1, 5, 10, 20 and 30  $mg L^{-1}$ ), oxygen (0.5, 2 and 3.5  $mg L^{-1}$ ), nitrate (1, 4 and 16  $mg L^{-1}$ ) and dissolved iron(II) (2, 8 and 32  $mg L^{-1}$ ) concentrations after one year simulation time.

## 5.10 Example 10: Dissolution, degradation and geochemical response

**5.10.1 Introduction** This is a second example demonstrating the degradation of hydrocarbon compounds. It illustrates a different, more geochemically based approach to simulating the biodegradation of oxidisable compounds. In contrast to the previous case (Example 9), where the primary biodegradation reactions were modelled as single oxidation-reduction reactions with a fixed reaction stoichiometry, here, a so-called two-step process modelling approach is employed (Brun and Engesgaard, 2002). The approach follows the argumentation of Postma and Jakobsen (1996) who point out, that if the first step of a redox reaction, the oxidation step, is the rate-limiting step, the second, electron-accepting step, can be viewed and modelled as a reversible equilibrium reaction. Given this assumption, kinetic biodegradation reactions of oxidisable organic substances can be modelled without pre-defining the redox sequence, i.e., the sequence of electron acceptor consumption. Instead, the reduction reaction is simply modelled through the addition of organic compounds (e.g.,  $C_7H_8$ , Toluene) as irreversible reaction to/with the inorganic background water (Prommer et al., 1999a). The progressing, kinetically controlled biodegradation reaction converts successively the organic carbon to inorganic carbon and consumes thereby the oxidation capacity provided by aqueous and mineral form electron acceptors. In the present example, a point source pollution is assumed to be created through the dissolution of benzene, toluene, ethylbenzene and xylene from a non aqueous phase liquid (NAPL) source zone into the uncontaminated passing groundwater. In the aqueous phase, benzene, toluene, ethylbenzene and xylene undergo advective-dispersive transport and biodegradation. Apart from the mineralisation reaction of the organic compounds, further geochemical changes, e.g., the precipitation of minerals, will occur in response to the primary biodegradation reaction. The background water composition in this simulation example is based on a water sample from a shallow sand aquifer in Perth/Western Australia. However, the originally anaerobic background water composition was equilibrated with oxygen.

**5.10.2 Spatial discretisation and flow problem** The model domain consists of an idealised, heterogeneous unconfined aquifer of 200 m length, 50 m width and 10 m thickness. It is discretised into 80 columns, 40 rows and 1 layer using equally sized grid-cells. The groundwater flow is driven by a head difference of 2 m between the influent and the effluent model boundary. A non-uniform flow field results from the zonal conductivity distribution that is depicted in Figure 5.12.

Table 5.22: Flow and transport parameters used in Example 10.

Flow simulation	steady state
Total simulation time ( <i>days</i> )	500
Stress period	1
Time steps	50
Grid spacing (Columns/Rows) ( <i>m</i> )	$2.5 \times 1.25$
Model length ( <i>m</i> )	200
Model width ( <i>m</i> )	50
Aquifer type	unconfined
Horizontal hydraulic conductivity $kf1, kf2, kf3$ ( $m\ d^{-1}$ )	10,4,2
Height datum aquifer (bottom) ( <i>m</i> )	0
Height datum aquifer (top) ( <i>m</i> )	10
Prescribed head influent boundary ( <i>m</i> )	5
Prescribed head effluent boundary ( <i>m</i> )	3
Porosity	0.30
Longitudinal dispersivity ( <i>m</i> )	0.5
Transversal horizontal dispersivity ( <i>m</i> )	0.1

The parameters used for the flow simulation are summarised in Table 5.22 while Figure 5.13 shows head contours and streamlines of the simulated flow field.

**5.10.3 Data input for the database file** The reaction network of this case includes all major anions and cations (see Table 5.23), the BTEX compounds (dissolved and as NAPL phase) and 3 minerals. As discussed for previous examples, only the organic compounds (both dissolved and NAPL) will need to be

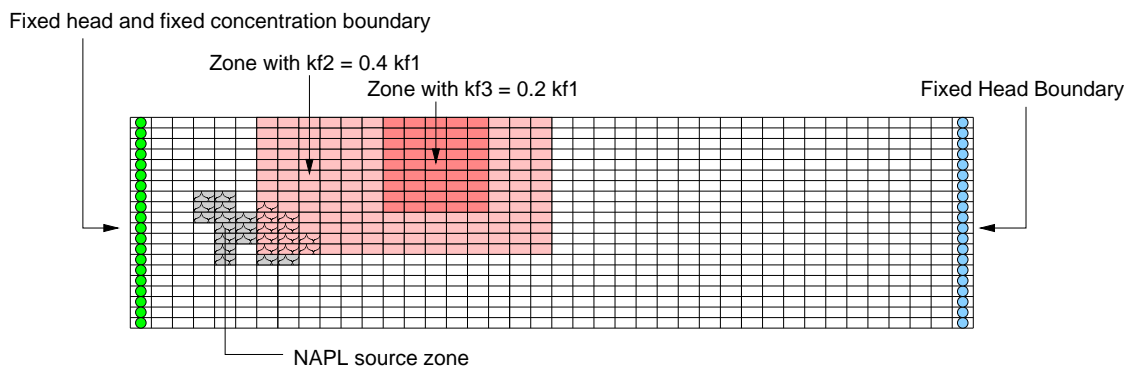


Figure 5.12: Model grid, boundary conditions, hydraulic conductivity zonation and location of contaminant source used in Example 10

Table 5.23: Concentrations of mobile aqueous components used in Example 10.

Aqueous component	$C_{init}$ ( $mol L_w^{-1}$ )	Aqueous component	$C_{init}$ ( $mol L_w^{-1}$ )
pH	6.77	Fe(2)	$1.99 \times 10^{-22}$
pe	13.85	Fe(3)	$6.97 \times 10^{-14}$
C(4)	$9.59 \times 10^{-3}$	K	$4.63 \times 10^{-4}$
C(-4)	0.0	Ca	$4.21 \times 10^{-3}$
O(0)	$5.00 \times 10^{-4}$	Mg	$2.64 \times 10^{-3}$
N(5)	$4.31 \times 10^{-6}$	K	$4.63 \times 10^{-5}$
N(3)	0.0	Cl	$5.41 \times 10^{-3}$
N(0)	0.0	Al	$1.27 \times 10^{-7}$
Amm	0.0	Benzene	0.0
S(6)	$3.03 \times 10^{-3}$	Toluene	0.0
S(-2)	0.0	Ethylbenzene	0.0
Na	$4.61 \times 10^{-3}$	Xylene	0.0

Table 5.24: Mineral concentrations used in Example 10.

Mineral	$C_{init}$ ( $mol L_v^{-1}$ )
Calcite ( $CaCO_3$ )	1.0
Goethite ( $FeOOH$ )	$1 \times 10^{-3}$
Pyrite ( $FeS_2$ )	0.0

treated as kinetic species. All other aqueous complexation reactions may be assumed to undergo equilibrium reactions. Similarly the included minerals (calcite, goethite and pyrite) are in the present case also assumed to be in equilibrium with the aqueous phase, an assumption that does not always hold in reality. The details of the inclusion of equilibrium-based aqueous components into the database file has been discussed previously for other examples and is not repeated here. However, the formulation used for the kinetically controlled processes will be discussed. Among the many possibilities for rate expressions that describe kinetically controlled biodegradation of oxidisable organic contaminants (Brun and Engesgaard, 2002; Barry et al., 2002), a simple formulation, a first order reaction, was used in this example. For benzene it was assumed that degradation occurs much slower compared to toluene, which is modelled by assigning a lower reaction rate constant (first-order rate constant) to benzene. The entries into the database file **pht3d\_datab.dat** describing for example the rate of benzene degradation are:

**RATES**

**Benz**

**-start**

**30 mBenz = tot("Benz")**

**60 rate = parm(1)\* mBenz**

**70 moles = rate \* time**

**200 save moles**

**-end**

In this rate expressions the first order rate constant is handled as a variable parameter **parm(1)** that needs to be specified in **pht3d\_ph.dat**. If the conceptual for this problem was that benzene degradation under anaerobic condition is not occurring at all, this could simply be implemented by adding some additional statements to the **RATES** block, which would assure that the degradation rate of benzene is 0 once oxygen is depleted.

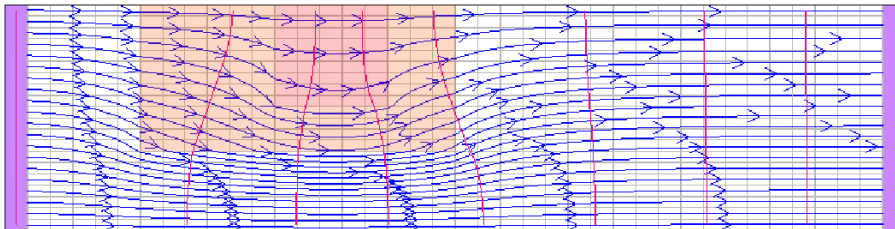


Figure 5.13: Head contours and streamlines of the heterogeneous flow field.

**RATES****Benz****-start****20 mOx = tot("O(0)")****30 mBenz = tot("Benz")****40 if (mOx <= 1e-10) then goto 200****60 rate = parm(1)\* mBenz****70 moles = rate \* time****200 save moles****-end**

Dissolution of NAPLs will occur at grid elements where the concentration of individual or all NAPL compounds is  $> 0$ . The mass transfer rate  $r_{dis_i}$  between the immobile NAPL phase and the dissolved phase is modelled as:

$$r_{dis_i} = \omega_i (C_{sat,mc}^i - C_i) \quad (5.10.3.1)$$

where  $\omega_i$  ( $T^{-1}$ ) is a rate-transfer coefficient approaching infinity for equilibrium dissolution,  $C_i$  ( $ML^{-3}$ ) is the aqueous species concentration of the  $i^{th}$  organic compound and  $C_{sat,mc}^i$  ( $ML^{-3}$ ) is the multicomponent solubility of the  $i^{th}$  organic compound. The multicomponent solubility is calculated according to *Raoult's law*:

$$C_{sat,mc}^i = C_{sat}^i \gamma_i m_i \quad (5.10.3.2)$$

where  $C_{sat}^i$  ( $ML^{-3}$ ) is the single-species solubility,  $\gamma_i$  is the activity coefficient of the  $i^{th}$  organic compound (in the present model assumed to be unity), and  $m_i$  is the mole fraction of the  $i^{th}$  organic compound. The mole fraction is defined as:

$$m_i = \frac{C_n^i}{C_n^{tot}} \quad (5.10.3.3)$$

where  $C_n^i$  is the molar concentration of compound  $i$  in the NAPL phase and  $C_n^{tot}$  is the total molar concentration of all organic compounds in the NAPL phase. The rate expressions for this case can be formulated in the following way:

**Benznapl****-start****10 mBenznapl = tot("Benznapl")****15 if (mBenznapl <= 1e-10) then goto 200****20 solub\_Benz = 0.022820**

```

25 mBenz = tot("Benz")
32 mTolunapl = tot("Tolunapl")
34 mEthynapl = tot("Ethynapl")
36 mXylnapl = tot("Xylnapl")
38 mLowsolubnapl = tot("Lowsolubnapl")
40 m_napl_tot = mBenznapl + mTolunapl + mEthynapl + mXylnapl + mLowsolubnapl
42 if (m_napl_tot <= 1e-10) then goto 200
50 msolub_Benz = mBenznapl / m_napl_tot * solub_Benz
60 rate = parm(1) * (msolub_Benz - mBenz)
70 moles = rate * time
80 if (moles > m) then moles = m
200 save moles
-end

```

Note, that **Benz**, **Tolu**, **Ethy**, **Xyl**, **Benznapl**, **Tolunapl**, **Ethynapl** and **Xylnapl** also need to be defined as **SOLUTION\_MASTER\_SPECIES** and as **SOLUTION\_SPECIES** in the database file as it was previously demonstrated for other kinetic reactants, e.g., for **Species** in **Example 1**.

**5.10.4 Data input for the PHREEQC interface package file** The interface package file contains, apart from the details that were discussed for previous examples, the essential information that is needed to simulate the geochemical response to the degradation of the organic compounds within the inorganic hydrogeochemistry of the aquifer, i.e., changes in aqueous component and mineral concentrations.

```

2 25 0 1E-10 .001
0
18
3
0 0
0
4 0 0 4
Benz 1
1E-08
-formula Benz -1.0 C6H6 1.0
Tolu 1

```

.0000002  
-formula Tolu -1.0 C7H8 1.0  
Ethy 1  
2E-10  
-formula Ethy -1.0 C8H10 1.0  
Xyl 1  
2E-10  
-formula Xyl -1.0 C8H10 1.0  
Al  
C(4)  
C(-4)  
Ca  
Cl  
Fe(2)  
Fe(3)  
K  
Mg  
N(3)  
N(5)  
N(0)  
Na  
O(0)  
S(-2)  
S(6)  
pH  
pe  
Benznapl 1  
.0000001  
-formula Benznapl -1.0 Benz 1.0  
Tolunapl 1  
.0000001  
-formula Tolunapl -1.0 Tolu 1.0  
Ethynapl 1  
.0000001  
-formula Ethynapl -1.0 Ethy 1.0  
Xylnapl 1  
.0000001

**-formula Xylnapl -1.0 Xyl 1.0**

**Calcite**

**Goethite**

**Pyrite**

The stoichiometric relationship between organic compound removal and the changes in the inorganic aquifer geochemistry is defined through the lines **-formula Benz -1.0 C6H6 1.0**, **-formula Tolu -1.0 C7H8 1.0**, **-formula Xyl -1.0 C8H10 1.0** and **-formula Ethy -1.0 C8H10 1.0**, For example, the removal rate of benzene, computed according to its definition in **RATES**, is then multiplied with a factor of **-1.0** whereas a stoichiometric factor of **1.0** applies for the rate at which  $C_6H_6$  is added to the aqueous solution and as a result consumes oxidation capacity.

**5.10.5 Data input for the basic transport package file** The basic transport package file contains the initial concentrations which in this case are defined by the hydrogeochemistry of the uncontaminated aquifer and the NAPL mass that is assumed to be present at the beginning of the simulation. The initial concentrations of the aqueous components are summarised in Table 5.23 and the initial concentrations of the three included minerals are listed in Table 5.24. The contamination source is defined through a total of 104 grid cells at which the initial concentrations of the components **Benznapl**, **Tolunapl**, **Ethynapl** and **Xylnapl** are  $> 0$ . The location of these grid-cells can be seen in Figure 5.12. The boundary conditions to be used for the transport simulations are defined in this package. A fixed concentration boundary condition (**ICBUND** = -1) is used for the influent (upstream) boundary, as indicated in Figure 5.12. This means that the inflow water composition is kept constant. This inflow water composition, which is similar to the initial uncontaminated water composition, was equilibrated with respect to the minerals that are assumed to be present in the aquifer. The equilibration was carried out outside of PHT3D through a PHREEQC-2 batch-type simulation.

**5.10.6 Data input for the advection package file** The MMOC scheme is used for the simulation of advective transport. The entries for the advection package input file **pht3dadv.dat** are:

**2 .75 5000 0**

**3 .5**

**1 0 15**

**5.10.7 Data input for the dispersion package file** A longitudinal dispersivity of 0.5 *m* and transversal dispersivities of 0.1 *m* (horizontal) and 0.05 *m* (vertical) were used in the simulations. The resulting entries for the dispersion package input file **pht3ddsp.dat** are:

```
0 0.5(20G14.0) -1 C1. Longit. disp. of layer 1
0 0.2(1G14.0) -1 C2. TRPT=(horiz. transv. disp.) / (Long. disp.)
0 0.1(1G14.0) -1 C3. TRPV=(vert. transv. disp.) / (Long. disp.)
0 0(1G14.0) -1 C4. effective molec. diffusion coeff. [L2/T]
```

**5.10.8 Simulation results** Like in the previous example (**Example 9**), the degradation of the petroleum hydrocarbon compounds creates a geochemically reduced zone with the most reducing, the methane producing zone in the plume centre. As can be seen in Figure 5.14, at the end of the 500 day simulation period dissolved benzene forms a rather wide plume that reaches the effluent end, i.e., the downstream boundary of the model domain. In contrast, the toluene plume, which degrades at a much higher rate, is much smaller and has stabilised in size within the model domain as a result of both aerobic and anaerobic degradation. The partial mineralisation of the organic compounds is accompanied by the consumption of oxygen, nitrate, goethite and sulphate which act as electron acceptors. After the 500 days of simulation time, oxygen is depleted in a large area downstream of the NAPL source (see Figure 5.14). The extent of the depleted zone is smallest in size for the less thermodynamically favourable aqueous electron acceptors, e.g., sulphate and goethite. Methane forms at locations where  $CO_2$  acts as electron acceptor, once all other more favourable electron acceptors are depleted. In response to the mineralisation reactions, secondary reactions occur and modify concentrations of other dissolved species/components and minerals. For example, calcite precipitation or dissolution acts in the present example as a buffer preventing strong changes of pH during the mineralisation reactions. Accordingly, the initially homogeneous distribution of (dissolved) calcium is also changing in response to the biodegradation reactions (Figure 5.14).

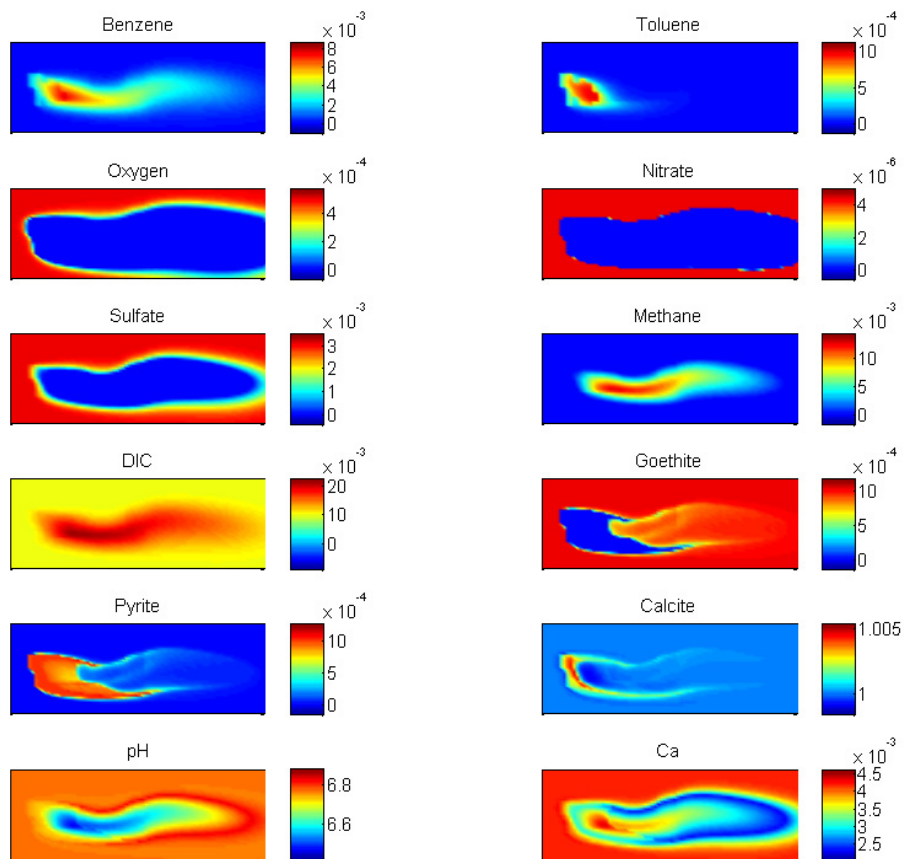


Figure 5.14: Simulated aqueous and mineral concentrations after 500 days simulation time.

## 5.11 Example 11: Biogeochemical and isotopic changes during BTEX/PAH degradation

**5.11.1 Introduction** As already discussed for the last two examples (Examples 9 and 10), oxidisable compounds such as aromatic hydrocarbons may be degraded by a combination of various redox reactions involving both dissolved (oxygen, nitrate, sulfate) or mineral-form (e.g., iron/manganese oxides) electron acceptors. Several numerical studies (Cirpka et al., 1999; Prommer et al., 2006), controlled laboratory-scale experiments (Bauer et al., 2008, 2009a,b; Rees et al., 2007) and field investigations (Davis et al., 1999; Tuxen et al., 2006; van Breukelen and Griffioen, 2004) suggested that biochemical turnover rates may be particularly high at contaminant plume fringes where soluble electron donors and acceptors mix due to transverse hydrodynamic dispersion. This conceptual model implies the occurrence of steep geochemical gradients and the formation of narrow bioactive zones at locations where electron donors and electron acceptors overlap. In addition, scenario-type numerical modeling of fringe-controlled degradation processes by van Breukelen and Prommer (2008) indicated that the associated accelerated isotopic enrichment in fringe zones may also lead to the formation of distinct isotopic gradients across contaminant plumes.

Following from the modelling concepts introduced in some of the previously discussed problems, Example 11 illustrates particularly the simulation capabilities related to (i) the quantification of microbial processes and (ii) the associated isotope fractionation processes that occur during the microbially mediated degradation of organic compounds.

In this specific example the simultaneous degradation of multiple hydrocarbon compounds under sulfate reducing conditions and the associated carbon and sulfur isotope fractionation processes were simulated for a selected transect along a contaminant plume's centre axis. The contaminated site and various research activities related to its pollution has been described by several publications (Anneser et al., 2008; Winderl et al., 2008). The modelling study itself was reported in full detail in Prommer et al. (2009).

**5.11.2 Field Site** The study site is located at a former gasworks site. The aquifer below the site received considerable input of mono- and polycyclic aromatic hydrocarbons (especially toluene and naphthalene) during the production of tar oil compounds from 1897 to 1967. The saturated zone is characterized by relatively homogeneous quaternary sediments exhibiting a mean hydraulic conductivity of  $1 \times 10^{-3} \text{ ms}^{-1}$ . A layer of low permeable Tertiary fine sand confines the aquifer

at the bottom. Groundwater flows from east to west along a hydraulic gradient of 0.006 at an estimated mean pore velocity of  $1.5 \text{ m d}^{-1}$  (Anneser et al., 2008)

Excavation of soil ( $> 55,000 \text{ t}$ ) between 1995 and 1997 removed most of the tar oil from the unsaturated zone, but failed to completely remove the nonaqueous phase liquid (NAPL) contaminant from the saturated portion of the aquifer, especially where soils were covered by buildings. The remaining contaminants formed a plume of about 200 m length and 30 m width, consisting mainly of aromatic hydrocarbons, above all toluene, xylenes, and naphthalene. A network of several fully screened and multilevel sampling wells was established in order to monitor the distribution of the contaminants (Figure 5.15). In June 2005, a novel high spatial resolution multilevel well with vertical sampling intervals of 2.5-33 cm was installed in the centerline of the BTEX plume, approximately 15 m downstream of the presumed tar oil source. Simultaneous sampling of up to 32 filter ports at low pumping rates using protocols specifically tailored to the analysis of low sampling volumes allowed the identification of steep geochemical and isotopic gradients as well as various microbiological parameters. Compound-specific stable isotope analysis of aromatic hydrocarbons ( $\delta^{13}\text{C}$ ) and for groundwater sulfate ( $\delta^{34}\text{S}$ ) was performed at the high resolution multilevel well in addition to the standard geochemical analysis.

**5.11.3 Model Setup** The dimension of the modelled transect (40 m) was selected such that the model would capture the plume evolution between the source zone and the multilevel well. In vertical direction, the model domain extended between 22 m asl (above sea level; bottom of aquifer) and 34 m asl (i.e., above the groundwater table). Groundwater flow at the site was generally unsteady, exhibiting small interannual water table fluctuations of mostly  $< 40 \text{ cm}$ . However, around the time for which the model was set up and calibrated, the time-scale of the transport between source zone and the monitoring well (8 days) was smaller than the time-scale of significant water table changes. For this study it was therefore assumed that the flow field and the contaminant plumes were approximately at steady state. The reactive transport model was run for a spin-up period until microbial lag times were overcome and steady state concentrations were established throughout the model domain for all aqueous species. Further details on the model discretization and the flow model setup are listed in Table 5.25.

**5.11.4 Reaction Network** A conceptual model for the reactive processes was developed by qualitatively interpreting the measured hydrogeochemical data

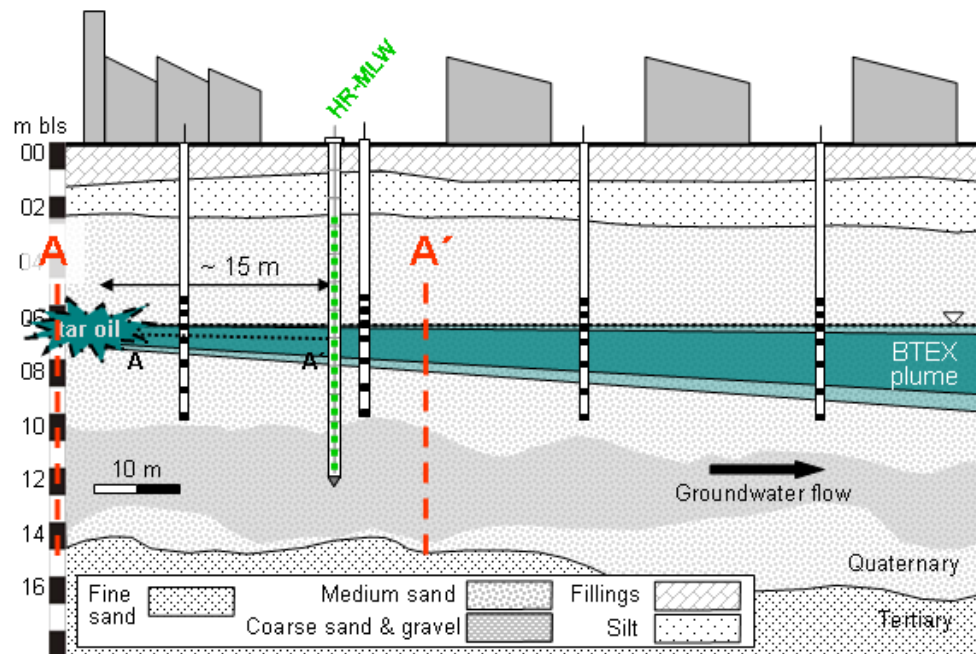


Figure 5.15: Example 11 - Study site, including the high-resolution multilevel well (HR-MLW) in relation to the main contaminant source and the BTEX/PAH plumes (cross-sectional view). In order to enhance removal of the contaminants, a pump and treat scheme was implemented and groundwater from the hydrocarbon-impacted areas is now constantly extracted and treated off-site in a bioreactor. The treated water is re-infiltrated into the aquifer via an infiltration ditch located 125 m upstream of the extraction wells. To characterize and monitor the distribution of the contaminants, more than 50 fully screened wells were installed at the site between 1995 and 2007. In addition, since 1997, 18 multilevel monitoring wells were installed. These provided an improved delineation of the contaminant plume with concentration profiles available both along and across the plume axis.

Table 5.25: Flow/transport model parameters used in Example 11

Flow and physical transport parameters	Value,Unit
model dimensions $l_x \times l_y \times l_z$	40 m $\times$ 1 m $\times$ 13 m
number of layers	58
layer thickness $\Delta z$	0.05 m – 1 m
hydraulic conductivity $k_f$	$1 \times 10^{-3} \text{ m s}^{-1}$
porosity $n_e$	0.3
longitudinal dispersivity $\alpha_L$	0.05 m
transversal dispersivity $\alpha_T$	0.005 m
(average) pore velocity in longitudinal direction	$1.53 \text{ m d}^{-1}$
simulation time	60 d

and translating it into a numerical model by formulating a reaction network of mixed equilibrium and kinetically controlled homogeneous and heterogeneous reactions. This site-specific reaction network was then implemented into the **pht3d\_ph.dat** file. The final version of the reaction network contained

- all major ions
- a limited number of minerals/mineral reactions potentially affecting aqueous concentrations
- all major dissolved organic contaminants found at the site
- the corresponding immobile NAPL compounds and
- biomass consisting of sulfate-reducing bacteria.

The specific organic compounds included in the reaction network were

- benzene ( $C_6H_6$ )
- toluene ( $C_7H_8$ )
- ethylbenzene ( $C_8H_{10}$ )
- o-xylene ( $C_8H_{10}$ )
- m/p-xylene ( $C_8H_{10}$ )
- naphthalene ( $C_{10}H_8$ )

- acenaphthene ( $C_{12}H_{10}$ )
- and fluorene ( $C_{13}H_{10}$ ).

Among these compounds, toluene is generally seen to be the most readily oxidisable compound (Edwards et al., 1992; Thierrin et al., 1993), followed by the other monoaromatic hydrocarbons and naphthalene, whereas acenaphthene and fluorene are considered to degrade slowly or potentially to be recalcitrant under sulfate reducing conditions (Meckenstock et al., 2004; Spormann and Widdel, 2000). For each organic compound two separate species were defined (van Breukelen and Prommer, 2008; Prommer et al., 2008; van Breukelen et al., 2005), one representing the lighter carbon pool ( $^{12}C$ ) and one describing the heavier fraction ( $^{13}C$ ). Similarly, redox states of sulfur, S(VI) and S(-II), were separated into a heavier ( $^{34}S$ ) and a lighter ( $^{32}S$ ) fraction. The equilibrated aqueous solution representing the ambient water composition is given in 5.26.

Previous investigations at the study site have identified microbially mediated sulfate reduction as the key process that is generally predominantly responsible for the mineralization of aromatic hydrocarbons and for the secondary geochemical changes triggered by the primary biodegradation reactions (Anneser et al., 2008; Winderl et al., 2008; Wisotzky and Eckert, 1997). For example, molecular analysis of the microbial community identified sulfate reducers (i.e., *Desulfocapsa* and *Desulfosporosinus*) as dominant microorganisms in the aquifer (Winderl et al., 2008).

These studies also found that >97% of the microbial community is attached to the sediments. In the numerical model, microbial activity was represented by a consortium of sediment-bound sulfate reducing bacteria (SRB). Concentrations of SRB were assumed to be affected by growth and decay, as discussed in, for example, Prommer et al. (2002b, 2006):

$$\frac{\partial X}{\partial t} = \frac{\partial X}{\partial t} \Big|_{growth} + \frac{\partial X}{\partial t} \Big|_{decay} \quad (5.11.4.1)$$

where  $X$  is the concentration of the SRB. Microbial growth, which quantifies the rate at which organic carbon from  $n_{org}$  different organic compounds (i.e., from the various aromatic hydrocarbons) is converted to cell material, was modelled as

$$\frac{\partial X}{\partial t} \Big|_{growth} = \sum_{i=1, n_{org}} v_{max,i} Y_{X,i} \frac{C_{Org,i}}{K_{Org,i} + C_{Org,i}} \frac{C_{Sulf}}{K_{Sulf} + C_{Sulf}} X \quad (5.11.4.2)$$

where  $v_{max}$  is the maximum microbial uptake rate,  $C_{org}$  is the concentration of the hydrocarbon compound,  $C_{sulf}$  is the sulfate concentration,  $K_{org}$ , and  $K_{sulf}$

Table 5.26: Initial (ambient) and upgradient boundary water composition used in Example 11, corresponding to measured values from an upgradient infiltration well.

aqueous component	concentration [mol L <sup>-1</sup> ] <sup>b</sup>
O(0) <sup>a</sup>	0
Ca	$4.629 \times 10^{-3}$
Mg	$7.748 \times 10^{-4}$
Na	$2.488 \times 10^{-3}$
K	$2.943 \times 10^{-4}$
Fe(2) <sup>a</sup>	$5.871 \times 10^{-10}$
Fe(3) <sup>a</sup>	0
Cl	$3.007 \times 10^{-3}$
C(4) <sup>a</sup>	$6.652 \times 10^{-3}$
N	$1 \times 10^{-4}$
pH	7.288
pe	-4.007
sulfate (light)	$2.192 \times 10^{-3}$
sulfate (heavy)	$1.021 \times 10^{-4}$
sulfide (light)	0
sulfide (heavy)	0

<sup>a</sup> Values in parentheses indicate valence.

<sup>b</sup> Except pH and pe at bottom of the table.

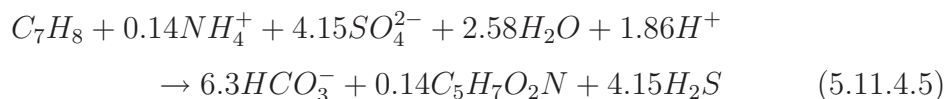
are the appropriate halfsaturation constants and  $Y_x$  is a stoichiometric factor expressing microbial yield. Many factors may influence bacterial decay, including protozoan grazing, contaminant toxicity, and lack of nutrients. However, little quantitative information is available to describe these effects on microbial decay, in particular under in situ conditions. Therefore, the decay term was described using the standard assumption of a linear dependence on the biomass concentration:

$$\left. \frac{\partial X}{\partial t} \right|_{decay} = -k_{dec}X \quad (5.11.4.3)$$

where  $k_{dec}$  is a decay rate constant. The removal rate of the  $i^{th}$  organic compound was proportional to the microbial growth rate:

$$\frac{\partial C_{Org,i}}{\partial t} = v_{max,i} Y_{Org,i} \frac{C_{Org,i}}{K_{Org,i} + C_{Org,i}} \frac{C_{Sulf}}{K_{Sulf} + C_{Sulf}} X \quad (5.11.4.4)$$

The stoichiometric factor  $Y_{Org,i}$  can be determined from the balanced degradation reactions that incorporate growth and thus a partial incorporation of the (degraded) organic carbon into cell mass. A microbial efficiency of 10% was assumed for sulfate reduction (Beller et al., 1992). For example, the reaction stoichiometry for toluene degradation under sulfate-reducing condition is then



where  $C_5H_7O_2N$  is the nominal molecular formula for the microbes. Thus, the stoichiometric factor  $Y_{Toluene}$  yields 0.14 (see Table 5.27 for all other reactions).

**5.11.5 Carbon Isotope Fractionation** While the use of stable isotope signatures as indicators of microbially mediated removal of aromatic hydrocarbons has become a standard tool (Griebler et al., 2004; Meckenstock et al., 2004; Richnow et al., 2003), multidimensional numerical modelling studies that included isotope fractionation processes associated with a complex set of biogeochemical reactions were not yet reported for field-scale problems. Molecules containing the heavier isotope  $^{13}C$  degrade at relatively slower rates than those composed exclusively of the more abundant light isotope  $^{12}C$  (Meckenstock et al., 2004). This results in a successively increasing isotopic ratio,  $\delta^{13}C$ , of the residual contaminant during biodegradation. To consider this effect in the numerical model, separate light and heavy fractions were included in the reaction network for each dissolved organic compound (van Breukelen and Prommer, 2008; Prommer et al.,

Table 5.27: Example 11 - Stoichiometry of degradation reactions that include microbial growth, assuming that 10% of the organic carbon is incorporated into biomass.

Compound	Stoichiometry
benzene	$C_6H_6 + 0.12NH_4^+ + 3.45SO_4^{2-} + 2.64H_2O + 1.38H^+$ $\rightarrow 4.40HCO_3^- + 0.12C_5H_7O_2N + 3.45H_2S$
toluene	$C_7H_8 + 0.14NH_4^+ + 4.15SO_4^{2-} + 2.58H_2O + 1.86H^+$ $\rightarrow 6.30HCO_3^- + 0.14C_5H_7O_2N + 4.15H_2S$
ethylbenzene	$C_8H_{10} + 0.16NH_4^+ + 4.85SO_4^{2-} + 2.52H_2O + 2.34H^+$ $\rightarrow 7.20HCO_3^- + 0.16C_5H_7O_2N + 4.85H_2S$
xylene	$C_8H_{10} + 0.16NH_4^+ + 4.85SO_4^{2-} + 2.52H_2O + 2.34H^+$ $\rightarrow 7.20HCO_3^- + 0.16C_5H_7O_2N + 4.85H_2S$
naphthalene	$C_{10}H_8 + 0.2NH_4^+ + 5.50SO_4^{2-} + 5.40H_2O + 1.80H^+$ $\rightarrow 9.00HCO_3^- + 0.20C_5H_7O_2N + 5.50H_2S$

2008; van Breukelen et al., 2005). Therefore, the concentrations of both the lighter and heavier fractions could be tracked individually and the spatial distribution of the isotopic ratios could be computed subsequently from the simulated concentrations of the two fractions. In the model two different microbial uptake rates are assumed for the lighter and heavier fraction, respectively. While the uptake rate of the lighter isotopes was computed after eq 4, the uptake of the heavier isotopes was calculated from

$$\frac{\partial^{13}C_{Org,i}}{\partial t} = \frac{\partial C_{org,i}}{\partial t} \frac{^{13}C_{org,i}}{^{12}C_{org,i}} \alpha_{Org,i} \quad (5.11.5.1)$$

where  $\alpha_{Org,i}$  represents the kinetic isotope fractionation factor, which equals the ratio of the two reaction rates. It can be determined from the enrichment factor  $\epsilon$ :

$$\alpha_{Org,i} = \epsilon + 1 \quad (5.11.5.2)$$

All  $\epsilon$  values used in this study (see Table 2) were adopted from values reported in the literature. Under sulfate-reducing conditions, values for  $\epsilon$  range between -1.8 and -3.7% for monoaromatic hydrocarbons (Meckenstock et al., 2004; Morasch et al., 2004; Wilkes et al., 2000), whereas for naphthalene  $\epsilon$  was assumed to be -1.1% (Griebler et al., 2004).

**5.11.6 Sulfate Reduction and Sulfur Isotope Fractionation** As for carbon isotope fractionation, the preferential conversion of isotopically lighter sulfate during microbial reduction causes an enrichment of the heavier  $^{34}S$  in the residual sulfate pool (Einsiedl and Mayer, 2005). The differential consumption of  $^{32}S$  and  $^{34}S$  sulfate pools is governed by

$$\frac{\partial^{34}SO_4^{-2}}{\partial t} = \frac{\partial SO_4^{-2}}{\partial t} \frac{^{34}SO_4^{-2}}{^{32}SO_4^{-2}} \alpha_{SO_4^{-2}} \quad (5.11.6.1)$$

with  $\alpha_{SO_4^{-2}}$  representing the kinetic isotope fractionation factor for sulfate reduction. The consumption of sulfate as electron acceptor during hydrocarbon mineralization was computed from:

$$\frac{\partial SO_4^{-2}}{\partial t} = \sum_{i=1, n_{org}} \frac{\partial C_{org,i}}{\partial t} Y_{SO_4^{-2},i} \quad (5.11.6.2)$$

where the stoichiometric factor  $Y_{SO_4^{-2},i}$  links the degradation rates of individual hydrocarbon compounds with the corresponding sulfate consumption rates. The overall sulfate reduction rate is governed by the sum of the  $n_{org}$  consumption rates. Following previous reports of enrichment factors from field studies (Bottrell et al.,

1995; Spence et al., 2005), a mean  $\epsilon$  value of -13‰ was used for sulfate isotope fractionation. Measured concentrations of dissolved sulfide were very low, thus suggesting that reduced sulfur was quickly precipitating as  $FeS$  or pyrite. Since the measured dissolved iron concentrations in the ambient water ( $2.0 \times 10^{-7}$  mol  $L^{-1}$ ) as well as in the plume core ( $<5 \times 10^{-6}$  mol  $L^{-1}$ ) were far below the required amount for stoichiometric  $FeS$  or pyrite precipitation, dissolution of goethite was assumed to be acting as primary source of iron in the model. Such a reaction between ferric iron and biogenic sulfide has been reported earlier by Beller et al. (1992) for a case of toluene degradation under sulfate-reducing conditions.

**5.11.7 Contaminant Source Geometry, Source Composition and Dissolution Kinetics** The measurements of dissolved contaminant concentrations and biogeochemical parameters indicated the presence of two distinct contamination sources. Therefore, in the numerical model, two NAPL source zones located 15 m upstream of the multilevel well were assumed to continuously release BTEX and PAH constituents. The thickness of the upper source zone was assumed to be 0.3 m. The lower zone, which was quantitatively less significant and presumably consisted of entrapped NAPL residuals, was only 0.05m thick. The kinetically controlled dissolution rate for each compound from these source zones was computed from Prommer et al. (2002b):

$$\frac{-\partial C_{org,napl}}{\partial t} = \omega (C_{org,aqu} - C_{org,mc}) \quad (5.11.7.1)$$

where  $C_{org,napl}$  and  $C_{org,aqu}$  are the immobile (NAPL) and the aqueous concentration of the hydrocarbon compound, respectively,  $C_{org,mc}$  is the multicomponent solubility and  $\omega$  is a rate transfer constant. Following *Raoult's law*,  $C_{org,mc}$  in eq 10 can be computed from the known single-species solubility of the hydrocarbon compound and its mole fraction  $\gamma_{org}$  in the NAPL mixture:

$$C_{org,mc} = \gamma_{org} C_{org,solub} \quad (5.11.7.2)$$

However, in the present study the NAPL composition and the molar fractions  $\gamma_{org}$  were unknown and had to be estimated during the model calibration (see Table 2).

**5.11.8 Data input for the PHREEQC interface package file** For the PHT3D simulations, the above discussed reaction network can be implemented via

- 12 aqueous components (**NR\_SOL\_MST\_SPEC\_EQU** = 15)

- 3 equilibrium minerals (**NR\_MIN\_EQU** = 3)
- 18 mobile kinetic reactants (**NR\_MOB\_KIN** = 18)
- 9 immobile kinetic reactants (**NR\_IMOB\_KIN** = 9)

The dissolved forms of the organic compounds are modelled as kinetic reactants, whereby the majority of them (benzene, toluene, ethylbenzene, m/p-xylene, o-xylene and naphtalene) occur separately as lighter and heavier isotopes. In contrast, the carbon isotope fractionation of acenaphthene (*Ace*) and fluorene (*Fluor*) was not modelled and both compounds occur only once. Unlike in the standard PHREEQC database, sulfate and sulfide were decoupled from the redox-equilibrium and modelled as kinetic reactants. Additionally they were separated into lighter (*Sulf\_l*, *Sulfid\_l*) and heavier (*Sulf\_h*, *Sulfid\_h*) isotopes. As a result of the decoupling of sulfate/sulfide from the redox equilibrium the partial equilibrium approach demonstrated for Example 10 is not applicable. Therefore the stoichiometry of the degradation reactions under sulfate-reducing conditions is defined in detail for each compound.

The 9 immobile kinetic reactants included in the simulation are the 9 immobile NAPL compounds. The kinetic reaction associated with these compounds is the mass-transfer (NAPL dissolution) reaction. While during this dissolution mass is removed the NAPL compounds the same mass is added as dissolved compounds to the groundwater. However, the added dissolved mass is separately allocated into the lighter and heavier fraction of the compounds, respectively. By adjusting the stoichiometry of this reaction accordingly (i.e., the lighter vs the heavier fraction) it is possible to force the organic compounds to occur at a specific carbon isotope ratio and therefore a specific  $\delta^{13}C$  representative of the undegraded compounds.

The 3 equilibrium minerals included in the simulations occur at the end of the **pht3d\_ph.dat** file. Note, that calcite equilibrium is attained for an SI of 0.41 rather than 0.0 (=default), as indicated by value following the mineral name.

```

2 15 1 0 0
0
12
3
0 0
0
18 0 0 9
Benz_l 2

```

.000025  
.00003  
-formula Benz\_l -1.0 H2O -2.64 H+ -1.38 HCO3- 5.4 Srb 0.12 C5H7O2N -0.12  
-3.6  
-formula Benz\_h -1.0 H2O -2.64 H+ -1.38 HCO3- 5.4 Srb 0.12 C5H7O2N -0.12  
Tolu\_l 2  
.0005  
.00003  
-formula Tolu\_l -1.0 H2O -2.58 H+ -1.86 HCO3- 6.3 Srb 0.14 C5H7O2N -0.14  
Tolu\_h 1  
-2  
-formula Tolu\_h -1.0 H2O -2.58 H+ -1.86 HCO3- 6.3 Srb 0.14 C5H7O2N -0.14  
Ethyl\_l 2  
.0001  
.00003  
-formula Ethyl\_l -1.0 H2O -2.52 H+ -2.34 HCO3- 7.2 Srb 0.16 C5H7O2N -0.16  
Ethyl\_h 1  
-3.7  
-formula Ethyl\_h -1.0 H2O -2.52 H+ -2.34 HCO3- 7.2 Srb 0.16 C5H7O2N -0.16  
Xyl\_l 2  
.000075  
.00003  
-formula Xyl\_l -1.0 H2O -2.34 H+ -1.86 HCO3- 7.2 Srb 0.16 C5H7O2N -0.16  
Xyl\_h 1  
-1.8  
-formula Xyl\_h -1.0 H2O -2.34 H+ -1.86 HCO3- 7.2 Srb 0.16 C5H7O2N -0.16  
Oxy\_l 2  
.0001  
.00003  
-formula Oxy\_l -1.0 H2O -2.34 H+ -1.86 HCO3- 7.2 Srb 0.16 C5H7O2N -0.16  
Oxy\_h 1  
-1.5  
-formula Oxy\_h -1.0 H2O -2.34 H+ -1.86 HCO3- 7.2 Srb 0.16 C5H7O2N -0.16  
Naph\_l 2  
.0001  
.00003  
-formula Naph\_l -1.0 H2O -5.40 H+ -1.80 HCO3- 9.0 Srb 0.2 C5H7O2N -0.2

Naph\_h 1  
-1.1  
-formula Naph\_h -1.0 H2O -5.40 H+ -1.80 HCO3- 9.0 Srb 0.2 C5H7O2N -0.2  
Ace 2  
0  
.00003  
-formula Ace -1.0 H2O -6.28 H+ -2.26 HCO3- 10.8 Srb 0.24 C5H7O2N -0.24  
Fluor 2  
0  
.00003  
-formula Fluor -1.0 H2O -7.22 H+ -2.24 HCO3- 11.7 Srb 0.26 C5H7O2N -0.26  
Sulf\_l(6) 1  
.0001  
-formula Sulf\_lO4-2 -1.0 H2Sulfid\_l 1.0  
Sulf\_h(6) 1  
-13  
-formula Sulf\_hO4-2 -1.0 H2Sulfid\_h 1.0  
Sulfid\_l(-2) 1  
0  
-formula H2Sulfid\_h 0.0  
Sulfid\_h(-2) 1  
0  
-formula H2Sulfid\_h 0.0  
O(0)  
Ca  
Mg  
Na  
K  
Fe(2)  
Fe(3)  
Cl  
C(4)  
N  
pH  
pe  
Benznapl 2  
.0001

.00006  
-formula Benznapl -1.0 Benz\_l 0.989150872302019 Benz\_h 0.0108491276979814  
Tolunapl 2  
.0001  
.155  
-formula Tolunapl -1.0 Tolu\_l 0.9891624689 Tolu\_h 0.0108375311  
Ethylnapl 2  
.0001  
.0225  
-formula Ethylnapl -1.0 Ethyl\_l 0.9891613694 Ethyl\_h 0.0108386306  
Xylnapl 2  
.0001  
.21  
-formula Xylnapl -1.0 Xyl\_l 0.9891569715 Xyl\_h 0.0108430285  
Oxylnapl 2  
.0001  
.1  
-formula Oxylnapl -1.0 Oxy\_l 0.9891604608 Oxy\_h 0.0108395392  
Naphnapl 2  
.0001  
.4  
-formula Naphnapl -1.0 Naph\_l 0.9891569715 Naph\_h 0.0108430285  
Acenapl 2  
.0001  
.08235  
-formula Acenapl -1.0 Ace 1.0  
Flnnapl 2  
.0001  
.11  
-formula Flnnapl -1.0 Fluor 1.0  
Srb 2  
.00001  
.000001  
-formula Srb -1.0 C5H7O2N 1.0  
Calcite 0.41  
Goethite  
Pyrite

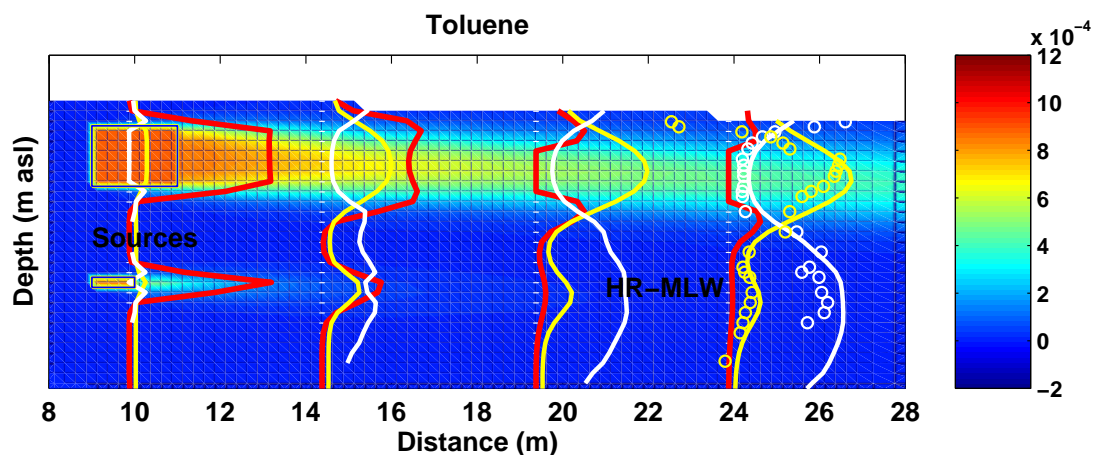


Figure 5.16: Simulated concentration contours of toluene and selected depth profiles of simulated toluene degradation rates (solid red lines) in comparison with the simulated carbon isotope signature of toluene (solid white lines) and sulfur isotope signature (solid yellow lines). Circles indicate corresponding values measured at the high-resolution multilevel well. The dashed white lines show the carbon isotope signature resulting from the simulation in which the lower source zone was deactivated.

**5.11.9 Simulated Fate of BTEX and PAH** In the model simulations, uncontaminated sulfate-containing groundwater passed through the NAPL source zones, where, for each of the simulated organic compounds, mass was transferred to the aqueous phase. At locations where both sulfate and aromatic hydrocarbons were simultaneously present, microbial growth occurred, thereby degrading the various hydrocarbons at compound-specific and spatially varying rates. Figure 5.16 shows the simulated steady-state toluene concentration contours and selected depth profiles of the simulated toluene degradation rates. These depth profiles suggest that near the source zone degradation occurred across the whole NAPL contaminated zone. However, further downgradient, biodegradation became most pronounced at the plume fringe due to the lack of sulfate in the plume core (Figure 5.18). At these locations mixing by transverse dispersion (calibrated  $\alpha_T = 0.5$  mm) allows the degradation to proceed further. Figure 3 shows a detailed comparison of simulated hydrocarbon concentration profiles with the concentrations measured at the well. The plots also show the results from the corresponding (nonreactive) simulations, in which NAPL dissolution could occur but all biodegradation processes were switched off. For all hydrocarbon compounds considered, model simulations

agreed favorably with the measured data. The only noteworthy discrepancy is the slight overestimation of m/p-xylene concentrations in the lower part of the profile, which corresponds to the lower source zone. Substantial differences between simulated reactive and nonreactive concentration profiles at the monitoring well existed mainly for toluene and ethylbenzene, whereas the other concentration profiles were less clearly affected by biodegradation. Note that in the absence of better information, the simplifying assumption was made that the NAPL mixture (mole fractions) was similar in both source zones. In reality, mixtures and thus multicomponent solubilities may differ in space as a result of the spatially varying source depletion rates of the various compounds. The degradation behavior that can be inferred from the model-based interpretation agrees with literature reports that anaerobic oxidation of toluene proceeds appreciably faster compared to other aromatic hydrocarbons. In the calibrated model the computed toluene mass flux reduction between the source zone and the multilevel well was 53% (naphthalene 32%, m/p-xylene 15%, o-xylene 26%, ethylbenzene 46%, benzene 69%) and accounted for 56% of the oxidation capacity (naphthalene 18%, m/p-xylene 12%, o-xylene 10%, ethylbenzene 3%, benzene 0.02%, see also Figure 5.17).

**5.11.10 Simulated Carbon Isotope Signatures** Both measurements and simulation results exhibit clear variations in the carbon isotope enrichment and distinct spatial variations. These were most pronounced for the most degradable compound toluene while being less clear for the more slowly degradable compounds. Similar to the measured data, the simulations for toluene showed significant differences in the isotopic enrichment between the plume center ( $\leq 0.5\text{‰}$ ) and the plume fringes (see Figures 5.18 and 5.19 for comparison). At the lower plume fringe, an enrichment of up to 3.3‰ was measured at the multilevel well, which was accurately reproduced by the model. Figure 5.16 shows the evolution of the simulated carbon isotope ratios between the source zones and the groundwater well via selected depth profiles, whereas Figure 5.18 shows contour plots of both simulated concentrations as well as the corresponding isotope ratios. In the present case the smaller carbon isotope enrichment for toluene in the plume core results from a combination of factors. First, a significant part of the toluene mass removal occurred in the source zone itself, where degradation triggered additional dissolution of toluene that had the initial (non-enriched) carbon isotope ratio. Second, further downgradient of the source zone, degradation proceeded solely at the plume fringes, as discussed before and as indicated by the degradation rate depth profiles shown in Figure 5.16. It was also investigated to what extent the plume originating from the lower source, which was degraded more completely,

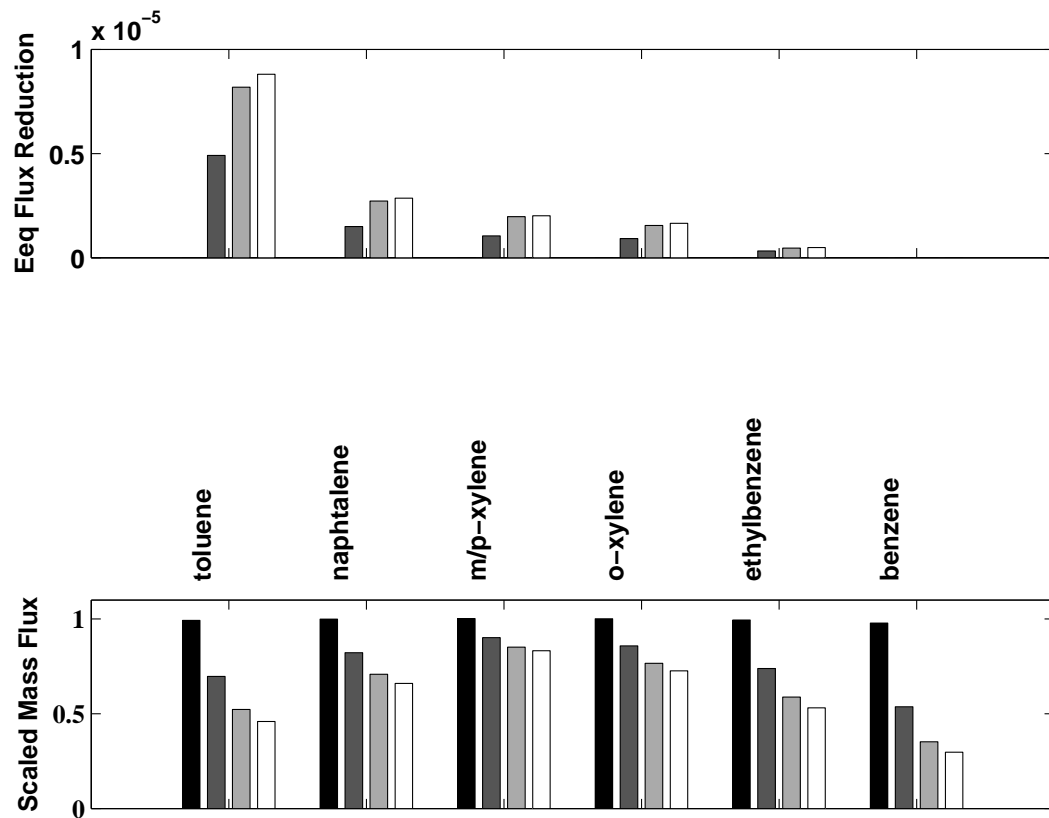


Figure 5.17: Modelled degradation-induced reduction in electron flux at four discrete positions along the flow line between source zone and HR-MLW.

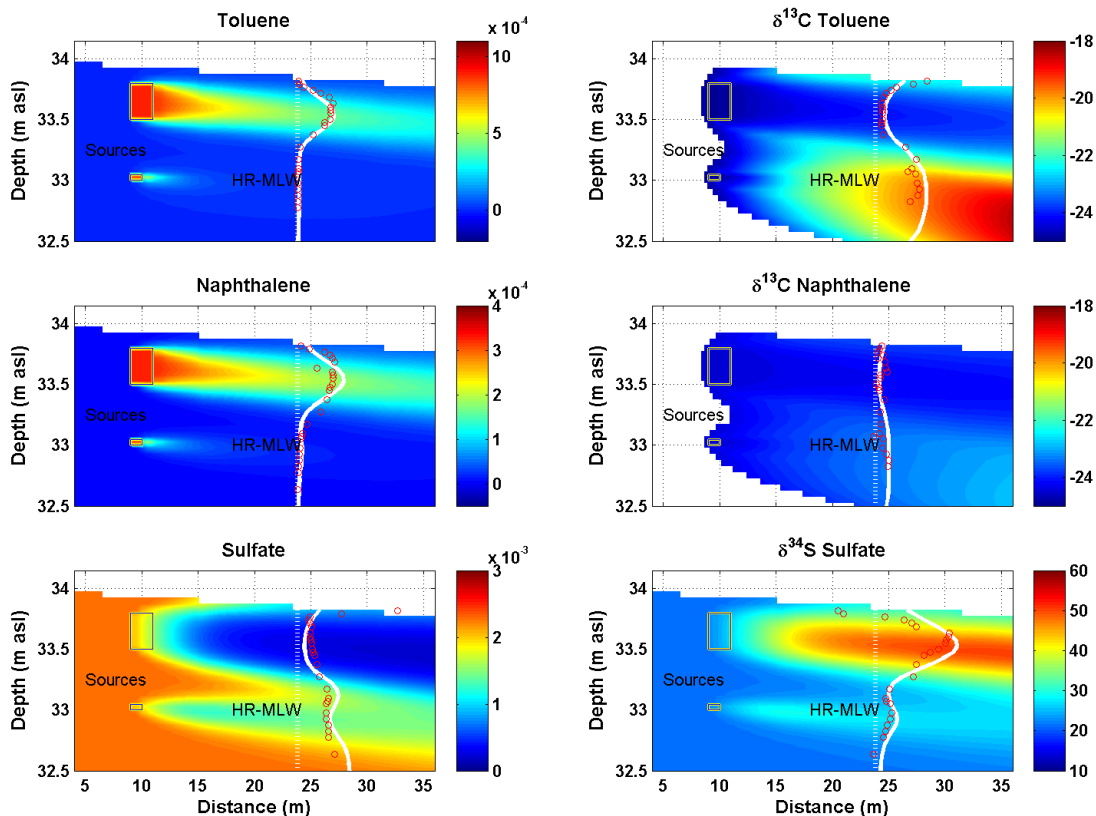


Figure 5.18: Simulated concentration contours of toluene, naphthalene, sulfate and associated isotope signatures. Solid white lines indicate simulated and red circles indicate measured values at the high-resolution well.

affected the carbon isotope profile. While these comparative simulations without the lower source zone indicated some influence on the lower part of the carbon isotope profiles, including the high-resolution well location, the lower source was not responsible for the strong gradients (Figure 5.16). In contrast to toluene, only slight changes in the isotope signatures were observed for the more slowly degrading m/p-xylene and for naphthalene, where the higher number of C atoms in the molecule is additionally responsible for the moderate isotope fractionation (Figure 5.19). Measured benzene concentrations were below the detection limit of the CSIA method, thus isotope ratios were not determined.

**5.11.11 Simulated Sulfate Reduction and Sulfate Isotope Signatures** While groundwater passed through the upper NAPL source zone, oxidation of hydrocarbon compounds consumed most of the sulfate for which the background water concentration was  $2.3 \times 10^{-3} \text{ mol L}^{-1}$ . Downstream of the upper NAPL source zone, sulfate remained at low concentrations throughout the core of

the plume. As shown in Figure 3, the profile of the sulfur isotope signature at the multilevel well exhibits an enrichment of up to 30‰. In contrast to the toluene carbon isotopes, which showed a maximum enrichment outside the plume, the maximum  $^{34}\text{S}$  enrichment occurred in the center of the upper contaminant plume. In the plume core, where most of the sulfate was degraded, the sulfate pool remained enriched in the heavier  $^{34}\text{S}$  isotope, whereas at the plume fringe, transverse dispersion leads to a dilution of the enriched isotope signature. In the lower, presumably much smaller source zone, sulfate was only partially consumed by the hydrocarbons released from the NAPL. Given the numerous simplifying assumptions made for the source definition (geometry, mass transfer rates, contaminant mixture), the modelled sulfate concentration profiles as well as the associated sulfur isotope signature (Figure 5.19) agreed very well with the data collected from the high-resolution well. As Figure 5.19 shows, modelled  $\delta^{34}\text{S}$ -values just below the groundwater table overestimated the measured values, which decreased to 6.6‰ in this zone, i.e., to values below the  $\delta^{34}\text{S}$  value that were assumed to represent ambient conditions. The lower values could possibly point to the reoxidation of previously precipitated iron sulfides when oxidants can access the sulfides during water table fluctuations. However, as a steady state flow was assumed, these oxidation processes could not be represented in the current model. The reoxidation of iron sulfides could also explain the pronounced decrease of the measured pH toward the groundwater table, where it dropped to below the ambient values found deeper in the saturated zone. At this location the simulated pH overestimates the measured values, whereas it is in good agreement elsewhere.

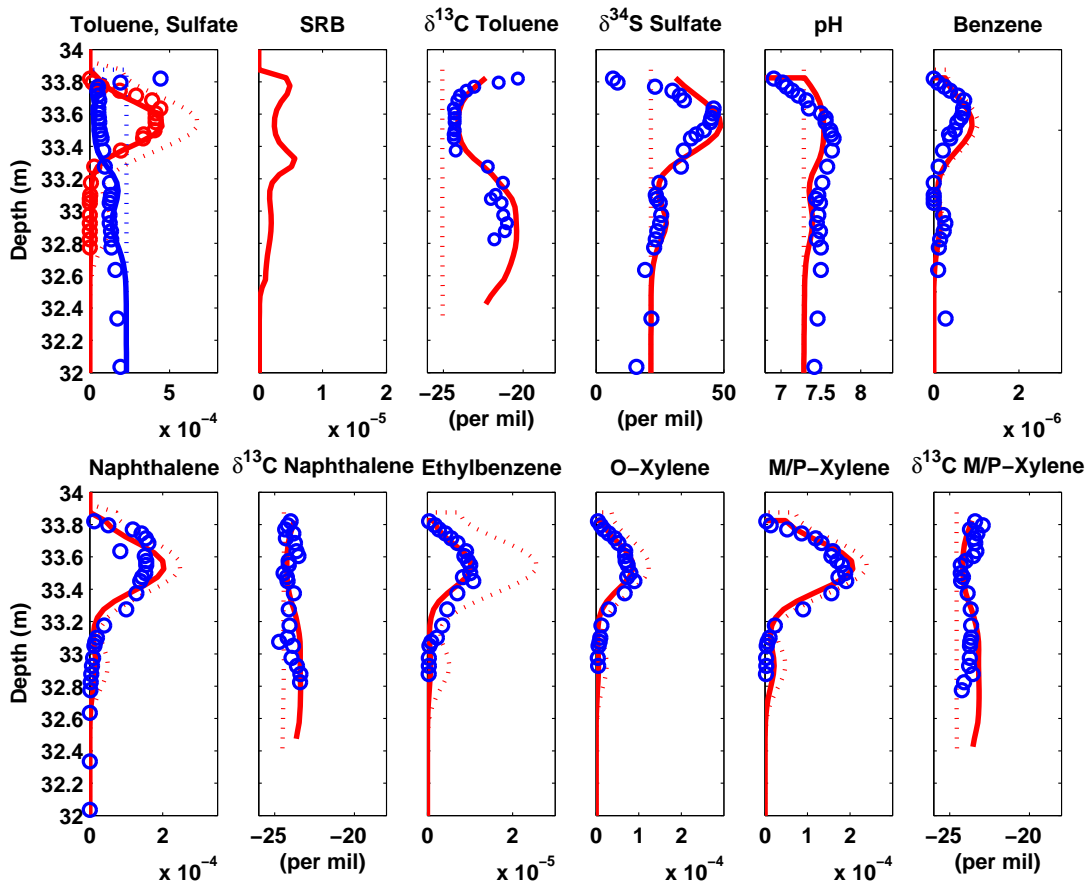


Figure 5.19: Selected simulated (reactive and nonreactive: solid and dot lines, respectively) and measured concentration (circles) depth profiles and associated isotopic signatures at the multilevel well. All concentrations, including microbial concentrations, are given in  $\text{mol L}^{-1}$ .

## 5.12 Example 12: Transport and surface complexation of uranium

**5.12.1 Introduction** Example 12 describes a study that was reported earlier by Kohler et al. (1996), who modelled transport, aqueous complexation and surface complexation of U(VI) during a column experiment. In the original work of Kohler et al. (1996) a whole range of column experiments was carried out and modelled for several different column inflow solutions to investigate the fate of U(VI) under variable chemical conditions. A number of conceptual models were tested to explain the observed breakthrough behaviour and measured concentration profiles. The present simulation example refers to experiment 7 and model C5 of the original paper.

**5.12.2 Spatial discretisation and flow problem** Like in the previous examples, the first step of setting up the simulation is to define the flow model parameters for a one-dimensional MODFLOW model.

The longitudinal extent of the model domain that represents the experimental column is 0.211 *m*. This length is discretised into 212 grid cells of 0.001 *m*. The area perpendicular to the flow direction is set to  $3.80 \times 10^{-4} \text{ m}^2$ , which corresponds to the inner diameter of the column of 2.2 *cm*. This is achieved by setting the layer thickness to  $3.80 \times 10^{-4} \text{ m}$ , while the width of the row is set to 1 *m*.

A flux boundary condition is defined by assigning an injection well to the first grid-cell (i.e., at the upstream boundary), while a constant hydraulic head is assigned to the model's downstream boundary. The (positive) flux of the well is set to  $Q_{well} = 4.8 \times 10^{-4} \text{ m}^3 \text{ d}^{-3}$  to represent the flux applied in the experiment. The effective porosity is set to  $n_{eff} = 0.42$ , as reported by Kohler et al. (1996). The total simulation time is 1.12252 days, which corresponds to 16 pore volumes. The total simulation time is subdivided into 2 different stress periods. The first stress period represents the initial inflow of an uranyl-containing aqueous solution for a period of 0.08333 days (corresponding to 40 *mL* of solution). The second stress period represents the subsequent flushing period of 1.03919 days in which both uranyl and tracer were absent from the inflow solution. Stress periods 1 and 2 were discretised into 520 and 6264 time steps, respectively. At this temporal discretisation level operator splitting errors will be minimal. All relevant parameters defining the flow model for this example are summarised in Table 5.28.

**5.12.3 Data input for the database file** The modelled reaction network in this example consists of 17 aqueous complexation reactions and includes 3 different types of binding sites on a quartz surface to which ions can sorb (S\_a, S\_b and S\_c). Dissolution and precipitation of minerals are not considered in the

present example. All homogeneous and heterogeneous reactions are assumed to be in thermodynamic equilibrium. The equilibrium constants of all reactions as reported by Kohler et al. (1996) are given in Table 5.29. The list of reactions also involves complexation reactions for fluoride. However, these reactions are only relevant for the experiments 3, 4 and 6 of Kohler et al. (1996), while in the present example, which only simulates experiment 7, fluoride is absent.

The total surface site density is  $5.3235 \times 10^{-4}$  ( $mol L_{bulk}^{-1}$ ). The site density is un-equally distributed between the three types of surface sites (see Table 5.29). Note, that the surface complexation model defined by Kohler et al. (1996) did not include corrections for electrostatic interactions between charged surfaces and adsorbing ions.

The compositions of the inflow and initial solutions for the simulated column are given in Table 5.30.

To be consistent with the definitions of Kohler et al. (1996), the valence states of N and U were fixed to +5 and +6, respectively. This is done by including solely N(5) and U(6) as redox components in the database file **pht3d\_ph.dat**, while excluding, for example, N(3), N(0), U(4) and other valences of N and U. The sodium concentrations were adjusted to achieve a fully charge-balanced aqueous solution. The resulting change of the ionic strength is negligible. To ensure that

Table 5.28: Flow and transport model setup and discretisation used in Example 12.

Flow simulation	steady state
Total simulation time ( <i>days</i> )	1.12252
Stress periods	2
Length stress period 1	0.08333
Length stress period 2	1.03919
Time steps (stress period 1)	520
Time steps (stress period 2)	6264
Grid spacing ( <i>m</i> )	0.001
Model length ( <i>m</i> )	0.211
Darcy Flux ( $m d^{-3}$ )	$4.8 \times 10^{-4}$
Effective Porosity	0.42
Total surface site density ( $mol L_{bulk}^{-1}$ )	$5.3235 \times 10^{-4}$
Longitudinal dispersivity ( <i>m</i> )	$7.5 \times 10^{-5}$

the physical (non-reactive) transport is adequately simulated a tracer has been included in the simulations.

**5.12.4 Data input for the PHREEQC interface package file** The **pht3d\_ph.dat** file for the present example includes only a few aqueous components and the three different surface sites. It also includes the definition of the type of surface calculation of these three sites, here indicated by the **-no\_edl**

Table 5.29: Reaction network definition for Example 12.

Reactions	Log K (I=0.0)	Site density ( $mol L_{bulk}^{-1}$ )
$UO_2^{+2} + H_2O = UO_2OH^+ + H^+$	-5.20	
$UO_2^{+2} + 2H_2O = UO_2(OH)_2 + 2H^+$	-12.00	
$UO_2^{+2} + 3H_2O = UO_2(OH)_3^- + 3H^+$	-20.00	
$UO_2^{+2} + 4H_2O = UO_2(OH)_4^{-2} + 4H^+$	-33.00	
$2UO_2^{+2} + H_2O = (UO_2)_2(OH)^{+3} + H^+$	-2.80	
$2UO_2^{+2} + 2H_2O = (UO_2)_2(OH)_2^{+2} + 2H^+$	-5.63	
$3UO_2^{+2} + 4H_2O = (UO_2)_3(OH)_4^{+2} + 4H^+$	-11.90	
$3UO_2^{+2} + 5H_2O = (UO_2)_3(OH)_5^+ + 5H^+$	-15.56	
$3UO_2^{+2} + 7H_2O = (UO_2)_3(OH)_7^- + 7H^+$	-31.00	
$4UO_2^{+2} + 7H_2O = (UO_2)_4(OH)_7^+ + 7H^+$	-21.9	
$UO_2 + 2 + NO_3^- = UO_2NO_3^+$	0.26	
$UO_2 + 2 + F^- = UO_2F^+$	5.09	
$UO_2 + 2 + 2F^- = UO_2F_2$	8.62	
$UO_2 + 2 + 3F^- = UO_2F_3^-$	10.90	
$UO_2 + 2 + 4F^- = UO_2F_4^{-2}$	11.70	
$H^+ + F^- = HF$	3.17	
$H^+ + 2F^- = HF_2^-$	3.75	
$S_{aOH} + UO_2^{+2} + H_2O = S_{aOUO_2OH} + 2H^+$	-4.9503 <sup>a</sup>	$5.1968 \times 10^{-3}$
$S_{bOH} + UO_2^{+2} + H_2O = S_{bOUO_2OH} + 2H^+$	-3.4703 <sup>a</sup>	$1.2562 \times 10^{-5}$
$S_{bOH} + UO_2^{+2} = S_{bOUO_2}^+ + H^+$	0.7766 <sup>a</sup>	$1.2562 \times 10^{-5}$
$S_{cOH} + UO_2^{+2} + H_2O = S_{cOUO_2OH} + 2H^+$	-1.0603 <sup>a</sup>	$1.0920 \times 10^{-7}$

<sup>a</sup> Re-calculated for ionic strength I=0.0. Equilibrium constants in Kohler et al. (1996) were given for an ionic strength of I = 0.01.

option. The file looks as follows:

```

2 25 0 0 0
0
7
0
0 0
3
0 0 0 0
Tracer
U(6)
Na
N(5)
F
pH
pe
S_aOH 0 0
S_bOH 0 0
S_cOH 0 0
-no_edl

```

Table 5.30: Compositions of initial and inflow solutions in Example 12.

Component	Inflow concentration ( $\text{mol L}^{-1}$ ) <sup>a</sup>	Initial concentration ( $\text{mol L}^{-1}$ ) <sup>a</sup>
Na	9.8456e-3	9.9398e-3
N(5)	0.01	0.01
U(6)	5e-5	0.0
F	0.0	0.0
Tracer	1e-6	0.0
pH	4.26	4.26
pe	4	4

<sup>a</sup> Except pH and pe.

**5.12.5 Data input for the basic transport package** As illustrated for previous examples, geometrical information, boundary conditions, initial concentrations temporal discretisation and several other parameters are defined in the **pht3dbtn.dat** file. For the present example the file looks as follows:

```

Example 12
Kohler et al., 1996
1 1 211 2 10 5
day m kg
T T T F T T F F F F
0
0 5.e-4 1 Column Thickness
0 3.80e-04 1 Row Thickness
0 1.0 1 Htop
0 1.0 1 Layer Thickness(DZ)
0 4.2e-1 1 Porosity (PRSITY)
0 1 -1 icbund
0 0 1 Starting Conc. Tracer
0 0 1 Starting Conc. U(6)
0 9.9398e-3 1 Starting Conc. Na
0 1.e-2 1 Starting Conc. N(5)
0 0 1 Starting Conc. F
0 4.26 1 Starting Conc. pH
0 4.0 1 Starting Conc. pe
0 1.2373e-3 1 S_aOH site density
0 2.9909e-5 1 S_bOH site density
0 2.6000e-7 1 S_cOH site density
-1.e30 1.e-2
0 0 0 0 T
-2
0 1
T 1
0.08333 520 1.
0. 10000 1. 0.
1.03919 6264 1.
0. 10000 1. 0.

```

**5.12.6 Data input for the advection package** For the present simulation the HMOC scheme was used and defined in the **pht3dadv.dat** file:

```
3 7.5e-1 10000 0
1 5.e-1
1.e-6 0 4 15 1 30 1.
1 0 15
1.e-6
```

**5.12.7 Data input for the dispersion package** The information controlling dispersion and molecular diffusion was implemented into **pht3ddsp.dat** as follows:

```
0 7.5e-5 (10G11.4) 0 long. dispersivity
100 1.00e+00 (10G11.4) 0 Horiz. Dispersivity
1.e-1
100 1.00e+00 (10G11.4) 0 Vert. dispersivity
1.e-2
100 1.00e+00 (10G11.4) 0 Molecular Diffusion
8.64e-5
```

**5.12.8 Data input for the source/sink package** The **pht3dssm.dat** file for the present example should look as follows:

```
T F F F F F F FWEL,FDRN,FRCH,FEVT,FRIV,FGHB,FSTR
2 Max source/Sink
1
1 1 1 1.e-6 2 1e-06 5e-05 0.00984564 0.01 0 4.26 4 0 0 0
1
1 1 1 0. 2 0 0 0.00993984 0.01 0 4.26 4 0 0 0
```

**5.12.9 Simulation results** Figures 5.20-5.22 show the simulation results of PHT3D along with the experimental and modelling results of Kohler et al. (1996). Figure 5.20 shows the PHT3D-simulated tracer breakthrough, which is essentially

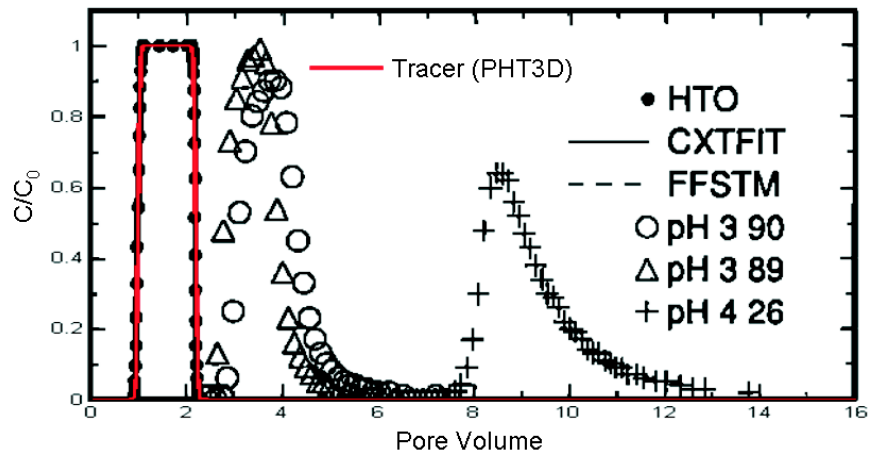


Figure 5.20: Simulated and experimental normalized tracer breakthrough.

identical with the breakthrough that was observed in the experiment, indicating that advective-dispersive, non-reactive transport is adequately simulated.

During the first stress period, i.e., the inflow of the uranium-rich solution into the column, uranium starts to partially occupy the different sorption sites ( $S_a$ ,  $S_b$  and  $S_c$ ) on the quartz surface while protons are released into the solution. This leads to a retardation of the uranium migration and a decrease of the pH. The pH decrease can be seen downstream of the uranium front for a simulation time of 1.5 hours (Figures 5.22a and 5.22b). After this time the first pore volume has almost been flushed through the column. The equilibrated initial water composition still persists near the column outlet. This can for example be seen in the plot that shows the pH profile within the column after 1.5 hours simulation time (Figure 5.22b)

The inflow of the uranium-free solution that starts after 2 hours (0.08333 *days*) allows the desorption of uranium that proceeds until the reservoir of adsorbed uranium is exhausted. After a simulation time of 3 *hours*, the first 1 *cm* (measured from the column inlet) contains no more uranium as the uranium has completely desorbed from the quartz surface. A step increase in the aqueous uranium concentrations from 0 to 15  $\mu\text{mol L}^{-1}$  reflects the beginning of the zone where uranium desorbs. This zone extends to about 13 *cm* from the inlet. The concentration drop from 20  $\mu\text{mol L}^{-1}$  to 10  $\mu\text{mol L}^{-1}$  (in upstream direction) at approximately 13 *cm* from the inlet reflects the end of the uranium-rich inflow (end of stress period 1) into the column. Where uranium desorbs, protons can adsorb on the quartz surface, which leads to a pH increase. In the uranium desorption zone uranyl concentrations and pH slightly decrease in flow direction. This is because

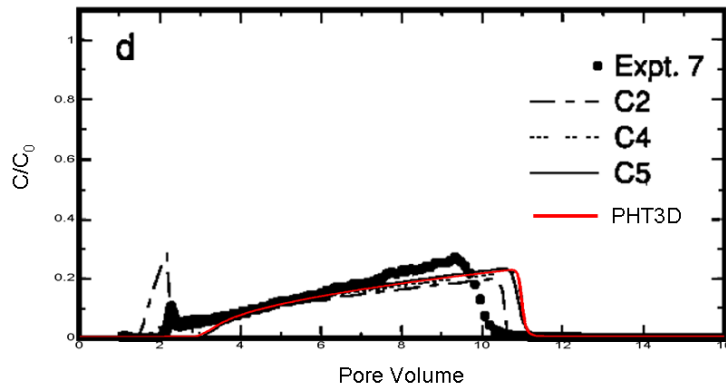


Figure 5.21: Simulated and measured normalized uranyl breakthrough curves (Experiment 7).

the concentrations of sorbed uranyl are highest at the upstream end of this zone, while successively decreasing further downstream. As the sorbed uranyl species are in thermodynamic equilibrium with the dissolved uranyl species, dissolved uranyl also decreases in flow direction. After 12.5 *hours* (i.e., 7.65 pore volumes), the desorbing zone has shifted further towards the outlet of the column while the principal shape of the concentration profile has barely changed. As a result, breakthrough concentrations of uranium increase steadily with time (Figure 5.21). A full discussion of the breakthrough behaviour is given by Kohler et al. (1996).

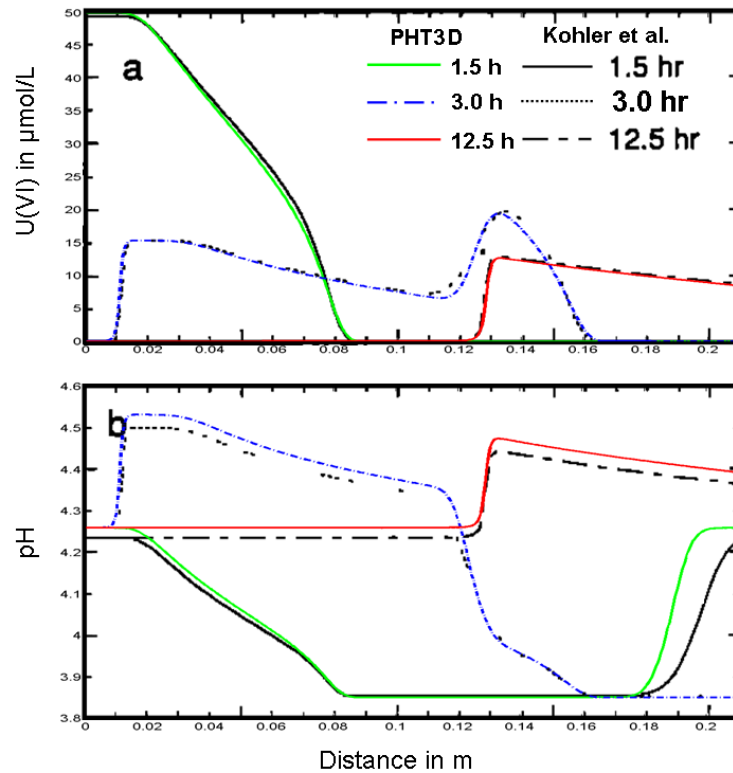


Figure 5.22: Top: Simulated concentrations profiles of uranyl; Bottom: Simulated pH profiles (Experiment 7). Note that there is a typing error in Kohler et al. 1996 for the label of the profiles at 3h; in Kohler et al. 1996 the label showed 2.5h instead of 3h (pers. comm. Gary Gurtis)

### 5.13 Example 13: Modelling of an oxidation experiment

**5.13.1 Introduction** Example 13 describes the simulation of an oxidation experiment with marine pyrite-containing sediments. This modelling study was, together with the experimental work, originally reported by Appelo et al. (1998). The conceptual hydrochemical model and the implemented reaction network proposed for this experiment consists of a complex set of reactive processes. This includes

- the oxidation of pyrite, which is the primary driver of hydrochemical changes
- secondary reactions, such as dissolution of calcite, CO<sub>2</sub> sorption, cation and proton exchange and
- oxidation of organic matter, a reaction that competes for the oxidation capacity supplied by the inflow solution.

The modelling study considers three distinct phases of the experiment. In the first part the sediment material collected in the field was equilibrated with a 280 mmol MgCl<sub>2</sub> solution. In this phase the pore space becomes completely filled with the MgCl<sub>2</sub> solution and the exchangers sites are filled with Mg. In the second phase the column was fed with a more dilute MgCl<sub>2</sub> solution, while in the third phase the column was flushed for 4 pore volumes (at the same flow rate) with a hydrogen peroxide (H<sub>2</sub>O<sub>2</sub>) containing oxidising solution. Particularly the second phase provided the data that allowed to characterise the non-reactive transport behaviour.

**5.13.2 Spatial discretisation and flow problem** The experimental column used by Appelo et al. (1998) was 5.3 cm long and had an inner diameter of 6.0 cm. In the model the length of the column is discretised into 16 grid cells of 0.0033125 m length. The area perpendicular to the flow direction is therefore  $2.87433 \times 10^{-3} m^2$ , which was modelled by defining the layer thickness and row width accordingly (i.e.,  $2.87433 \times 10^{-3} m \times 1 m$ ). In this way the modelled cross-sectional area agrees with the area of the experimental column.

As in several previous examples the flux boundary condition for the one-dimensional domain was defined by assigning an injection well to the first grid cell (upstream boundary), and a constant hydraulic head at the downstream boundary. The flux of the well at the upstream boundary was set to  $Q_{well} = 0.00024 m^3 d^{-3}$ , which then results in a Darcy velocity similar to that in the experimental columns. The porosity is set to  $n_{eff} = 0.376$ . All relevant parameters defining the flow model for this example are summarised in Table 5.31.

Table 5.31: Flow/transport model setup and spatial/temporal discretisation used in Example 13.

Length of column ( $m$ )	0.053
Inner diameter of column ( $m$ )	0.06
Cross-sectional area ( $m^2$ )	0.00287433
Flow simulation	steady state
Total simulation time ( $days$ )	2.39666
Stress periods	2
Length stress period 1	0.9333
Length stress period 2	1.45833
Time steps (stress period 1)	64
Time steps (stress period 2)	100
Grid spacing ( $m$ )	0.0033125
Flow rate column inlet ( $mLh^{-1}$ )	10
Flow rate column inlet ( $m d^{-3}$ )	$2.4 \times 10^{-4}$
Effective Porosity	0.376
Longitudinal dispersivity ( $m$ )	.00537
Temperature ( $^{\circ}C$ )	7.5

**5.13.3 Data input for the database file** Based on a stepwise increase in complexity and using the experimental data as constraints Appelo et al. (1998) successively developed a reaction network which, in its final version, included

- selected major ions and redox-sensitive species/components ( $Ca$ ,  $Cl$ ,  $Mg$ ,  $Fe(2)$ ,  $Fe(3)$ ,  $S(6)$ ,  $S(-2)$ ,  $C(4)$ ,  $C(-4)$ )
- $pH$  and  $pe$
- equilibrium mineral reactions for *goethite*
- kinetically controlled oxidation of *pyrite*
- kinetically controlled dissolution of *calcite*
- multi-site ion exchange with seven different exchanger sites ( $X$ ,  $Y_a$ ,  $Y_b$ ,  $Y_c$ ,  $Y_d$ ,  $Y_e$ ,  $Y_f$ )
- kinetically controlled oxidation of sediment bound (i.e., immobile) organic matter (*Orgc\_sed*)
- sorption reactions to an *HfO\_w* surface site, whereby the concentration of the surface site is directly linked to the simulated *Goethite* concentration.

The most important aspects of this reaction network will be discussed in the following, while the full details of its identification and construction are reported in much greater depth in the original paper of Appelo et al. (1998). The standard PHREEQC database file serves as a starting point for the necessary reaction network adaptations of the numerical model to adequately represent the details of the conceptual hydrochemical model. The major adaptations of the standard database included

- the definition of rate expressions for the kinetically controlled oxidation reactions of pyrite and organic matter and
- the definition of additional ion exchanger sites.

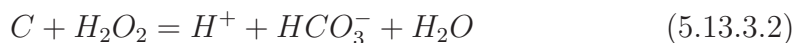
A kinetically controlled pyrite oxidation by oxygen was incorporated by Appelo et al. (1998) through a rate expression that was originally proposed by Williamson and Rimstidt (1994). In this rate expression the specific oxidation rate for pyrite,  $r_{pyr}$ , with  $O_2$  is modelled as:

$$r_{pyr} = k_p m_{O_2}^{0.5} m_{H^+}^{-0.11} \quad (5.13.3.1)$$

where  $k_p = 10^{-10.19} \text{ mol dm}^{-2} \text{ s}^{-1}$  at  $25(^{\circ}\text{C})$ ,  $m_{\text{O}_2}$  is the concentration of dissolved oxygen in  $\text{mol L}^{-1}$ , and  $m_{\text{H}^+}$  is the concentration of protons in  $\text{mol L}^{-1}$ . The corresponding BASIC program for this rate expression is:

```
#####
#Pyrite
#####
# Example of KINETICS data block for pyrite rate:
# KINETICS 1
# Pyrite
# -tol 1e-8
# -m0 5.e-4
# -m 5.e-4
# -parms -5.0 0.1 .5 -0.11
Pyrite
-start
1 rem parm(1) = log10(A/V, 1/dm) parm(2) = exp for (m/m0)
2 rem parm(3) = exp for O2 parm(4) = exp for H+
10 if (m <= 0) then goto 200
20 if (si("Pyrite")) >= 0 then goto 200
30 rate = -10.19 + parm(1) + parm(3)*ln("O2") + parm(4)*ln("H+") + parm(2)*log10(m/m0)
40 moles = 10*rate * time
50 if (moles > m) then moles = m
60 if (moles >= (mol("O2")/3.5)) then moles = mol("O2")/3.5
200 save moles
-end
```

This rate expression is included under the RATES keyword in the databasefile **pht3d\_datab.dat**. In addition, organic matter degradation, here for example by hydrogen peroxide



was also considered as a kinetically controlled reaction. For oxygen concentrations  $C_{\text{O}_2} \leq 1 \text{ mmol L}^{-1}$  the degradation of the organic matter was modelled through a first order degradation rate.

$$r_C = k_c C_{\text{SOM}} \quad (5.13.3.3)$$

where  $k_c$  is the first order reaction constant and  $C_{SOM}$  is the concentration of organic matter. However, for concentrations  $C_{O_2} > 1 \text{ mmol L}^{-1}$  the rate was also assumed to be dependent on the oxygen concentrations  $C_{O_2}$ .

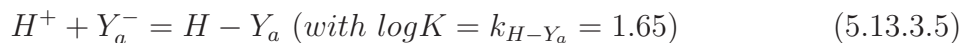
$$r_C = k_c C_{SOM} C_{O_2} \quad (5.13.3.4)$$

The corresponding RATES expression that accordingly is included in the database file **pht3d\_datab.dat** is

```
#####
# Organic Matter (Organic C in sediments)
#####
Orgc_sed
-start
5 mOrgc_sed = tot("Orgc_sed")
10 mO2 = mol("O2") * parm(1)
20 if mO2 < 1 then mO2 = 1.0
30 moles = parm(1) * mO2 * mOrgc_sed * time
40 save moles
```

In the above rate expression the first order reaction constant  $k_c$  is included as `parm(1)`, which allows the user to vary the reaction rate constant in the file **pht3d\_ph.dat**.

To replicate the ion exchanging reactions in the experimental columns Appelo et al. (1998) included three different types of ion exchangers in their reaction network. The X exchanger, which is already included in the PHREEQC standard database, was assumed to account mainly for the Mg/Ca exchange reactions occurring with the  $< 2\mu\text{m}$  fraction of the sediment material. To account for the observed proton buffering reactions Appelo et al. (1998) represented the ion exchange capacity provided by the organic matter as an additional set of exchangers  $Y_a, Y_b, \dots, Y_f$ . Exchange reactions were defined, here for example for hydrogen, as



Finally, sorption to amorphous Fe-oxyhydroxide was considered via surface complexation reactions. A complete list of the considered exchange and surface complexation reactions and their reaction constants is given in Table 5.32.

**5.13.4 Data input for the PHREEQC interface package file** The PHREEQC interface package file **pht3d\_ph.dat** defines the actual reaction net-

Table 5.32: Ion exchange and surface complexation reactions defined for Example 13.

Cations	X	Na-X	Mg-X <sub>2</sub>	Ca-X <sub>2</sub>			
	log K	0.0	0.8	1.1			
i=a,...,f	Y <sub>i</sub>	Na-Y <sub>i</sub>	K-Y <sub>i</sub>	Mg-(Y <sub>i</sub> ) <sub>2</sub>	Ca-(Y <sub>i</sub> ) <sub>2</sub>		
	log K	-1.0	-0.75	-0.2	0.1		
Protons	Y	H-Y <sub>a</sub>	H-Y <sub>b</sub>	H-Y <sub>c</sub>	H-Y <sub>d</sub>	H-Y <sub>e</sub>	H-Y <sub>f</sub>
	log K	1.65	3.3	4.95	6.85	9.6	12.35
Anions	Z	H <sub>2</sub> O-Z	H <sub>2</sub> CO <sub>3</sub> -Z	HCl-Z			
	log K	0.0	-3.3	-7.05			

work that is used for the Example 13 simulations. It defines that the simulation includes 14 mobile aqueous equilibrium components, one immobile, kinetically controlled component (*Orgc<sub>sed</sub>*), one equilibrium mineral (*Goethite*), 7 different exchanger sites (*X*, *Y<sub>a</sub>*, *Y<sub>b</sub>*, *Y<sub>c</sub>*, *Y<sub>d</sub>*, *Y<sub>e</sub>* and *Y<sub>f</sub>*), one surface (*HfO<sub>w</sub>*) and two kinetically controlled minerals/mineral reactions (*Pyrite* and *Calcite*).

Following the numbers of the various species/component types are the names of these entities.

The list of the names of the kinetic immobile species and the 14 aqueous equilibrium components is then followed by the name of the equilibrium mineral (*Goethite*). The line with the name of the mineral also contains a saturation index (SI) of 3.0. Appending a saturation index to the mineral name will change the saturation index to which PHREEQC is normally equilibrated during a reaction step. Instead of attaining SI = 0 the equilibration for goethite will be made for SI of 3.0. Following the equilibrium minerals the exchanger sites (*X*, *Y<sub>a</sub>*, ...) are listed, each followed by the value -1.0. The latter value indicates that after the start of a simulation (at t = 0) PHT3D will carry out an initial equilibration step to determine the occupancy of the exchanger site that is in equilibrium with the initial water composition. The exchange capacity for each exchanger is defined by allocating the respective capacity of each exchanger as initial concentrations in the file **pht3dbtn.dat**. At the end of the file and next after the exchanger definitions,

**2 7.5 1 0 0**  
**0**

11  
1  
7 0  
1  
0 2 0 1  
C(4)  
C(-4)  
Ca  
Cl  
Fe(2)  
Fe(3)  
Mg  
S(6)  
S(-2)  
pH  
pe  
Orgc\_sed 1  
 $9.5 \times 10^{-5}$   
-formula Orgc\_sed -1.0 C 1.0 Goethite 3.0  
X -1.0  
Ya -1.0  
Yb -1.0  
Yc -1.0  
Yd -1.0  
Ye -1.0  
Yf -1.0  
Hfo\_w 600 0.2 Goethite equilibrium  
  
Calcite 2  
100  
0.6  
Pyrite 4  
3.42  
0.0  
0.5  
0.0

Note also that the fourth number in the first line (i.e., 7.5) indicates the temperature that is used for the PHREEQC calculations, here corresponding to the experimental conditions reported by Appelo (1996).

**5.13.5 Data input for the basic transport package** The initial concentrations as well as the time parameters are defined in the file **pht3dbtn.dat**. The compositions of the inflow and initial solutions for the simulated column are given in Table 5.34. The complete and detailed content of the **pht3dbtn.dat** is not further discussed here, as it follows from previously discussed examples. However, important points to note are that

- the exchange capacities (CEC) of the various exchanger sites are defined as initial concentrations
- the surface site concentrations of the *HfO<sub>w</sub>* surface are defined as initial concentrations.

As discussed for the previous examples, the order of the definition of the initial concentrations is controlled by the order defined in the **pht3d\_ph.dat** file.

### Example 13

Appelo et al. (1998)

1 1 16 2 23 9

T L M

T T T F T T

3

100 1(5G14.0) -1 A7. DELR(NCOL)

0.0033125 0.0033125 0.0033125 0.0033125 0.0033125

0.0033125 0.0033125 0.0033125 0.0033125 0.0033125

0.0033125 0.0033125 0.0033125 0.0033125 0.0033125

0.0033125

100 1(1G14.0) -1 A8. DELC(NROW)

1

100 1(5G14.0) -1 A9. HTOP(NCOL,NROW); Top of the first layer

2.87433E-03 2.87433E-03 2.87433E-03 2.87433E-03 2.87433E-03

2.87433E-03 2.87433E-03 2.87433E-03 2.87433E-03 2.87433E-03

2.87433E-03 2.87433E-03 2.87433E-03 2.87433E-03 2.87433E-03

2.87433E-03

0 2.874E-03 -1 A10. Thickness of layer 1

```

0 .376 -1 A11. Effective porosity of layer 1
0 1 -1 A12. ICBUND matrix of Layer 1
0 .000586 -1 A13. Init conc species 1 C(4)
0 0 0 A13. Init conc species 2 C(-4)
0 .000386 -1 A13. Init conc species 3 Ca
0 .02007 -1 A13. Init conc species 4 Cl
0 .000001 -1 A13. Init conc species 5 Fe(2)
0 0 0 A13. Init conc species 6 Fe(3)
0 .01 -1 A13. Init conc species 7 Mg
0 0 0 A13. Init conc species 8 S(-2)
0 .00001 -1 A13. Init conc species 9 S(6)
0 9.104 -1 A13. Init conc species 10 pH
0 -4.812 -1 A13. Init conc species 11 pe
0 .89 -1 A13. Init conc species 12 Orgc_sed
0 0 0 A13. Init conc species 13 Goethite
100 1(5G14.0) -1 A13. Init conc species 14 X
.032712 .032712 .032712 .032712 .029704
.029704 .029704 .029704 .040608 .040608
.040608 .040608 .045496 .045496 .045496
.045496
100 1(5G14.0) -1 A13. Init conc species 15 Ya
.001316 .001316 .001316 .001316 .0014664
.0014664 .0014664 .0014664 .0030456 .0030456
.0030456 .0030456 .0036848 .0036848 .0036848
.0036848
100 1(5G14.0) -1 A13. Init conc species 16 Yb
.001316 .001316 .001316 .001316 .0014664
.0014664 .0014664 .0014664 .0030456 .0030456
.0030456 .0030456 .0036848 .0036848 .0036848
.0036848
100 1(5G14.0) -1 A13. Init conc species 17 Yc
.001316 .001316 .001316 .001316 .0014664
.0014664 .0014664 .0014664 .0030456 .0030456
.0030456 .0030456 .0036848 .0036848 .0036848
.0036848
100 1(5G14.0) -1 A13. Init conc species 18 Yd
.001316 .001316 .001316 .001316 .0014664

```

```

.0014664 .0014664 .0014664 .0030456 .0030456
.0030456 .0030456 .0036848 .0036848 .0036848
.0036848
100 1(5G14.0) -1 A13. Init conc species 19 Ye
.001316 .001316 .001316 .001316 .0014664
.0014664 .0014664 .0014664 .0030456 .0030456
.0030456 .0030456 .0036848 .0036848 .0036848
.0036848
100 1(5G14.0) -1 A13. Init conc species 20 Yf
.001316 .001316 .001316 .001316 .0014664
.0014664 .0014664 .0014664 .0030456 .0030456
.0030456 .0030456 .0036848 .0036848 .0036848
.0036848
0 0.001 -1 A13. Init conc species 21 HfO_w
0 1.504 -1 A13. Init conc species 22 Calcite
0 .01504 -1 A13. Init conc species 23 Pyrite
1E+30 .05
0 0 0 0 T
49
0 .05 .1 .15 .2 .25 .3 .35
.4 .45 .5000001 .5500001 .6000001 .6500001 .7000001 .7500001
.8000001 .8500001 .9000002 .9500002 1 1.05 1.1 1.15
1.2 1.25 1.3 1.35 1.4 1.45 1.5 1.55
1.6 1.649999 1.699999 1.749999 1.799999 1.849999 1.899999 1.949999
1.999999 2.049999 2.099999 2.149999 2.199999 2.249999 2.299999 2.349999
2.391666
0 1
T 1
.9333333 64 1
0 50000 1 0
1.458333 100 1
0 50000 1 0

```

**5.13.6 Data input for the advection package** For the present simulation the TVD scheme was used and defined in pht3adv.dat:

```
-1 .75 5000 0
```

Table 5.33: Cation exchange capacities of exchangers defined for Example 13.

Component	CEC cells 1-4 ( $mol L^{-1}$ )	CEC cells 5-8 ( $mol L^{-1}$ )	CEC cells 9-12 ( $mol L^{-1}$ )	CEC cells 13-16 ( $mol L^{-1}$ )
X	0.087	0.079	0.108	0.121
Y_a	0.0035	0.0039	0.0081	0.0098
Y_b	0.0035	0.0039	0.0081	0.0098
Y_c	0.0035	0.0039	0.0081	0.0098
Y_d	0.0035	0.0039	0.0081	0.0098
Y_e	0.0035	0.0039	0.0081	0.0098
Y_f	0.0035	0.0039	0.0081	0.0098

Table 5.34: Compositions of initial and inflow solutions in Example 13.

Component	Initial concentration ( $mol L^{-1}$ ) <sup>a</sup>	Inflow stress period 1 ( $mol L^{-1}$ ) <sup>a</sup>	Inflow stress period 2 ( $mol L^{-1}$ ) <sup>a</sup>
Ca	0.000386	.000001	1.e-7
Cl	0.020070	.005301	0.0102
Mg	0.010000	0.00265	0.0051
Fe(2)	0.000001	1E-08	2.e-7
Fe(3)	0	0	0
S(6)	0.00001	1.0e-8	2.e-7
S(-2)	0	0	0
C(4)	0.000586	1.0e-6	1.e-7
C(-4)	0	0	0
pH	9.104	7.00	7.00
pe	-4.812	15.8715	14.5

<sup>a</sup> Except pH and pE.

**5.13.7 Data input for the dispersion package** The information for dispersion can be implemented into pht3ddsp.dat as follows:

```
0 7.5e-5 (10G11.4) 0 long. dispersivity
100 1.00e+00 (10G11.4) 0 Horiz. Dispersivity
1.e-1
100 1.00e+00 (10G11.4) 0 Vert. dispersivity
1.e-2
100 1.00e+00 (10G11.4) 0 Molecular Diffusion
8.64e-5
```

**5.13.8 Data input for the source/sink package** The pht3ssm.dat file for the present example should look as follows:

```
T F F F F F
2002
1
1 1 1 0 2 .000001 0 .000001 .005301 1E-08 0 .00265 .3491 0 1E-08 7 15.8715 0 0
0 0 0 0 0 0 0 0 0 0
1
1 1 1 0 2 .0000001 0 .0000001 .0102 1E-08 0 .0051 1.145E-06 0 .0000002 7 14.5
0 0 0 0 0 0 0 0 0 0 0
```

**5.13.9 Simulation results** Figures 5.23 shows the simulation results of PHT3D in comparison with the corresponding PHREEQC results and observed concentration values.

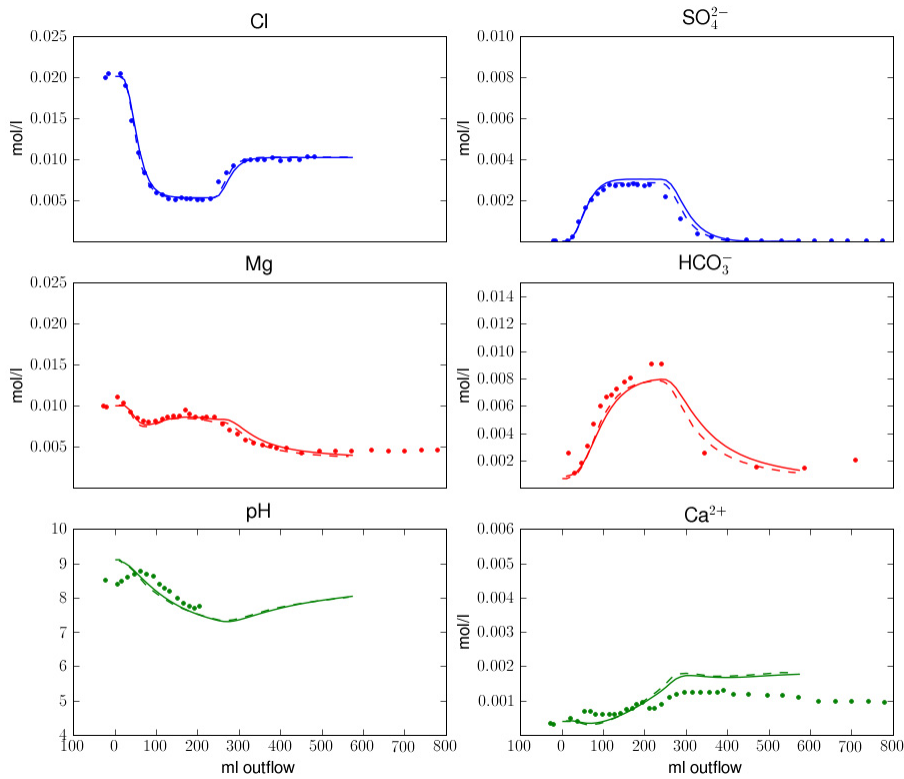


Figure 5.23: Simulated and measured breakthrough curves.

## File formats

### 6.1 ASCII Output file format

The output format for the concentrations in the ASCII files is (one concentration result per line):

```

C at timestep 1, layer 1, row 1, column 1
C at timestep 1, layer 1, row 1, column 2
...
C at timestep 1, layer 1, row 1, column  $col_{max}$ 
C at timestep 1, layer 1, row 2, column 1
C at timestep 1, layer 1, row 2, column 2
...
C at timestep 1, layer 1,  $row_{max}$ , column  $col_{max}$ 
C at timestep 1, layer 2, row 1, column 1
C at timestep 1, layer 2, row 1, column 2
...
C at timestep 1, layer  $lay_{max}$ , row  $row_{max}$ , column  $col_{max}$ 
C at timestep 2, layer 1, row 1, column 1
C at timestep 2, layer 1, row 1, column 2
...
C at timestep  $time_{max}$ , layer  $lay_{max}$ , row  $row_{max}$ , column  $col_{max}$ 

```

In other words, the results can be read into appropriate visualisation tools with a code/script resembling:

```

nr = 1;
for t = 1:t_max
  for k = 1:lay_max
    for j = 1:row_max
      for i = 1:col_max
        conc(t,k,j,i) = pht3d_ucn_data(nr);
        nr = nr + 1;
      end
    end
  end
end
end

```



## Further information

### 7.1 Web resources

- Executables, updated versions of this manual, modelling examples, dates for PHT3D short-courses and other, related information can be found under <http://www.pht3d.org>
- The MT3DMS manual, source code and up-to-date information on MT3DMS can be obtained from <http://hydro.geo.ua.edu/mt3d> and from <http://www.mt3d.org>
- PHREEQC-2 executables, manual, source code and GUI can be downloaded from [http://wwwbrr.cr.usgs.gov/projects/GWC\\_coupled/phreeqc/index.html](http://wwwbrr.cr.usgs.gov/projects/GWC_coupled/phreeqc/index.html)
- A nice Windows-based user interface for PHREEQC-2 was written by Vincent van Post and can be obtained from <http://www.geo.vu.nl/users/posv/phreeqc/index.html> .
- Tony Appelo's page: PHREEQC-2 courses and other PHREEQC-2 related information can be found at <http://www.xs4all.nl/~appt/>



## Bibliography

- Anneser, B., Einsiedl, F., Meckenstock, R. U., Richters, L., Wisotzky, F., and Griebler, C. (2008). High-resolution monitoring of biogeochemical gradients in a tar oil-contaminated aquifer. *Applied Geochemistry*, 23(6):1715–1730.
- Appelo, C., Verweij, E., and Schäfer, H. (1998). A hydrogeochemical transport model for an oxidation experiment with pyrite/calcite/exchangers/organic matter containing sand. *Appl. Geochem.*, (13):257–268.
- Appelo, C. A. J. (1994). Cation and proton exchange, pH variations, and carbonate reactions in a freshening aquifer. *Water Resour. Res.*, 30(10):2793–2805.
- Appelo, C. A. J. (1996). Multicomponent ion exchange and chromatography in natural systems. In Lichtner, P. C., Steefel, C. I., and Oelkers, E. H., editors, *Reactive Transport in Porous Media: General Principles and Applications to Geochemical Processes*, pages 193–227. Mineralogical Society of America, Washington D.C.
- Appelo, C. A. J. and Postma, D. (1993). *Geochemistry, Groundwater and Pollution*. A.A. Balkema, Rotterdam.
- Barry, D. A., Miller, C. T., and Culligan-Hensley, P. J. (1996). Temporal discretisation errors in non-iterative split-operator approaches to solving chemical reaction/groundwater transport models. *J. Contam. Hydrol.*, 22:1–17.
- Barry, D. A., Miller, C. T., Culligan-Hensley, P. J., and Bajracharya, K. (1997). Analysis of split operator methods for nonlinear and multispecies groundwater chemical transport models. *Mathem. Comp. Simul.*, 43:331–341.
- Barry, D. A., Prommer, H., Miller, C. T., Engesgaard, P., and Zheng, C. (2002). Modelling the fate of oxidisable organic contaminants in groundwater. *Adv. Water Res.*, 25:899–937.
- Bauer, R. D., Maloszewski, P., Zhang, Y., Meckenstock, R. U., and Griebler, C. (2008). Mixing-controlled biodegradation in a toluene plume - Results from two-dimensional laboratory experiments. *J. Contam. Hydrol.*, 96(1-4):150–168.
- Bauer, R. D., Rolle, M., Bauer, S., Eberhardt, C., Grathwohl, P., Kolditz, O., Meckenstock, R. U., and Griebler, C. (2009a). Enhanced biodegradation by hydraulic heterogeneities in petroleum hydrocarbon plumes. *J. Contam. Hydrol.*, 105(1-2):56–68.

- Bauer, R. D., Rolle, M., Kuerzinger, P., Grathwohl, P., Meckenstock, R. U., and Griebler, C. (2009b). Two-dimensional flow-through microcosms - Versatile test systems to study biodegradation processes in porous aquifers. *J. Hydrol.*, 369(3-4, Sp. Iss. SI):284–295.
- Bauer-Gottwein, P., Langer, T., Prommer, H., Wolski, P., and Kinzelbach, W. (2007). Okavango Delta Islands: Interaction between density-driven flow and geochemical reactions under evapo-concentration. *Journal of Hydrology*, 335:389–405.
- Beller, H. R., Grbic-Galic, D., and Reinhard, M. (1992). Microbial degradation of toluene under sulfate-reducing conditions and the influence of iron on the process. *Appl. Environ. Microbiol.*, 58(16):768–793.
- Bottrell, S., Hayes, P., Bannon, M., and Williams, G. (1995). Bacterial Sulfate Reduction and Pyrite Formation in a Polluted Sand Aquifer. *Geomicrobiol. J.*, 13(2):75–90.
- Brown, P. L., Haworth, A., Sharland, S. M., and Tweed, C. J. (1991). HARPHRQ: A Geochemical Speciation Code Based on PHREEQE. Technical report, Harwall Laboratories.
- Brun, A. and Engesgaard, P. (2002). Modelling of transport and biogeochemical processes in pollution plumes: model formulation and development. *J. Hydrol.*, 256(3-4):211–227.
- Carey, G. R., Geel, P. J. V., and Murphy, J. R. (1999). BioRedox-MT3DMS V2.0: A Coupled Biodegradation-Redox Model for Simulating Natural and Enhanced Bioremediation of Organic Pollutants - User's Guide. Technical report, Conestoga-Rovers & Associates, Waterloo, Ontario, Canada.
- Cirpka, O., Frind, E., and Helmig, R. (1999). Numerical simulation of biodegradation controlled by transverse mixing. *J. Contam. Hydrol.*, 40(2):159–182.
- Clement, T. P. (1997). A modular computer code for simulating reactive multi-species transport in 3-dimensional groundwater aquifers. Technical report, Pacific Northwest National Laboratory, Richland.
- Clement, T. P. (2001). A generalized analytical method for solving multi-species transport equations coupled with a first-order reaction network. *Water Resour. Res.*, 37:157–163.

- Cohen, E. L., Patterson, B. M., McKinley, A. J., and Prommer, H. (2008). Zvi remediation of a mixed brominated ethene contaminated groundwater. *Journal of Contaminant Hydrology*, 103:109–118.
- Colombani, N., Mastrocicco, N., Gargini, A., Davis, G. B., and Prommer, H. (2009). Modelling the fate of styrene in a mixed petroleum hydrocarbon plume. *Journal of Contaminant Hydrology*, 105:38–55.
- Davis, G. B., Barber, C., Power, T. R., Thierrin, J., Patterson, B. M., Rayner, J. L., and Wu, Q. (1999). The variability and intrinsic remediation of a BTEX plume in anaerobic sulphate-rich groundwater. *J. Contam. Hydrol.*, 36(3-4):265–290.
- Edwards, E. A., Wills, L. E., Reinhard, M., and Grbic-Galic, D. (1992). Anaerobic degradation of toluene and xylene by aquifer microorganisms under sulfate-reducing conditions. *Appl. Environ. Microbiol.*, 58(3):794–800.
- Einsiedl, F. and Mayer, B. (2005). Sources and processes affecting sulfate in a karstic groundwater system of the Franconian Alb, southern Germany. *Environmental Science and Technology*, 39(18):7118–7125.
- Engesgaard, P. and Kipp, K. L. (1992). A geochemical transport model for redox-controlled movement of mineral fronts in groundwater flow systems: A case of nitrate removal by oxidation of pyrite. *Water Resour. Res.*, 28(10):2829–2843.
- Essaid, H. I. and Bekins, B. A. (1997). BIOMOC, A multispecies transport model with biodegradation. Technical report, U.S. Geological Survey techniques of Water-Resources Investigations Report 97-4022.
- Fehlberg, E. (1969). Low-order classical Runge-Kutta formulas with stepsize control and their application to some heat transfer problems. Technical report, NASA.
- Greskowiak, J., Prommer, H., Massmann, G., and Nützmann, G. (2006). Identification of temperature-dependent water quality changes during a deep well injection experiment in a pyritic aquifer. *Environmental Science and Technology*, 40:6615–6621.
- Greskowiak, J., Prommer, H., Vanderzalm, J., Pavelic, P., and Dillon, P. (2005). Modeling of carbon cycling and biogeochemical changes during injection and recovery of reclaimed water at bolivar, south australia. *Water Resour. Res.*, 41(12):3539–3551.

- Griebler, C., Safinowski, M., Vieth, A., Richnow, H., and Meckenstock, R. (2004). Combined application of stable carbon isotope analysis and specific metabolites determination for assessing in situ degradation of aromatic hydrocarbons in a tar oil-contaminated aquifer. *Environmental Science and Technology*, 38(2):617–631.
- Guerin, M. and Zheng, C. (1998). GMT3D - Coupling multicomponent, three-dimensional transport with geochemistry. In Poeter, E. P., Zheng, C., and Hill, M. C., editors, *MODFLOW'98*, pages 413–420. Proc. International conference, Colorado School of Mines, Golden, CO.
- Ham, P. A. S., Prommer, H., Olsson, A. H., Schotting, R. J., and Grathwohl, P. (2007). Predictive modelling of dispersion controlled reactive plumes at the laboratory-scale. *Journal of Contaminant Hydrology*, 93:304–315.
- Ham, P. A. S., Schotting, R. J., Prommer, H., and Davis, G. B. (2004). Effects of hydrodynamic dispersion on plume lengths for instantaneous bimolecular reactions. *Adv. Water Resour.*, 27:803–813.
- Herzer, J. and Kinzelbach, W. (1989). Coupling of transport and chemical processes in numerical transport models. *Geoderma*, 44:115–127.
- Hindmarsh, A. C. (1983). ODEPACK, a systemized collection of ODE solvers. In Stepleman, R. S., editor, *Scientific Computing*, pages 55–64. North Holland, Amsterdam.
- Jung, H. B., Charette, M. A., and Zheng, Y. (2009). Field, Laboratory, and Modeling Study of Reactive Transport of Groundwater Arsenic in a Coastal Aquifer. *Environmental Science and Technology*.
- Kohler, M., Curtis, G. P., Kent, D. B., and Davis, J. A. (1996). Experimental investigation and modeling of uranium(VI) transport under variable chemical conditions. *Water Resour. Res.*, 32(12):3539–3551.
- Lu, G., Clement, T. C., Zheng, C., and Wiedemeier, T. H. (1999). Natural attenuation of BTEX compounds: Model development and field-scale application. *Ground Water*, 37(5):707–717.
- Ma, R., Zheng, C., Prommer, H., Greskowiak, J., Liu, C., Zachara, J., and Rockhold, M. (2009). A Field-Scale Reactive Transport Model for U(VI) Migration Influenced by Coupled Multi-rate Mass Transfer and Surface Complexation Reactions. *Water Resour. Res.*

- Meckenstock, R., Morasch, B., Griebler, C., and Richnow, H. (2004). Stable isotope fractionation analysis as a tool to monitor biodegradation in contaminated aquifers. *J. Contam. Hydrol.*, 75(3-4):215–255.
- Miller, C. T. and Rabideau, A. J. (1993). Development of split-operator, Petrov-Galerkin methods to simulate transport and diffusion problems. *Water Resour. Res.*, 29(7):2227–2240.
- Morasch, B., Richnow, H., Vieth, A., Schink, B., and Meckenstock, R. (2004). Stable isotope fractionation caused by glycol radical enzymes during bacterial degradation of aromatic compounds. *Appl. Environ. Microbiol.*, 70(5):2935–2940.
- Morshed, J. and Kaluarachchi, J. J. (1995a). Critical assessment of the operator-splitting technique in solving the advection-dispersion-reaction equation: 1. First-order reaction. *Adv. Water Res.*, 18(2):89–100.
- Morshed, J. and Kaluarachchi, J. J. (1995b). Critical assessment of the operator-splitting technique in solving the advection-dispersion-reaction equation: 2. Monod kinetics and coupled transport. *Adv. Water Res.*, 18(2):101–110.
- Nienhuis, P., Appelo, C. A. J., and Willemsen, G. (1994). User Guide PHREEQM-2D: A multi-component mass transport model. Technical report, IT Technology, Arnhem, The Netherlands.
- Noorishad, J., Carnahan, C. L., and Benson, L. V. (1987). Development of the non-equilibrium reactive chemical transport code CHMTRNS. Technical report, Lawrence Berkeley Laboratory, Earth Science Division.
- Parkhurst, D. L. (1995). User's guide to PHREEQC - A computer program for speciation, reaction-path, advective-transport, and inverse geochemical calculations. Technical Report 4227, U.S. Geological Survey Water-Resources Investigations Report.
- Parkhurst, D. L. and Appelo, C. (1999). User's guide to PHREEQC—A computer program for speciation, reaction-path, 1D-transport, and inverse geochemical calculations. Technical report, U.S. Geological Survey Water-Resources Investigations Report. in review.
- Parkhurst, D. L., Thorstenson, D. C., and Plummer, L. N. (1980). PHREEQE - A computer program for geochemical calculations. Technical report, U.S. Geological Survey techniques of Water-Resources Investigations Report 80-96.

- Parlange, J.-Y., Starr, J. L., Barry, D. A., and Braddock, R. D. (1984). Some approximate solutions of the transport equation with irreversible reactions. *Sci. Soc. Am. J.*, (137):434–442.
- Pooley, K. E., Blessing, M., Schmidt, T. C., Haderlein, S. B., MacQuarrie, K. T. B., and Prommer, H. (2009). Aerobic biodegradation of chlorinated ethenes in a fractured bedrock aquifer: quantitative assessment by compound-specific isotope analysis (CSIA) and reactive transport modelling. *Environmental Science and Technology*.
- Postma, D. and Jakobsen, R. (1996). Redox zonation: Equilibrium constraints on the Fe(III)/SO<sub>4</sub>-reduction interface. *Geochim. Cosmochim. Acta*, 60:3169–3175.
- Prommer, H. (2002). PHT3D - A Reactive Multicomponent Transport Model for Saturated Porous Media. Technical report, Contaminated Land Assessment and Remediation Research Centre, The University of Edinburgh.
- Prommer, H., Anneser, B., Rolle, M., Einsiedl, F., and Griebler, C. (2009). Biogeochemical and Isotopic Gradients in a BTEX/PAH Contaminant Plume: Model-Based Interpretation of a High-Resolution Field Data Set. *Environmental Science and Technology*, 43(21):8206–8212.
- Prommer, H., Aziz, L. H., Bolano, N., Taubald, H., and Schüth, C. (2008). Modelling of geochemical and isotopic changes in a column experiment for degradation of TCE by zero-valent iron. *Journal of Contaminant Hydrology*, 97:13–26.
- Prommer, H., Barry, D. A., and Davis, G. B. (1999a). A one-dimensional reactive multi-component transport model for biodegradation of petroleum hydrocarbons in groundwater. *Env. Model. Softw.*, 14(2/3):213–223.
- Prommer, H., Barry, D. A., and Davis, G. B. (2002a). Influence of transient groundwater flow on physical and reactive processes during biodegradation of a hydrocarbon plume. *J. Contam. Hydrol.*, 59:113–131.
- Prommer, H., Barry, D. A., and Davis, G. B. (2002b). Modelling of physical and reactive processes during biodegradation of a hydrocarbon plume under transient groundwater flow conditions. *Journal of Contaminant Hydrology*, 59:113–131.
- Prommer, H., Barry, D. A., and Zheng, C. (2003). MODFLOW/MT3DMS-based reactive multi-component transport modelling. *Ground Water*, 42(2):247–257.

- Prommer, H., Davis, G. B., and Barry, D. A. (1999b). PHT3D - A three-dimensional biogeochemical transport model for modelling natural and enhanced remediation. In Johnston, C. D., editor, *Proc. Contaminated site remediation: Challenges posed by urban and industrial contaminants, Fremantle, Western Australia, 21-25 March 1999*, pages 351–358.
- Prommer, H., Grassi, M. E., Davis, A. C., and Patterson, B. M. (2007). Modeling of microbial dynamics and geochemical changes in a metal bioprecipitation experiment. *Environmental Science and Technology*, 41:8433–8438.
- Prommer, H. and Stuyfzand, P. J. (2005). Identification of temperature-dependent water quality changes during a deep well injection experiment in a pyritic aquifer. *Environmental Science and Technology*, 39:2200–2209.
- Prommer, H., Tuxen, N., and Bjerg, P. L. (2006). Fringe-controlled natural attenuation of phenoxy acids in a landfill plume: Integration of field-scale processes by reactive transport. *Environmental Science and Technology*, 40:4732–4738.
- Rees, H. C., Oswald, S. E., Banwart, S. A., Pickup, R. W., and Lerner, D. N. (2007). Biodegradation processes in a laboratory-scale groundwater contaminant plume assessed by fluorescence imaging and microbial analysis. *Appl. Environ. Microbiol.*, 73(12):3865–3876.
- Richnow, H., Meckenstock, R., Reitzel, L., Baun, A., Ledin, A., and Christensen, T. (2003). In situ biodegradation determined by carbon isotope fractionation of aromatic hydrocarbons in an anaerobic landfill leachate plume (Vejen, Denmark). *J. Contam. Hydrol.*, 64(1-2):59–72.
- Rubin, J. and James, R. V. (1973). Dispersion-affected transport of reacting solutes in saturated porous media: Galerkin method applied to equilibrium-controlled exchange in unidirectional steady water flow. *Water Resour. Res.*, 9(5):1332–1352.
- Sardin, M., Krebs, R., and Schweich, D. (1986). Transient mass-transport in the presence of non-linear physico-chemical interaction laws: Progressive modelling and appropriate experimental procedures. *Geoderma*, 38:115–130.
- Spence, M., Bottrell, S., Thornton, S., Richnow, H., and Spence, K. (2005). Hydrochemical and isotopic effects associated with petroleum fuel biodegradation pathways in a chalk aquifer. *J. Contam. Hydrol.*, 79(1-2):67–88.

- Spormann, A. and Widdel, F. (2000). Metabolism of alkylbenzenes, alkanes, and other hydrocarbons in anaerobic bacteria. *Biodegradation*, 11(2-3):85–105.
- Steeffel, C. I. and MacQuarrie, K. T. B. (1996). Approaches to modelling of reactive transport in porous media. In Lichtner, P. C., Steefel, C. I., and Oelkers, E. H., editors, *Reactive Transport in Porous Media: General Principles and Applications to Geochemical Processes*, pages 83–129. Mineralogical Society of America, Washington D.C.
- Sun, Y., Petersen, J. N., Clement, T. P., and Skeen, R. S. (1999). Development of analytical solutions for multispecies transport with serial and parallel reactions. *Water Resour. Res.*, 35(1):185–190.
- Thierrin, J., Davis, G., Barber, C., Patterson, B. M., Pribac, F., Power, T. R., and Lambert, M. (1993). Natural degradation rates of BTEX compounds and naphthalene in a sulphate-reducing groundwater environment. *Hydro. Sci. J.*, 38(4):309–321.
- Tuxen, N., Albrechtsen, H.-J., and Bjerg, P. L. (2006). Identification of a reactive degradation zone at a landfill leachate plume fringe using high resolution sampling and incubation techniques. *J. Contam. Hydrol.*, 85(3-4):179–194.
- Valocchi, A. and Malmstead, M. (1992). Accuracy of operator splitting for advection-dispersion-reaction problems. *Water Resour. Res.*, 28(5):1471–1476.
- Valocchi, A. J. (1980). *Transport of ion-exchanging solutes during groundwater recharge*. Stanford University, Stanford, California. PhD thesis.
- Valocchi, A. J., Street, R. L., and Roberts, P. V. (1981). Transport of ion-exchanging solutes in groundwater: Chromatographic theory and field simulation. *Water Resour. Res.*, 17(5):1517–1527.
- van Breukelen, B. and Griffioen, J. (2004). Biogeochemical processes at the fringe of a landfill leachate pollution plume: potential for dissolved organic carbon, Fe(II), Mn(II), NH<sub>4</sub>, and CH<sub>4</sub> oxidation. *J. Contam. Hydrol.*, 73(1-4):181–205.
- van Breukelen, B., Hunkeler, D., and Volkering, F. (2005). Quantification of sequential chlorinated ethene degradation by use of a reactive transport model incorporating isotope fractionation. *Environmental Science and Technology*, 39(11):4189–4197.

- van Breukelen, B. M. and Prommer, H. (2008). Beyond the Rayleigh equation: Reactive transport modeling of isotope fractionation effects to improve quantification of biodegradation. *Environmental Science and Technology*, 42:2457–2463.
- van Genuchten, M. T. (1980). Determining Transport Parameters from Solute Displacement Experiments. Technical report, United States Department of Agriculture.
- Vencelides, Z., Sracek, O., and Prommer, H. (2007). Modelling of iron cycling and its impact on the electron balance at a petroleum hydrocarbon contaminated site in Hnevice, Czech Republic. *Journal of Contaminant Hydrology*, 89:270–294.
- Waddill, D. W. and Widdowson, M. A. (1998). SEAM3D: A Numerical Model for Three-Dimensional Solute Transport and Sequential Electron Acceptor-Based Bioremediation in Groundwater. Technical report, Virginia Tech., Blacksburg, Virginia.
- Wallis, I., Prommer, H., Simmons, C. T., Post, V., and Stuyfzand, P. J. (2010). Evaluation of Conceptual and Numerical Models for Arsenic Mobilization and Attenuation during Managed Aquifer Recharge. *Environmental Science and Technology*, 44:5035–5041.
- Walter, A. L., Frind, E. O., Blowes, D. W., and Ptacek, C. J. (1994). Modeling of multicomponent reactive transport in groundwater, 1, Model development and evaluation. *Water Resour. Res.*, 30(11):3137–3148.
- Wilkes, H., Boreham, C., Harms, G., Zengler, K., and Rabus, R. (2000). Anaerobic degradation and carbon isotopic fractionation of alkylbenzenes in crude oil by sulphate-reducing bacteria. *Org. Geochem.*, 31(1):101–115.
- Williamson, M. A. and Rimstidt, J. D. (1994). The kinetics and electrochemical rate-determining step of aqueous pyrite oxidation. *Geochim. Cosmochim. Acta*, 58:5443–5454.
- Winderl, C., Anneser, B., Griebler, C., Meckenstock, R. U., and Lueders, T. (2008). Depth-resolved quantification of anaerobic toluene degraders and aquifer microbial community patterns in distinct redox zones of a tar oil contaminant plume. *Applied and Environmental Microbiology*, 74(3):792–801.
- Wisotzky, F. and Eckert, P. (1997). Sulfat-dominiertes BTEX-Abbau im Grundwasser eines ehemaligen Gaswerksstandortes. *Grundwasser*, 3(1):11–20.

- Yeh, G. T. and Tripathi, V. S. (1989). A critical evaluation of recent developments in hydrogeochemical transport models of reactive multichemical components. *Water Resour. Res.*, 25(1):93–108.
- Zheng, C. (1990). A modular three-dimensional transport model for simulation of advection, dispersion and chemical reaction of contaminants in groundwater systems. Technical report, U.S. Environmental Protection Agency.
- Zheng, C. (1999). MT3D99: A modular three-dimensional multispecies transport simulator. Technical report, S. S. Papadopoulos & Associates, Inc., Bethesda, MD, USA.
- Zheng, C. and Wang, P. P. (1999). MT3DMS, A modular three-dimensional multispecies transport model for simulation of advection, dispersion and chemical reactions of contaminants in groundwater systems; documentation and user's guide. Technical report, U.S. Army Engineer Research and Development Center Contract Report SERDP-99-1, Vicksburg, MS.
- Zysset, A. (1993). *Modellierung des chemischen Zustandes in Grundwasser-Infiltrations-Systemen*. Institut f. Hydromechanik und Wasserwirtschaft, ETH Zürich. PhD thesis.
- Zysset, A., Stauffer, F., and Dracos, T. (1994). Modeling chemically reactive groundwater transport. *Water Resour. Res.*, 30(7):2217–2228.